



MODELING THE PATOS LAGOON AND INNER
SHELF HYDRODYNAMICS AND SEDIMENT
TRANSPORT – RIO GRANDE DO SUL - BRAZIL

Report by

Raphael Miguez Nogueira

Project: Cassino [z3672]

Universidade Federal do Rio de Janeiro – Rio de Janeiro – Brazil

12/feb – 13/apr
2006

CONTENTS

1. Introduction	7
2. Objectives.....	10
3. Data Available.....	11
3.1. 1998 Data set	12
3.2. 1999 Data set	14
3.3. 2000 Data set	14
4. Delft3D-Flow Module	17
4.1. Grid	17
4.2. Bathymetry	18
4.3. Water Elevation	19
4.4. Winds	21
4.5. River Discharges.....	22
5. Calibration.....	22
5.1. Water Elevation	22
5.2. Currents and Salinity.....	25
6. Behavior of the system	28
7. Delft3D-Flow Module with Cohesive Sediment.....	30
8. Conclusions and recommendations	32
9. References.....	34
10. Appendix.....	36

LIST OF FIGURES

Figure 1: Localization of the studied area. Adapted image taken from the website www.worldatlas.com/webimage/countrys/samerica/brlarge.htm	7
Figure 2: Astronomical tide spectra to the period of 01/04/99 till 30/09/99. X axe means the frequency in hours ⁻¹	8
Figure 3: Division of the studied area in accordance to literature. Axes are in UTM coordinates.	10
Figure 4: Plume of sediments formed in the inner shelf in front of Cassino beach, Rio Grande do Sul, south of Brazil.	10
Figure 5: Localization of the stations where the measured data were obtained.	12
Figure 6: The upper graphic is the measured water elevation on the jetties (M1 – blue line) and São José do Norte (M2 – magenta line). The second one is the measured salinity at 10 meters depth at station Praticagem (available data for 26/05-09/06). The third one is the measured wind speed and direction at station Praticagem. And the last is the Guaíba and Camaquã river discharges.....	13
Figure 7: The upper graphic is the measured water elevation in station Praticagem and New Port. The second one is the measured wind in station Praticagem. The third one is the flux through the sections A, B, C, D and E. The fourth one is the suspended matter in the same sections before. And the last one is the discharges of the Camaquã and Guaíba rivers.....	16
Figure 8: Measured salinity profiles for the period in the middle of each section.	17
Figure 9: Grid used in the model. Refined elements in the estuary and coast areas....	18
Figure 10: Bathymetry of the domain generated from the interpolation of the digitalized nautical charts.....	19
Figure 11: Water elevation measured at stations: Praticagem, Bojuru, Itapuã and São Lourenço.	20
Figure 12: Wind speed and direction measured at station Praticagem used in the model. The letters means: (a) May, (b) June, (c) July, (d) August and (e) September. The vectors were rotated in order to NE and SW winds match the main axis of the lagoon. NE winds are vertically downwards and SW vertically upwards. X axe is in days.....	21
Figure 13: Rose of the wins for the period. The color bar is the frequency of occurrence in percentage. The circles represent the speed in m/s.....	21
Figure 14: Guaíba and Camaquã river discharges used in the model.	22
Figure 15: Suspended matter from ANA website data for the Camaquã river. The concentration for the Camaquã river was chosen to 60 mg/l as a mean value of the may, july and october/99 data.	31
Figure 16: Amplified meteorological tide. Three different factors were used.	36
Figure 17: Water elevation spectral density at station Praticagem, using v1 amplification factor – run016. Ordinates in log scale.....	36
Figure 18: Water elevation spectral density at station Praticagem, using v2 amplification factor – run017. Ordinates in log scale.....	37
Figure 19: Water elevation spectral density at station Praticagem, using v3 amplification factor – run018. Ordinates in log scale.....	37

Figure 20: Water elevation plotted for transects. The red line is the lagoon transect. The black line is the middle lagoon transect. The blue line is the cross-estuary transect. The green is the along-estuary transect. The arrows indicate the beginning of each plotted transect in the graphics (x=0).38

Figure 21: Comparison of wind, water elevation, river discharges and cumulative discharge through the mouth for the modeled period. The blue balloons are correlated to NE winds and the green ones are to SW winds. In the upper graphic, the letters mean: (a) may, (b) june, (c) july, (d) august and (e) september of 1999.40

Figure 22: Salinity patterns under NE winds (a), (c) and (d) and SW winds (b). The upper part of each graphics is the location of Ponta da Feitoria. The color bar is in ppt. Results from model run_045.41

Figure 23: Constituent S2: amplitude and phase used to interpolate to the open boundary.....42

Figure 24: Constituent K1: amplitude and phase used to interpolate to the open boundary.....42

Figure 25: Constituent K2: amplitude and phase used to interpolate to the open boundary.....42

Figure 26: Constituent M2: amplitude and phase used to interpolate to the open boundary.....42

Figure 27: Constituent N2: amplitude and phase used to interpolate to the open boundary.....43

Figure 28: Constituent O1: amplitude and phase used to interpolate to the open boundary.....43

Figure 29: Constituent P1: amplitude and phase used to interpolate to the open boundary.....43

Figure 30: Constituent Q1: amplitude and phase used to interpolate to the open boundary.....43

Figure 31: Currents and salinity modeled comparison against measured data. Chezy bottom frictional law (C=50). Y units are in m/s (upper graphic) and ppt (lower graphic).44

Figure 32: Currents and salinity modeled comparison against measured data. Manning bottom frictional law (M=0.025). Y units are in m/s (upper graphic) and ppt (lower graphic).44

Figure 33: Currents and salinity modeled comparison against measured data. White-Colebrook bottom frictional law (k=0.01). Y units are in m/s (upper graphic) and ppt (lower graphic).....45

Figure 34: Modeled current and salinity comparison against measured data. k=0.005 and SGC discharge.....45

Figure 35: Modeled current and salinity comparison against measured data. k=0.001 and SGC discharge.....46

Figure 36: Modeled current and salinity comparison against measured data. k=0.015 and SGC discharge.....46

Figure 37: Modeled current and salinity comparison against measured data. k=0.05 and SGC discharge.....47

Figure 38: Modeled current and salinity comparison against measured data. $k=0.05$ and no SGC discharge.....47

Figure 39: Modeled current and salinity comparison against measured data. $k=0.015$ and no SGC discharge.....48

Figure 40: Modeled current and salinity comparison against measured data. $k=0.008$ and no SGC discharge.....48

Figure 41: Modeled current and salinity comparison against measured data. $k=0.005$ and no SGC discharge.....49

Figure 42: Modeled current and salinity comparison against measured data. $k=0.001$ and no SGC discharge.....49

Figure 43: Modeled current and salinity comparison against measured data. $k=0.008$ and SGC discharge.....50

Figure 44: Modeled current and salinity comparison against measured data. $k=0.01$ and no SGC discharge.....50

Figure 45: Modeled current and salinity comparison against measured data. Horizontal diffusivity in the estuary area set to $100 \text{ m}^2/\text{s}$51

Figure 46: Modeled current and salinity comparison against measured data. Horizontal diffusivity in the estuary area set to $150 \text{ m}^2/\text{s}$51

Figure 47: Modeled current and salinity comparison against measured data. Horizontal diffusivity in the estuary area set to $200 \text{ m}^2/\text{s}$52

Figure 48: Modeled current and salinity comparison against measured data. Horizontal diffusivity in the estuary area set to $300 \text{ m}^2/\text{s}$52

Figure 49: Modeled current and salinity comparison against measured data. Horizontal diffusivity in the estuary area set to $400 \text{ m}^2/\text{s}$53

Figure 50: Modeled current and salinity comparison against measured data. Horizontal diffusivity in the estuary area set to $500 \text{ m}^2/\text{s}$53

Figure 51: Modeled current and salinity comparison against measured data. Horizontal diffusivity in the estuary area set to $600 \text{ m}^2/\text{s}$54

Figure 52: Modeled current and salinity comparison against measured data. Horizontal diffusivity in the estuary area set to $700 \text{ m}^2/\text{s}$54

Figure 53: Modeled current and salinity comparison against measured data. Horizontal diffusivity in the estuary area set to $800 \text{ m}^2/\text{s}$55

Figure 54: Modeled current and salinity comparison against measured data. Horizontal diffusivity in the estuary area set to $900 \text{ m}^2/\text{s}$55

Figure 55: Modeled current and salinity comparison against measured data. Horizontal diffusivity in the estuary area set to $1000 \text{ m}^2/\text{s}$56

Figure 56: Modeled current and salinity comparison against measured data. Horizontal diffusivity in the estuary area set to $400 \text{ m}^2/\text{s}$ and SGC discharges included.....56

Figure 57: Modeled current and salinity comparison against measured data. Horizontal diffusivity in the estuary area set to $500 \text{ m}^2/\text{s}$ and SGC discharges included.....57

Figure 58: Modeled current and salinity comparison against measured data. Horizontal diffusivity in the estuary area set to $600 \text{ m}^2/\text{s}$ and SGC discharges included.....57

Figure 59: Modeled current and salinity comparison against measured data. Horizontal diffusivity for the whole domain set to 400 m²/s and SGC discharges included.....58

Figure 60: Modeled current and salinity comparison against measured data. Horizontal diffusivity for the whole domain set to 300 m²/s and SGC discharges included.....58

Figure 61: Modeled current and salinity comparison against measured data. Horizontal diffusivity for the whole domain set to 200 m²/s and SGC discharges included.....59

Figure 62: Modeled current and salinity comparison against measured data for Delft3D-Flow three dimensional module, 10 layers were used.59

Figure 63: Modeled current and salinity comparison against measured data for Delft3D-Flow three dimensional module, 10 layers were used.60

Figure 64: Available mass of sediments results for the models run048_Sed_041 (a), run048_Sed_042 (b), run048_Sed_043 (d) and run048_Sed_044 (c). Bathymetry isolines are spaced in 5 meters. Figures (a) and (d) are the same results but in different scales in order to better visualize the mud bank.61

Figure 65: Available mass of sediments results for the models run048_Sed_045 (a), run048_Sed_046 (b), run048_Sed_047 (d) and run048_Sed_048 (c). Bathymetry isolines are spaced in 5 meters. Figures (a) and (d) are the same results but in different scales in order to better visualize the mud bank.62

LIST OF TABLES

Table 1: Table of available data. The data set used in the models was the 1999.....11

Table 2: Harmonic analysis results made using T_Tide tool box.....24

Table 3: Comparison of the harmonic analyses and FES99 constituents used in the model.....24

Table 4: Table of correlation coefficients for the calibration process.....26

Table 5: Table of depth-averaged models evaluated for the work. Y = included; N = excluded; GB = Guaíba; CQ = Camaquã; SGC = São Gonçalo Channel; C = Chezy; Mn = Manning and W-C = White-Colebrook.28

Table 6: List of sediment models performed. The models with * means that the horizontal diffusivity was set to 400 m²/s for the whole domain and ** were set to 10 m²/s for the whole domain. GB = Guaíba river; CQ = Camaquã river and SGC = São Gonçalo Channel.....63

1. Introduction

This report is presented in order to register the work done with Delft3D-Flow module, implemented for the Patos Lagoon. The aims of the work were to implement Delft3D-Flow module to understand about the behavior of the Patos Lagoon during action of different forcing and to understand the cohesive sediment transport to the shore, with emphasis to Cassino beach.

The Patos Lagoon is considered the largest choked coastal lagoon in the world (Kjerfve, 1986). It is located in the southern Brazilian coastline between 30°32'15" S and 50°30' -52°15' W (Figure 1). With a length of 250 km and average width of 40 km, the lagoon has a surface of 10.360 km² and drains a hydrological basin of 200.000 km² (including the Mirim Lagoon basins), exhibiting Camaquã and Guaíba rivers as the main inflows of freshwater, with peaks (Guaíba) up to 3000 m³/s between August and October (spring), and during the El Niño phenomenon, it can reach peaks of 13000 m³/s (Moller et al, 2001).



Figure 1: Localization of the studied area. Adapted image taken from the website www.worldatlas.com/webimage/countrys/samerica/brlarge.htm

As the lagoon exhibits an average depth of 5 m, it is considered a shallow water body. Inside the main lagoon two morphological structures are found: sand banks and spits. These structures and the shallow bathymetry give to the lagoon a

high frictional behavior. The entire system can be separated into three distinct areas: the estuarine area, the main lagoon and the north portion of the lagoon.

The estuarine area can be defined as the area between the mouth and Ponta da Feitoria (Figure 3), it is connected to the ocean by a 20 km long and 1-2 km narrow inlet channel and is tidal classified as micro-tidal (Daves, 1964 in Fernandes et al, 2002), with mixed tides where the diurnal component is noticeable and amplitudes of 50 cm (Figure 2). The salinity is restricted to this area, with upper limit near Ponta da Feitoria in periods of low river discharges and south winds. The dynamics, i.e., the pressure gradients and the salinity distribution, are essentially dependent on the wind action and on the freshwater discharges, once that the tidal influence is small.

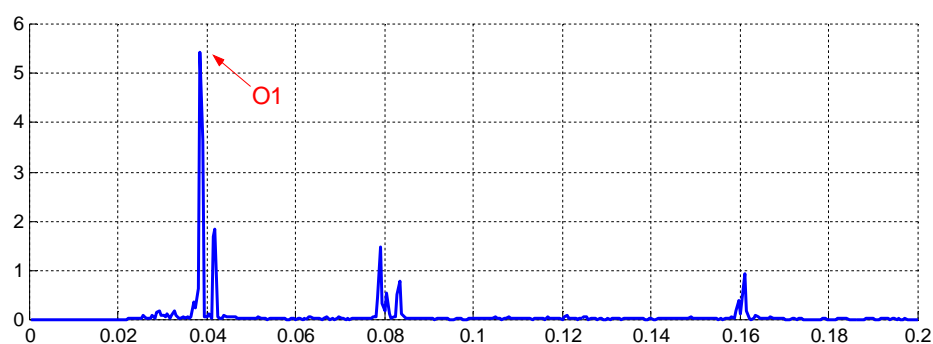


Figure 2: Astronomical tide spectra to the period of 01/04/99 till 30/09/99. X axe means the frequency in hours⁻¹.

In the north area of the estuary, on the west margin, there is a channel called São Gonçalo that makes the communication between the Patos Lagoon estuary and the Mirim Lagoon. Its length is 70 km long and its flow is usually in direction of the Patos Lagoon estuary. Some researches done by Hartmann et al (1990b & 1990c) showed a great contribution of sediments to the estuary zone. As cited in Hartmann et al (1990c), the São Gonçalo channel can export 13879 tons of suspended matter (fine sediments) during almost 7 months in currents of 0.40 m/s.

The main lagoon is the Patos Lagoon itself, exhibits four cells separated by spits, the main axis is NE-SW orientated, almost parallel to the coastline and is coincident with the dominant wind regime. Its waters are mainly fresh. The north portion of the lagoon is formed by the Guaíba river and the Casamento lagoon.

The hydrodynamics were subject to several works done by Moller et al (1996, 1999 & 2001), by Fernandes (2001) and by Fernandes et al (2002, 2004a, 2004b & 2004c). In Moller et al (1996), the authors concluded that the wind action in the lagoon can be observed through the difference in level generated inside the lagoon and between the lagoon and the ocean. Moller et al (1996) established that the

circulation of the inlet zone (between the mouth and Sao Jose do Norte) is mostly driven by the remote wind action; the circulation of the intermediate zone (between Sao Jose do Norte and Ponta da Feitoria) is mainly driven by the local wind action, although the remote wind has still some influence; and the circulation in the central lagoon is exclusively driven by the local wind through the so called set-up/set-down mechanism of oscillation.

Moller et al (2001) concluded that salt water enters the system due to a combination of both remote and local wind effects that favors the development of a pressure gradient towards the lagoon during southwesterly winds, and this situation is reversed when northeasterly winds dominate. During high flood periods, normally observed in late winter, the circulation is driven by freshwater discharge. They also concluded that the longitudinal component of the wind is the main responsible for the circulation of the system since its action is on the main axis of the lagoon. It is responsible for generate barotropic pressure gradient that produce landward (in case of SW winds) or seaward flows (in case of NE winds). As the NE wind is dominant during the year, frontal system passages from 3 to 16 days of period are the main forcing that can change the standard flow.

In relation to the stratification, saline intrusion and transverse flow, in Fernandes et al (2004a), the authors concluded that the basic mechanism controlling the along-shore flow and salinity distribution in the estuarine zone is given by the pressure gradient generated between the coast and the lagoon, resulting from the local and non-local wind action and freshwater discharge. Inside the main lagoon, which is a shallow water body, the transverse flow is driven by the local wind forcing. Lateral pressure gradients resulting from the interaction between longitudinal barotropic pressure gradients and the morphology control the transverse flow in shallower areas. In deeper areas subject to density stratification, the transverse flow results from the interaction between barotropic and baroclinic forces and bathymetry.

This report is divided into 10 chapters, being Introduction the first, References and Appendix the last two. In chapter 2, the main goals are described. In chapter 3, the available data to work with are defined and analyzed in accordance to literature. In chapter 4, the data used in the model, the grid and the bathymetry are presented. In chapter 5, the calibration process is evaluated in terms of water elevation, currents and salinity. In chapter 6, the behavior of the modeled system is analyzed against measured data. In chapter 7, most of all models used with sediments

are shown. In chapter 8, conclusions of all results and recommendations to future works in order to get better results are commented. In chapter 9, the literature used in this work is listed and in chapter 10 Appendix, is where all the figures results are.

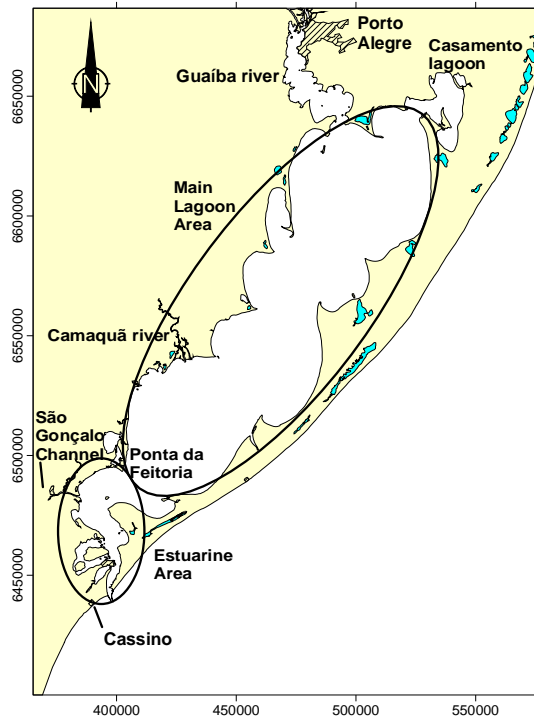


Figure 3: Division of the studied area in accordance to literature. Axes are in UTM coordinates.

2. Objectives

The main goals are to evaluate and calibrate the Delft3D-Flow using both depth-averaged and three dimensional modules and characterize the cohesive sediment transport to the inner shelf. Emphases are done to the formation of the mud bank that is created southwards from the jetties in front of Cassino beach (Figure 4).

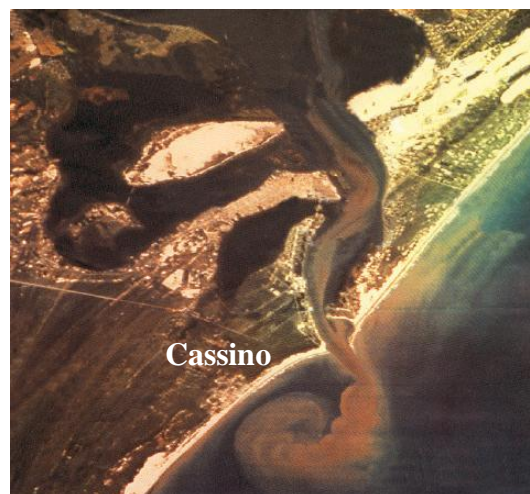


Figure 4: Plume of sediments formed in the inner shelf in front of Cassino beach, Rio Grande do Sul, south of Brazil.

3. Data Available

Three data sets were available to work with. The data are consisted in measured water elevations in some stations; wind speed and direction at the same station, Praticagem; rivers discharges for those that are the most important inflow of freshwater (Camaquã and Guaíba); salinity and currents in Rio Grande channel. The available data are shown in Table 1. The stations are located in the maps of Figure 5.

<i>Parameter</i>	<i>Station</i>	<i>Sampling Time</i>	<i>Begin</i>	<i>End</i>
Data 1998				
<i>Water Level</i>	Jetties (M1)	hour	23-05-1998	06-07-1998
	SJN (M2)	hour	23-05-1998	06-07-1998
<i>Wind</i>	Praticagem	hour	07-05-1998	17-06-1998
<i>Currents</i>	Praticagem	10 hour	26-05-1998	09-06-1998
<i>Salinity</i>	Praticagem	10 hour	26-05-1998	09-06-1998
<i>Density</i>	Praticagem	10 hour	26-05-1998	09-06-1998
<i>River Discharges</i>	Guaíba/Camaquã	day	01-05-1998	09-06-1998
Data 1999				
<i>Water Level</i>	Praticagem	hour	01-05-1999	30-09-1999
	Bojuru	hour	14-02-1999	30-09-1999
	Itapuã	hour	14-02-1999	30-09-1999
	São Lourenço	hour	14-02-1999	30-09-1999
<i>Wind</i>	Praticagem	hour	14-02-1999	30-09-1999
<i>Currents</i>	Praticagem	hour	02-08-1999	09-08-1999
<i>Salinity</i>	Praticagem	hour	02-08-1999	09-08-1999
<i>River Discharges</i>	Guaíba/Camaquã	day	01-05-1999	30-09-1999
Data 2000				
<i>Water Level</i>	Praticagem	hour	06-06-2000	21-06-2000
	New Port	hour	06-06-2000	21-06-2000
<i>Wind</i>	Praticagem	hour	06-06-2000	21-06-2000
<i>Currents</i>	New Port	6 hours	06-06-2000	20-06-2000
<i>Salinity</i>	New Port	6 hours	06-06-2000	20-06-2000
<i>Density</i>	New Port	6 hours	06-06-2000	20-06-2000
<i>Suspended Matter</i>	Transects	day	08-06-2000	19-06-2000
<i>Salinity and Temp Profiles</i>	Transects	4xMorning	07-06-2000	19-06-2000
<i>Discharges</i>	Transects	day	07-06-2000	19-06-2000
<i>River Discharges</i>	Guaíba/Camaquã	day	01-06-2000	01-07-2000

Table 1: Table of available data. The data set used in the models was the 1999.

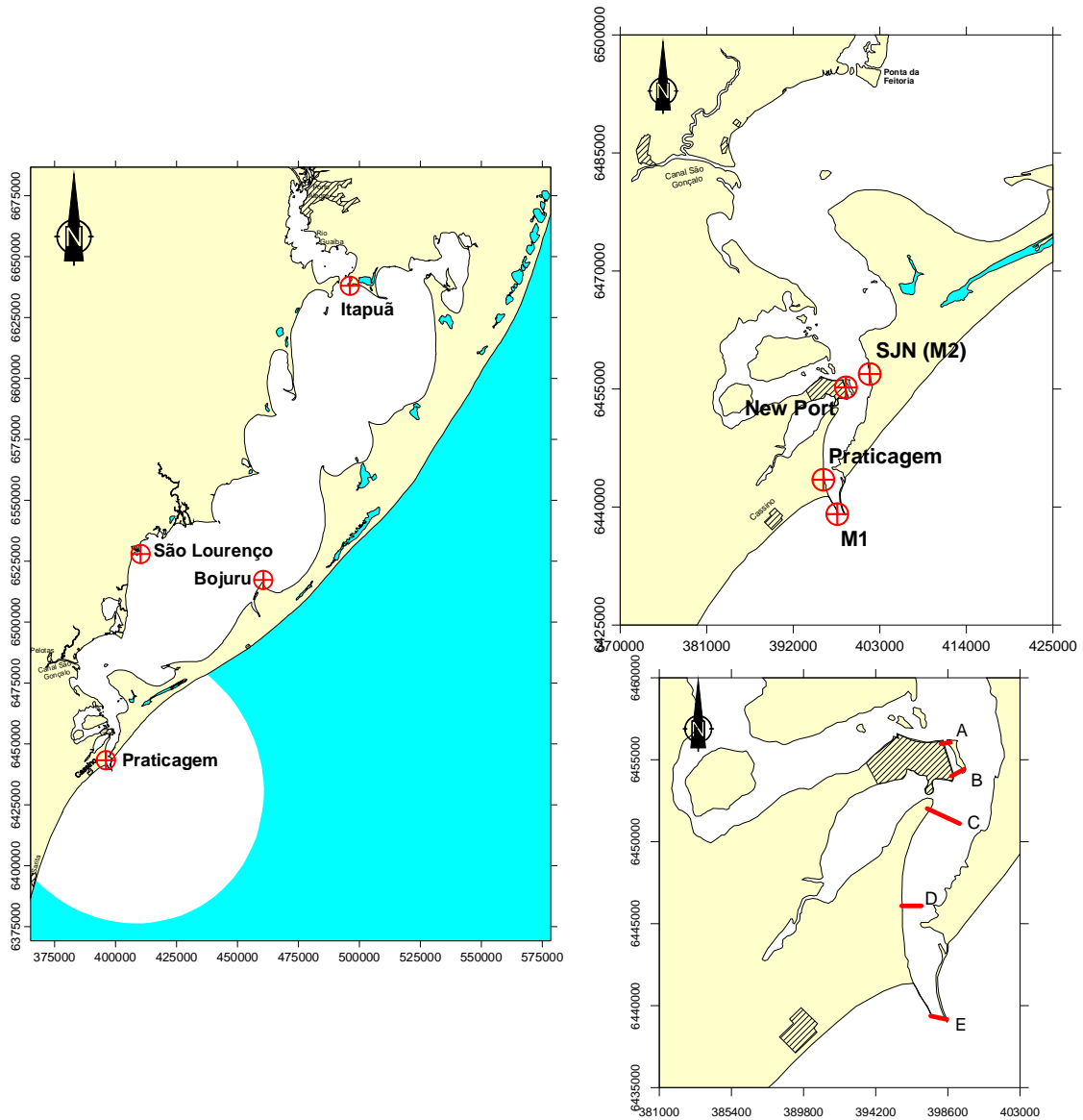
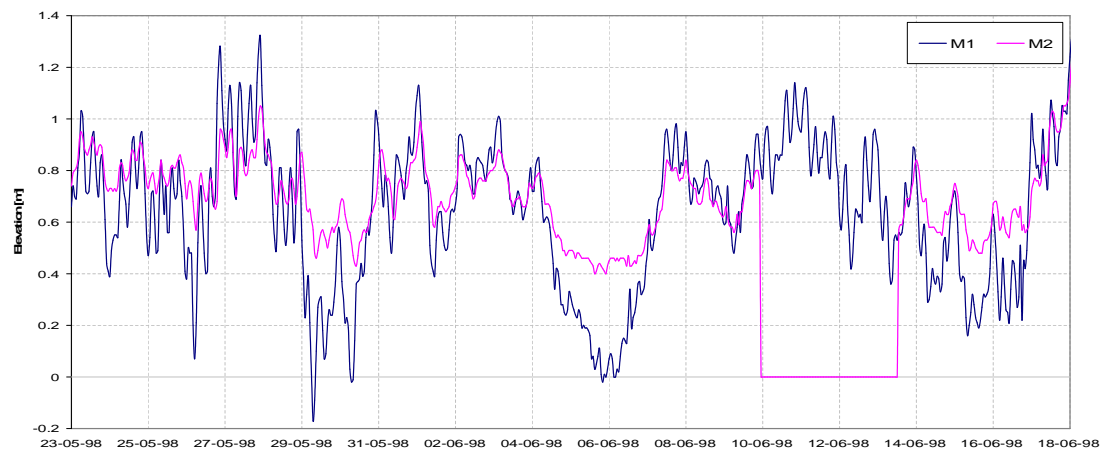


Figure 5: Localization of the stations where the measured data were obtained.

3.1. 1998 Data set



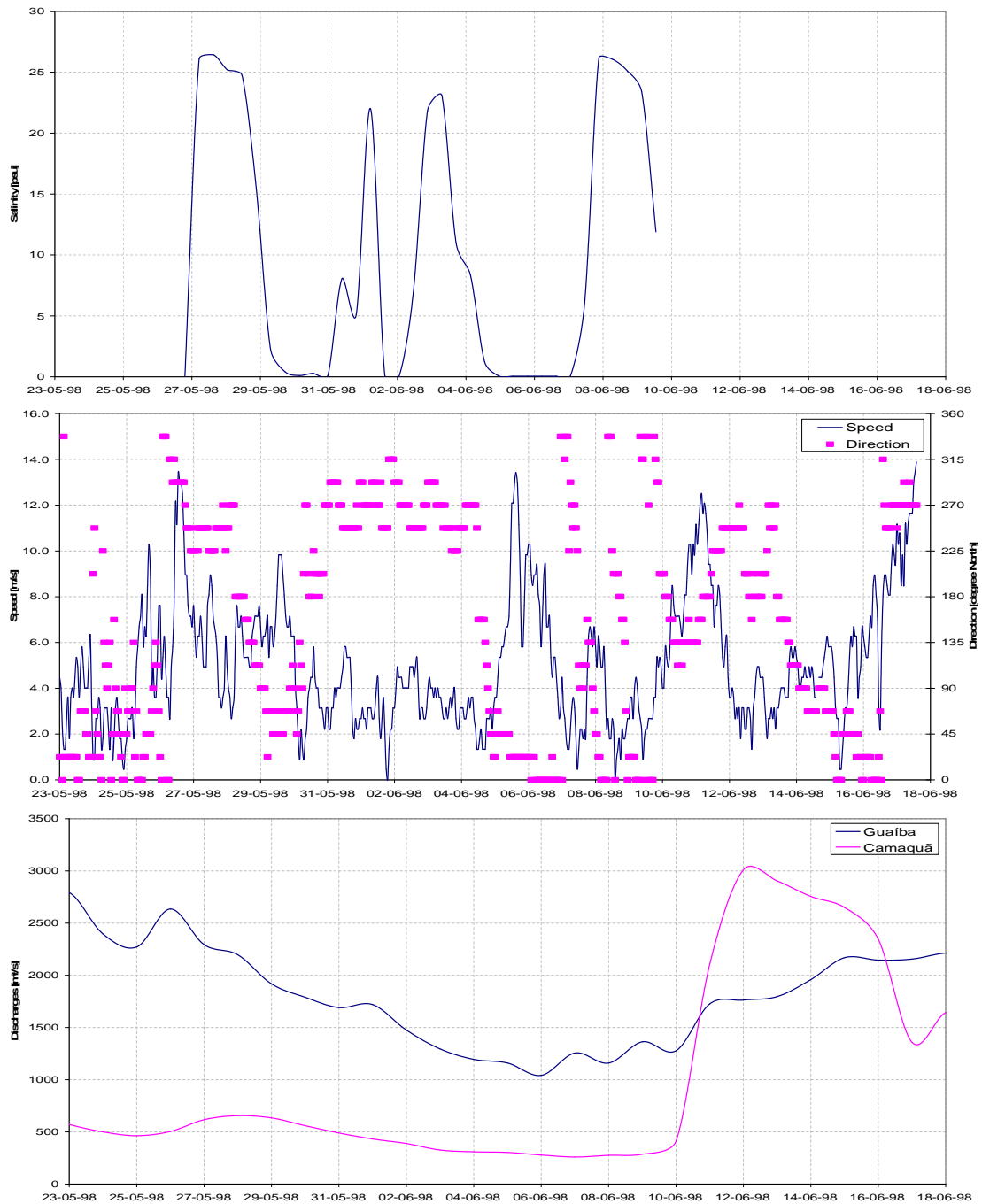


Figure 6: The upper graphic is the measured water elevation on the jetties (M1 – blue line) and São José do Norte (M2 – magenta line). The second one is the measured salinity at 10 meters depth at station Praticagem (available data for 26/05-09/06). The third one is the measured wind speed and direction at station Praticagem. And the last is the Guaíba and Camaquã river discharges.

From the Figure 6, it is noticeable that the wind is the main forcing which drives the hydrodynamics in this short period. The water elevation measurements were carried out in two stations, one at the outer point of the west jetty and the other on the pier of São José do Norte city. During north-east winds, there is a set down in the coast (days 23–26/05, 29-31/05, 04-07/06 and 14-17/06) and a pressure gradient is formed between the sea and the lagoon, favoring the outflow. The higher difference

between the coast and the estuary shown between days 29-31/05 may be due to the influence of the highest discharges occurred a few days before, and associated with high NE wind speed (10 m/s). The influence of the river discharges in this period can be associated with the decreasing of the salinity in the estuary. The second big difference is shown between days 04-07/06 and this one lasts more because of the influence of the N-NE highest wind speed that keeps blowing for several days, despite the relative small river discharges.

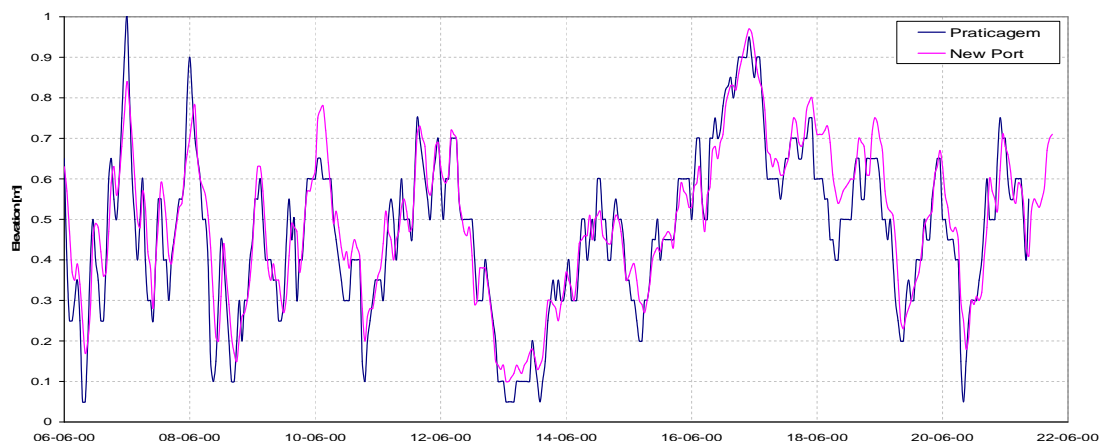
When south-west winds are blowing, the inversion of the process is observed. During the days 26-28/05, south-west wind speeds of 5-9 m/s cause a set up in the coast, creating a opposite pressure gradient that favors the saline water flows into the estuary. This mechanism can be verified when looking to the salinity graphic (days 31/05-01/06 and 02-03/06). South-east winds associated with low river discharges can also contribute to the saline intrusion as shown in the days 07-09/06.

3.2. 1999 Data set

The 1999 data are shown and analyzed in chapters 4 and 5. This set of data was used to simulate the hydrodynamics and sediment transport of the Patos Lagoon. These data were chosen due to their longer period of available measurements in comparison to the other two sets.

3.3. 2000 Data set

The 2000 data set is shown in Figure 7.



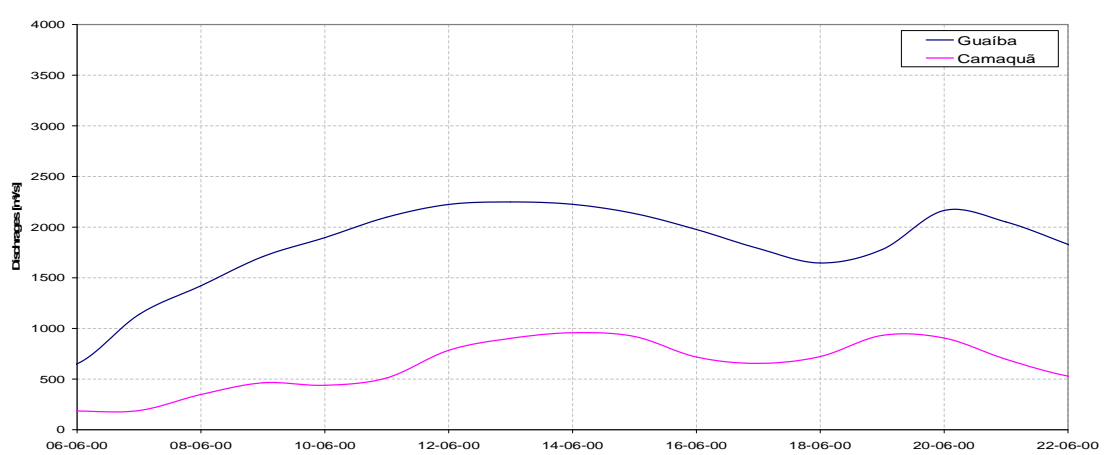
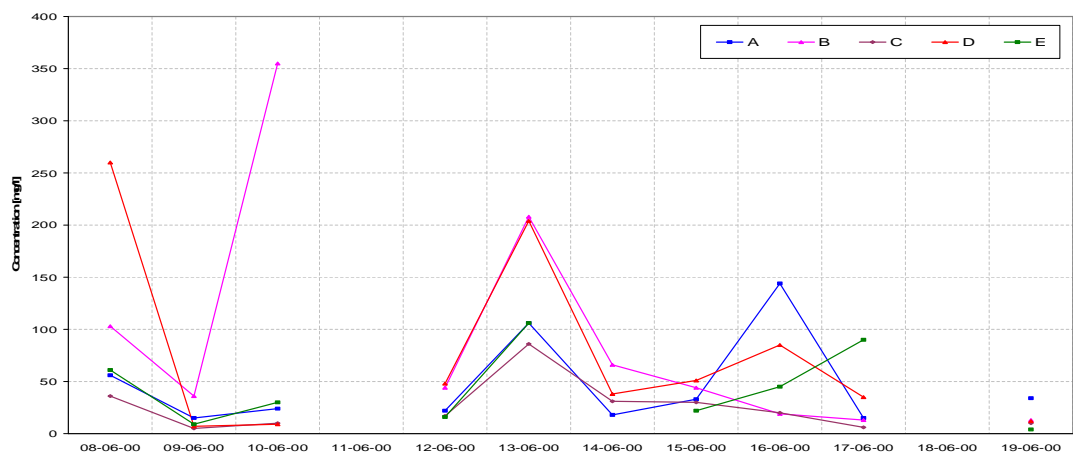
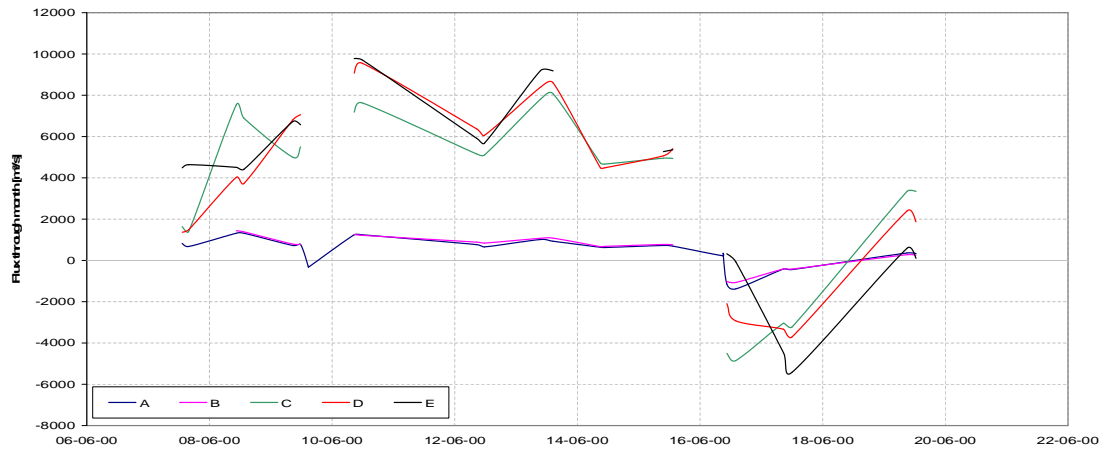
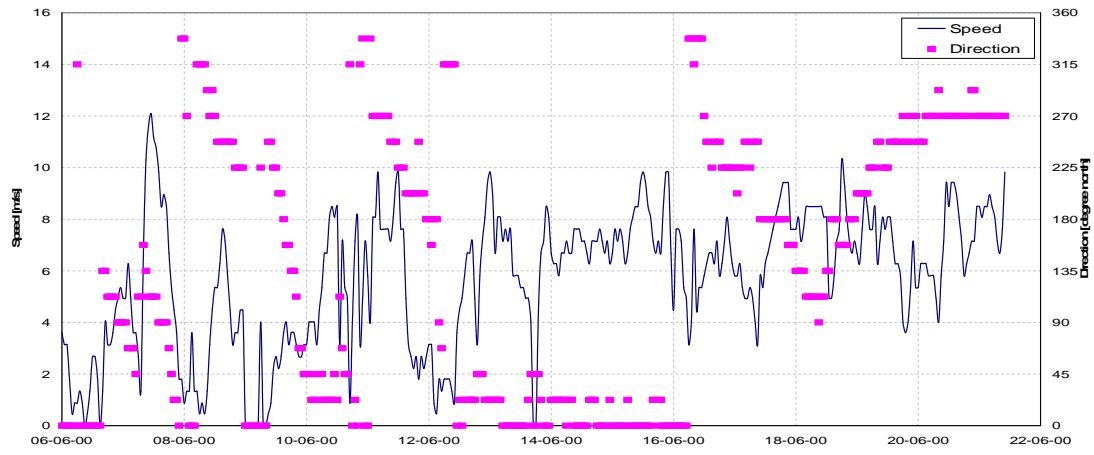
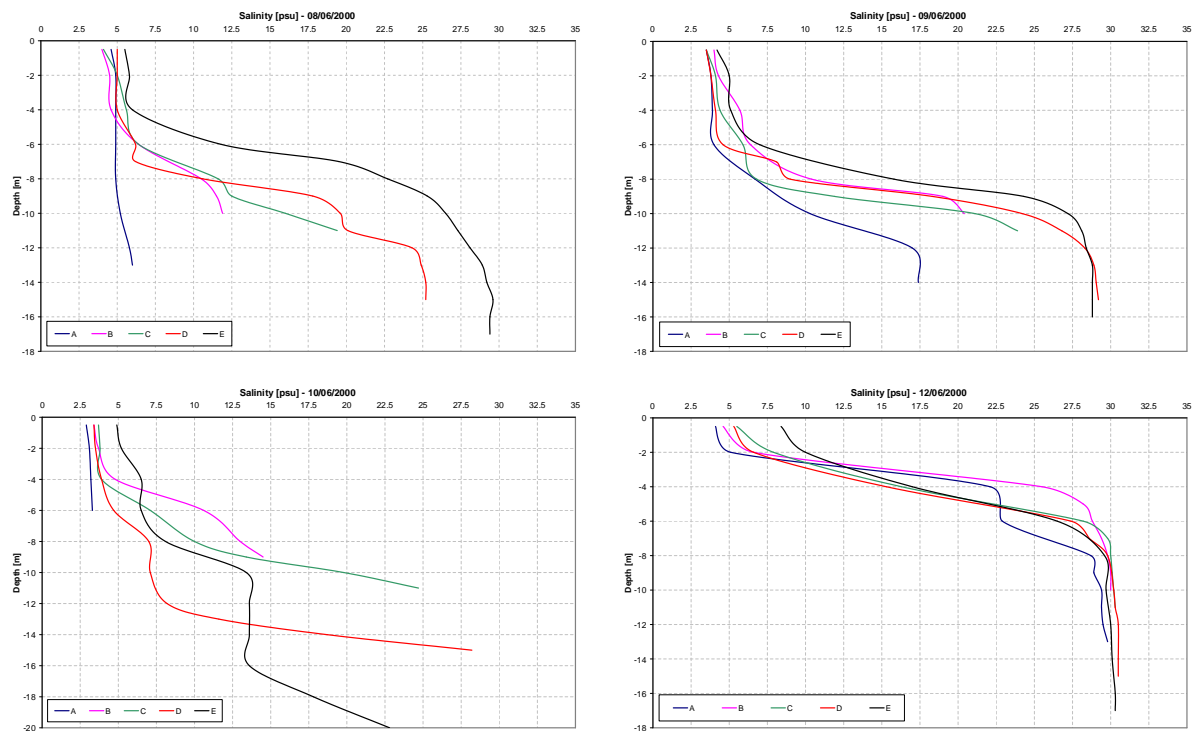


Figure 7: The upper graphic is the measured water elevation in station Praticagem and New Port. The second one is the measured wind in station Praticagem. The third one is the flux through the sections A, B, C, D and E. The fourth one is the suspended matter in the same sections before. And the last one is the discharges of the Camaquã and Guaíba rivers.

Unfortunately, for this data set there are no water level measurements in the coast, so it is not possible to mention about the pressure gradient between the lagoon and the coast. But still it is possible to check the behavior of the system for this short period. Comparing the wind against the sections flux, it is noticeable that the wind drives the ebb and flood. From the day 10 to 20/06, when the wind is blowing from NE an ebb flux is generated. The opposite cause occurs during SW winds. But for the period of 07-09/06 the mean flow is oceanwards despite the occurrence of some SW winds.

As mentioned in chapter 3.1., SW winds rules the salinity intrusion, and it is shown again in Figure 8. During the day 08/06, the SW winds promote the intrusion of the salinity below the fresh water layer, exhibiting a halocline between 4 and 10 meters depth. And during the next day, N winds are blowing and ebb is dominant, so a decrease in the halocline is noticeable from 4 to 6 and up to 10 meters depth. The graphic for the day 12/06 shows again the salinity intrusion, it is due to the consequence of the SW winds turning to NE winds in the day before and it is possible to check in the sections flux graphic, as the lines are decreasing.



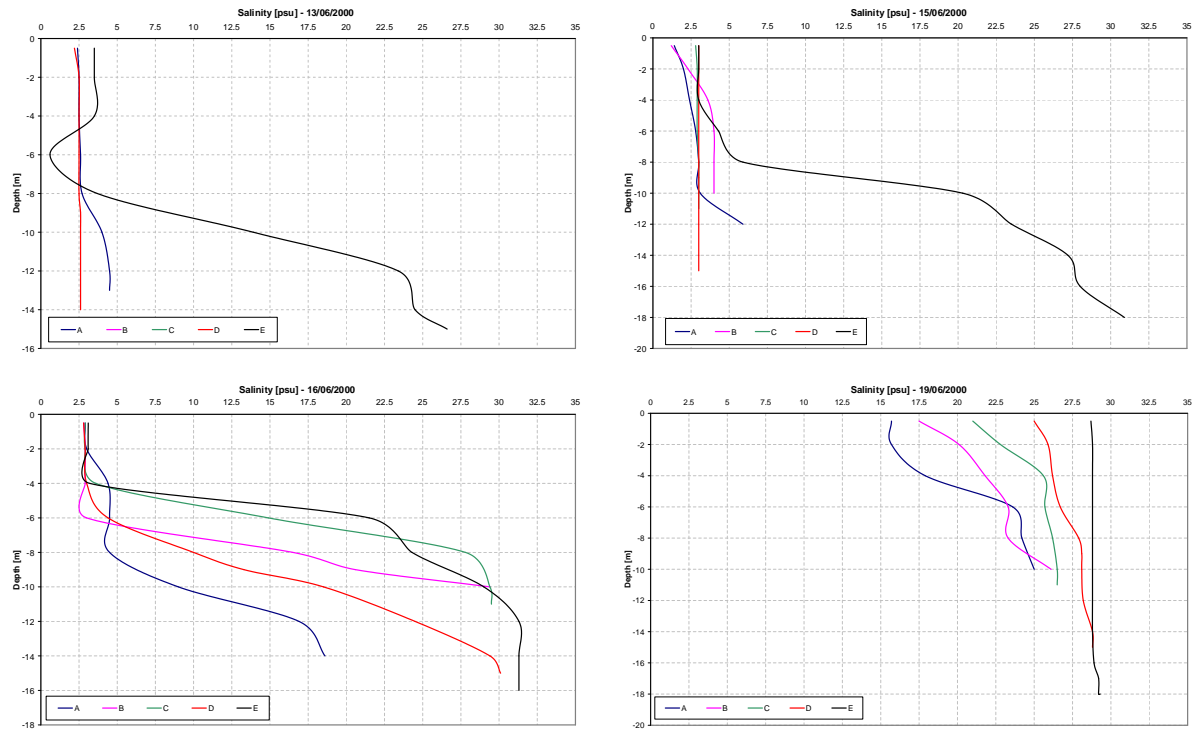


Figure 8: Measured salinity profiles for the period in the middle of each section.

4. Delft3D-Flow Module

4.1. Grid

A grid of finite difference quadrangular elements was created for the entire lagoon and for part of the inner shelf, reaching 50 meters depth. In order to save some computational time, the grid was built in different density. Coarser elements with sizes of 2700 x 5500 to 3100 x 5700 m² and smaller elements with sizes of 150 x 700 to 1500 x 1500 m² were implemented inside the lagoon and, estuary and inner shelf, respectively (Figure 9).

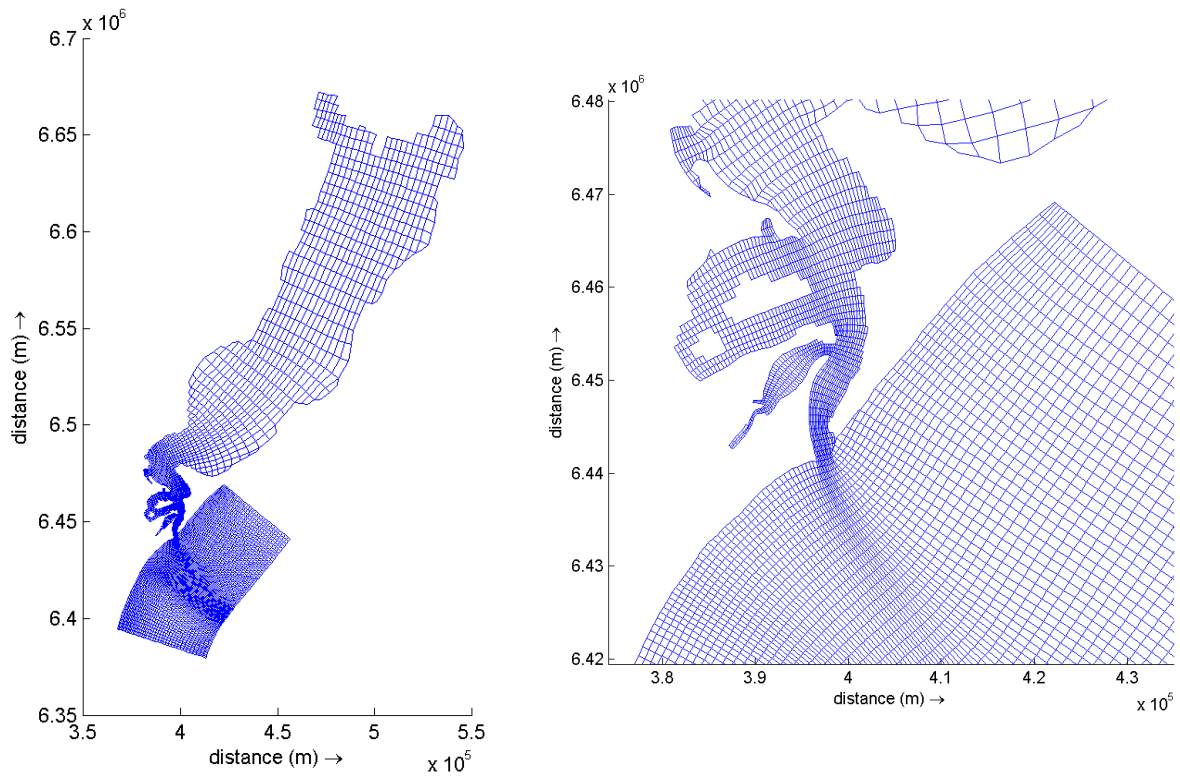


Figure 9: Grid used in the model. Refined elements in the estuary and coast areas.

4.2. Bathymetry

Nautical charts from the Hydrographical and Navigational Department of the Brazilian Navy (DHN) were used in order to specify the bottom boundary condition. The charts were digitalized using Golden Software Surfer 8 and each bathymetry point was correlated with its UTM coordinates.

The nautical charts used were:

- # 2100: Costa Sul: de Mostardas a Rio Grande, scale 1:269516;
Published in 31/10/1964. Reviewed in 15/10/1999; bathymetry related to the mean low-water spring tide;
- # 2112: Costa Sul: de Rio Grande a Feitoria, scale 1:80000;
Published in 21/03/1965. Reviewed in 30/09/2000; bathymetry related to the mean of the low-water levels;
- # 2140: Costa Sul: Lagoa dos Patos, scale 1:271653;
Published in 28/09/1965. Reviewed in 30/09/2000; bathymetry related to the mean low-water spring tide.

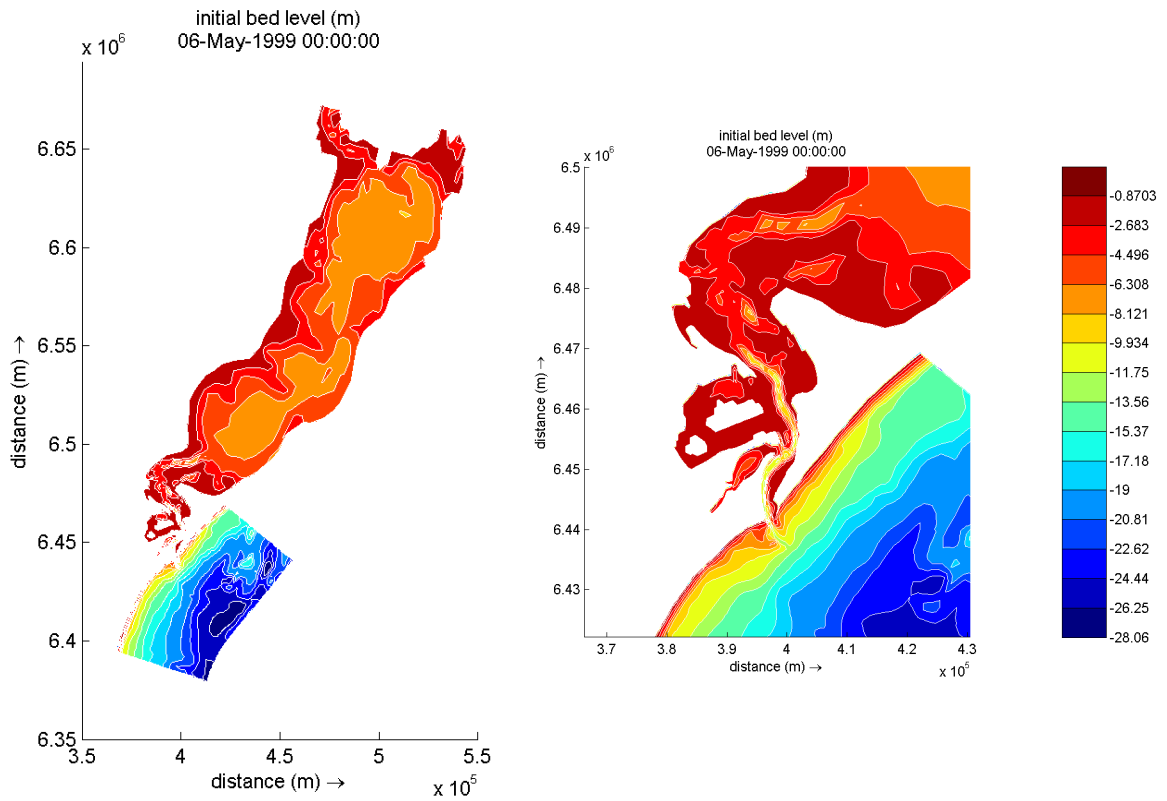


Figure 10: Bathymetry of the domain generated from the interpolation of the digitalized nautical charts.

4.3. Water Elevation

The water elevation used in the model was created from the sum of two time series of water elevation. One of them was generated from FES99 tidal constituents (as the astronomical tide) and the other one was removed from the measured water elevation in station Praticagem by the use of the Thompson filter (Thompson, 1983) (as the meteorological tide). The hourly measured water elevation data used in the model were kindly given by LOCFIS/FURG/RS/Brazil and is made of 5 months of water elevation measured in 4 stations which 3 are inside the main lagoon and the other one is inside the estuary close to the jetties.

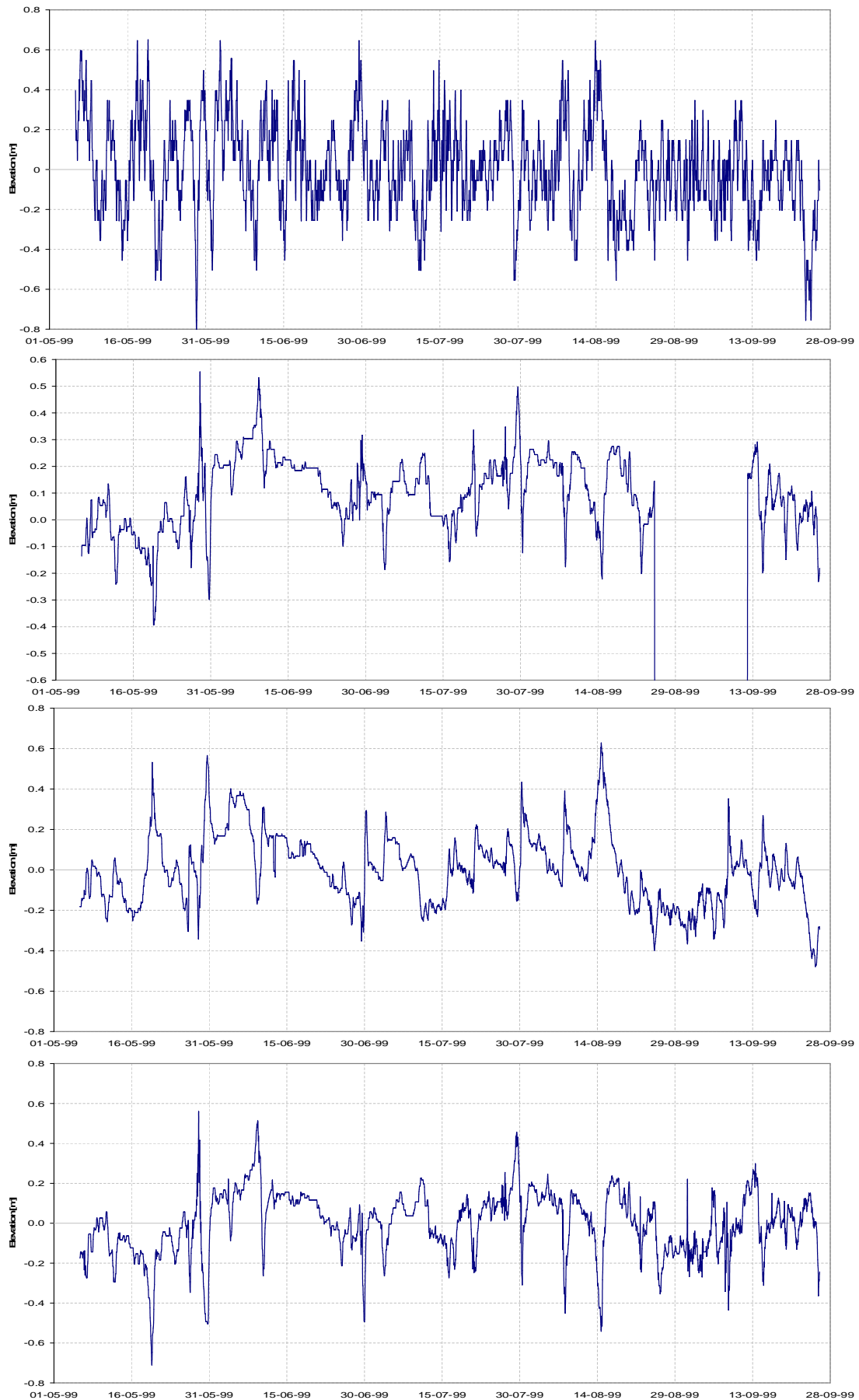


Figure 11: Water elevation measured at stations: Praticagem, Bojuru, Itapuã and São Lourenço.

4.4. Winds

A measured wind data set was used as constant for over the entire domain and varying in time. This data set is built of hourly wind direction and intensity measured at station Praticagem. From Figure 13 it is possible to observe the dominance of NE winds for this period.

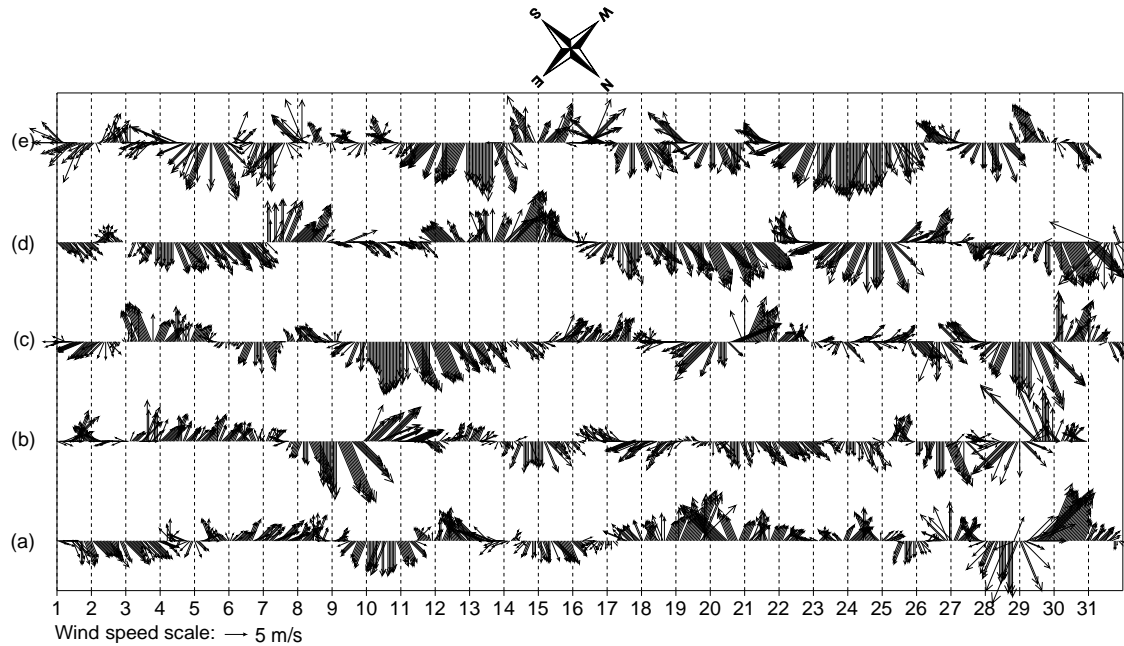


Figure 12: Wind speed and direction measured at station Praticagem used in the model. The letters means: (a) May, (b) June, (c) July, (d) August and (e) September. The vectors were rotated in order to NE and SW winds match the main axis of the lagoon. NE winds are vertically downwards and SW vertically upwards. X axe is in days.

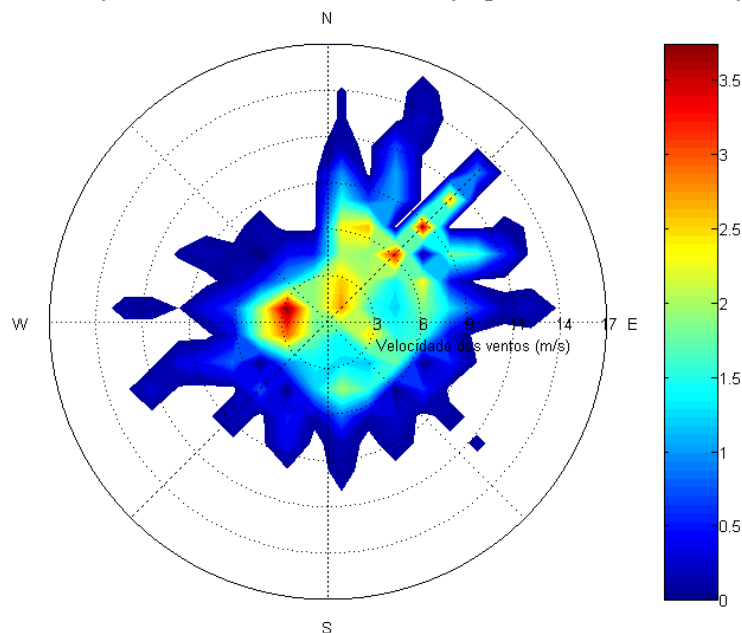


Figure 13: Rose of the wins for the period. The color bar is the frequency of occurrence in percentage. The circles represent the speed in m/s.

4.5. River Discharges

The river discharges were obtained from the Brazilian Water National Agency (ANA) website. Two data sets of daily measured river discharges were used: one for the Camaquã river and the other one for Guaíba river (Figure 14). A constant 200 m³/s discharge was described for the São Gonçalo Channel.

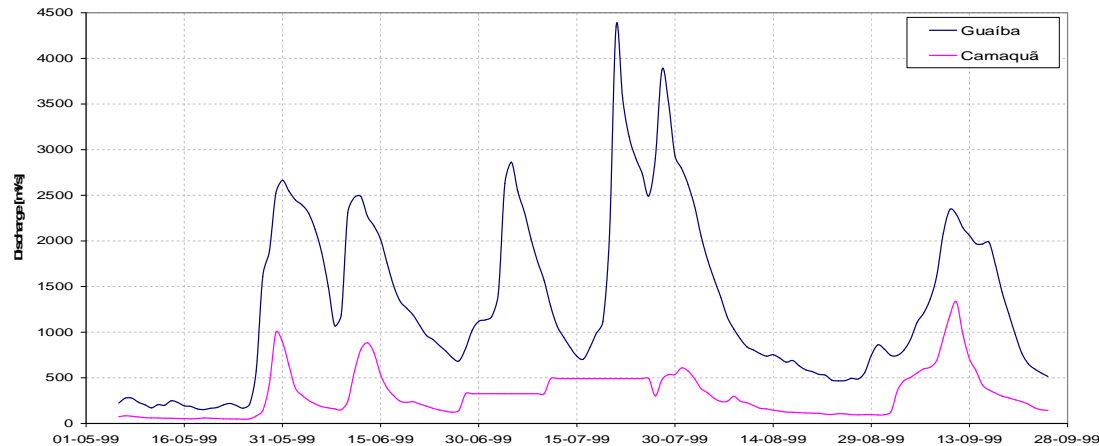


Figure 14: Guaíba and Camaquã river discharges used in the model.

5. Calibration

The calibration process was performed in order to increase the accuracy of the model against measured data. Comparison of modeled water elevation, current and salinity were done against measured data at station Praticagem. The water elevation comparison process was done for the whole period of simulation. The data set of measured salinity and currents were available just for few days, from the day 02/08/1999 to 10/08/1999. Currents and salinity were measured in two different depths, one at 3 and the other at 10 meters depth. The calibration process was done in two ways: first, three water elevation time series in the open boundary condition were tested in order to reproduce the measured data and second, varying roughness frictional law, roughness coefficients and horizontal diffusivity in order to get the best reproduction for currents and salinity.

5.1. Water Elevation

The water elevation calibration process started from the question: what can we specify in the ocean boundary condition so that we can simulate the measured data in station Praticagem, since there is no measured water elevation in the inner shelf for this period? So, in order to answer this question, we tried to adjust the water elevation

time series in the ocean boundary condition so that we could reproduce the measured water elevation at station Praticagem, or at least, reach the best fitting.

The ocean boundary condition was prescribed with the sum of two water elevation time series: one generated from FES99 tidal constituents (astronomical tide) and another of meteorological tide.

The astronomical tide was generated by the use of T_Tide toolbox tidal analyses (Pawlowicz et al, 2002) in Matlab interface using FES99 tidal constituents. The global tide finite solution FES99 (Lefèvre et al, 2002) is the last of four generation of the FES models, it is a improved version of the global hydrodynamics tide solutions, that is based on the resolution of the tidal barotropic equations on a finite element grid without any open boundary condition. This last version was improved by assimilating about 700 tide gauges and 687 TOUPEX/Poseidon (T/P) altimetric measurements in order to increase the accuracy of the tide solutions in the deep ocean and along the coastlines. The FES99 is available on a 0.25° x 0.25° grid, in each point the amplitude and phase of the eight constituents of the tidal spectra are given. The eight constituents used are M2, S2, N2, K2, P1, Q1, K1 and O1.

From the FES99 results close to the open boundary, the amplitude and phase values were interpolated to the open boundary nodes (Figure 23 to Figure 30). A good agreement between the amplitudes and phases of the FES99 constituents and the harmonic analysis of the measured water elevation was acquired (Table 3).

<i>Tide</i>	<i>Freq</i>	<i>Amp (m)</i>	<i>Amp_Err</i>	<i>Phase (°)</i>	<i>Pha_Err</i>	<i>SNR</i>
MM	0.001512	0.0027	0.039	188.04	269.3	0.0047
MSF	0.002822	0.0413	0.054	83.15	91.84	0.59
ALP1	0.034397	0.0076	0.011	272.34	87.58	0.52
2Q1	0.035706	0.0089	0.012	164.98	79.78	0.6
*Q1	0.037219	0.0248	0.013	80.09	30.63	3.8
*O1	0.038731	0.1099	0.013	102.04	7.4	67
*NO1	0.040269	0.0129	0.011	28.84	59.24	1.3
*K1	0.041781	0.0553	0.011	167.61	12.6	26
J1	0.043293	0.0051	0.009	123.17	129.02	0.33
OO1	0.044831	0.0061	0.013	274.1	146.85	0.22
UPS1	0.046343	0.0049	0.013	56.36	162.39	0.15
EPS2	0.076177	0.0015	0.006	175.2	181.61	0.059
MU2	0.07769	0.0037	0.006	269.88	113.31	0.38
*N2	0.078999	0.0404	0.007	255.37	11.85	36
*M2	0.080511	0.0243	0.007	286.2	18.75	11
L2	0.082024	0.0055	0.007	34.95	70.25	0.71
*S2	0.083333	0.0365	0.007	119.54	13.64	25
ETA2	0.085074	0.0018	0.007	143.32	192.5	0.056
MO3	0.119242	0.0025	0.004	128.36	134.06	0.33
*M3	0.120767	0.0067	0.006	276.52	46.36	1.4

*MK3	0.122292	0.0059	0.005	93.09	65.45	1.3
*SK3	0.125114	0.0071	0.006	114.58	49.76	1.5
*MN4	0.159511	0.0177	0.008	207.15	24.79	4.6
*M4	0.161023	0.0331	0.007	242.37	11.5	20
SN4	0.162333	0.0013	0.005	206.77	213.15	0.07
*MS4	0.163845	0.0109	0.007	319.39	41.34	2.2
S4	0.166667	0.0017	0.005	52.42	196.05	0.1
2MK5	0.202804	0.0016	0.003	164.96	124.28	0.29
2SK5	0.208447	0.0033	0.003	100.35	72.41	0.9
2MN6	0.240022	0.003	0.003	352.06	69.77	0.97
M6	0.241534	0.0016	0.003	101.24	110.53	0.27
*2MS6	0.244356	0.004	0.004	113.48	43.84	1.1
2SM6	0.247178	0.0014	0.003	216.91	152.99	0.23
3MK7	0.283315	0.0013	0.002	133.4	117.19	0.47
M8	0.322046	0.0003	0.001	69.89	214.23	0.033

Table 2: Harmonic analysis results made using T_Tide tool box.

Harmonic Analysis of the measured data in station Praticagem					
constituents	amp (m)	amp_err	phase (°)	pha_err	snr
Q1	0.0248	0.0130	80.09	30.63	3.8
O1	0.1099	0.0130	102.04	7.40	67
K1	0.0553	0.0110	167.61	12.60	26
N2	0.0404	0.0070	255.37	11.85	36
M2	0.0243	0.0070	286.20	18.75	11
S2	0.0365	0.0070	119.54	13.64	25
FES99 - at the ocean side of the model, perpendicular to the coast at the location of the jetties					
constituents	amp (m)	amp_err	phase (°)	pha_err	snr
Q1	0.0302	-	78.51	-	-
O1	0.1106	-	104.32	-	-
K1	0.0665	-	165.70	-	-
N2	0.0701	-	264.15	-	-
M2	0.0381	-	281.39	-	-
S2	0.0679	-	111.48	-	-
Absolute Difference					
constituents	amp (m)	amp_err	phase (°)	pha_err	snr
Q1	0.0054	-	1.58	-	-
O1	0.0007	-	2.28	-	-
K1	0.0112	-	1.91	-	-
N2	0.0297	-	8.78	-	-
M2	0.0138	-	4.81	-	-
S2	0.0314	-	8.06	-	-

Table 3: Comparison of the harmonic analyses and FES99 constituents used in the model.

Furthermore, time series were generated by the use t_predic , one of the tools that come with T_Tide, using the FES99 constituents for each open boundary section.

The measured water elevation in station Praticagem contains both the astronomical and meteorological tides since it is located close to the mouth. A Thompson filter was evaluated to remove high frequencies (less than 1 day of period) from the time series, generating the meteorological tide time series. One important mark is when performing the Thompson filter, 240 data are lost what in this case was 10 days (5 days in the beginning and 5 in the end of the series) in 5 months. Due to its location, which is inside the estuary and close to the mouth, this signal had been suffered attenuation (Fernandes et al, 2004b) and it could not be used directly as ocean boundary condition. So, a model (run009) was performed to estimate the amplification factor of the meteorological tide so that when applied in the open boundary, it could reproduce the measured water elevation. Spectra analyses were performed to compare both time series (measured and modeled) at station Praticagem. Three different factors (Figure 16 to Figure 19) were calculated, and the best one that fitted the measured data was on Figure 19.

In accordance to Zavialov et al (2002), that deployed a current meter in a depth of 50 meters in the inner shelf from the day 4 of march till 2 of august of 1997, through spectra analyses of the measured currents in four different bands, showed that the major part of the kinetic energy (59-51%) resides at periods between 2 and 10 days, associated with meteorological forcing, a considerable part of the energy corresponds to periods longer than 10 days (33-23%), and the diurnal and semi-diurnal bands are the least energetic ones, accounting together 8-26% of the energy. Each value-pair is respectively for the along and cross-shore components of the current. Maximum values of the along-shore currents are 1.21 N and 0.73 S m/s, and for the cross-shore are 0.58 W and 0.43 E m/s.

That is why is important to add the meteorological tide from the filtered water level at station Praticagem, since the meteorological tide is important to reproduce the hydrodynamics of the Patos Lagoon estuary, is also important to simulate the currents in the inner shelf, if there was no meteorological tide in the open boundary, the velocities in the inner shelf would be underestimated, since we don't have any measured data from the coast so that a comparison could be done.

5.2. Currents and Salinity

After calibrated the open boundary water elevation time series, the currents and salinity calibration process were done. Several tests were performed varying the

bottom frictional law and the roughness coefficient, and also the horizontal diffusivity. First of all, three models (run020, run021 and run022) were performed with different bottom frictional law, using the same values that Fernandes et al (2002) did (Figure 31, Figure 32 and Figure 33). The best result obtained was using the White-Colebrook.

Then, in order to improve the model results, 12 new models (run022 to run033) were performed with 6 different coefficient values ($k = 0.001, 0.005, 0.008, 0.01, 0.015$ and 0.05 m) with and without the influence of the São Gonçalo Channel (SGC) discharges. The aim of performing the models without the São Gonçalo channel discharge was to verify its influence in the salinity time series at station Praticagem. The results are shown in Figure 33 to Figure 44. The upper graphic of each figure is the comparison between measured and modeled water elevation, the second is the currents, the third the salinity, the fourth wind speed and direction and the last one is the sum of Camaquã and Guaíba rivers discharges.

In order to help the results analyses, correlation coefficients for water elevation, current and salinity were calculated. The correlation coefficient was evaluated for the same period of the measured data available, hence, for the water elevation, 5 months of measured and modeled data were used, but for current and salinity only the short period from 02/08/1999 to 10/08/1999 was used. For both current and salinity, two data sets are available, one measured in 3 and other in 10 meters depth. So, the correlation was performed using the average of these two depths since it is a depth-averaged model (Table 4).

Table of correlation coefficients			
Model	Salinity	Current	Water Elevation
<i>run022</i>	0.9239	0.9088	0.9055
<i>run023</i>	0.9239	0.9000	0.9060
<i>run024</i>	0.9108	0.8794	0.9064
<i>run025</i>	0.9219	0.9139	0.9052
<i>run026</i>	0.9128	0.9290	0.9037
<i>run027</i>	0.9184	0.9240	0.9050
<i>run028</i>	0.9239	0.9079	0.9066
<i>run029</i>	0.9199	0.8993	0.9071
<i>run030</i>	0.9156	0.8929	0.9073
<i>run031</i>	0.9006	0.8685	0.9074
<i>run032</i>	0.9243	0.9059	0.9057
<i>run033</i>	0.9217	0.9024	0.9070

Table 4: Table of correlation coefficients for the calibration process.

After the results analyses, the best ones were those that the roughness coefficient was set to 0.005 m. Both of the water elevation and the current seem to have a good agreement to the measured data, but salinity doesn't. In spite of the high correlation coefficient, in the end of the time series, when measured homogenous salinity is achieved, the model can't reproduce it. Hence, the horizontal diffusivity was changed. Eleven more models (run034 to run047) were evaluated varying the diffusivity from values of 100 m²/s to 1000 m²/s. The horizontal diffusivity was prescribed as varying in space, i.e., a different value for the estuarine area and for the rest of the domain was specified. The roughness frictional law and the Nikuradse coefficient were set to White-Colebrook and 0.005 m, respectively. The results for the short period of measured current and salinity available are shown in Figure 45 to Figure 61. In Figure 59 it is shown the result of the model with 400 m²/s constant diffusivity for the entire domain. This was necessary because while running the sediment transport model, some anomalies appeared in the limits of the prescribed diffusivity area. The best fit to the measured data were achieved with model run045, where the horizontal diffusivity was set to 400 m²/s (Figure 56).

In Figure 62 and Figure 63, the results of the calibration process for the three dimensional module is presented. The model was set to a 10 sigma-layers. The second one showed a improve in the salinity measurements, but the stratification still high in comparison to the observed data.

The list of all models performed for the tests are showed above:

Depth-Averaged Hydrodynamic Models												
Model Number	Open Boundary	t _{predic}	Discharges			Wind	Initial Condition Salt		Roughness		Horizontal Diffusivity	
			GB	CQ	SGC		Lagoon	Ocean	Law	Coef	Estuary	Domain
009	Orig Meteo	N	Y	Y	Y	Y	0	0	C	65	10	10
011	N	N	N	N	N	Y	0	0	C	65	10	10
016	v1 Meteo	N	Y	Y	Y	Y	0	35	C	65	10	10
017	v2 Meteo	N	Y	Y	Y	Y	0	35	C	65	10	10
018	v3 Meteo	N	Y	Y	Y	Y	0	35	C	65	10	10
019	v3 Meteo	N	Y	Y	Y	Y	0	35	C	50	10	10
020	v3 Meteo	Y	Y	Y	Y	Y	0	35	C	50	10	10
021	v3 Meteo	Y	Y	Y	Y	Y	0	35	Mn	0.025	10	10
022	v3 Meteo	Y	Y	Y	Y	Y	0	35	W-C	0.01	10	10
023	v3 Meteo	Y	Y	Y	Y	Y	0	35	W-C	0.005	10	10
024	v3 Meteo	Y	Y	Y	Y	Y	0	35	W-C	0.001	10	10
025	v3 Meteo	Y	Y	Y	Y	Y	0	35	W-C	0.015	10	10
026	v3 Meteo	Y	Y	Y	Y	Y	0	35	W-C	0.05	10	10
027	v3 Meteo	Y	Y	Y	N	Y	0	35	W-C	0.05	10	10
028	v3 Meteo	Y	Y	Y	N	Y	0	35	W-C	0.015	10	10

029	v3 Meteo	Y	Y	Y	N	Y	0	35	W-C	0.008	10	10
030	v3 Meteo	Y	Y	Y	N	Y	0	35	W-C	0.005	10	10
031	v3 Meteo	Y	Y	Y	N	Y	0	35	W-C	0.001	10	10
032	v3 Meteo	Y	Y	Y	Y	Y	0	35	W-C	0.008	10	10
033	v3 Meteo	Y	Y	Y	N	Y	0	35	W-C	0.01	10	10
034	v3 Meteo	Y	Y	Y	N	Y	0	35	W-C	0.005	100	10
035	v3 Meteo	Y	Y	Y	N	Y	0	35	W-C	0.005	150	10
036	v3 Meteo	Y	Y	Y	N	Y	0	35	W-C	0.005	200	10
037	v3 Meteo	Y	Y	Y	N	Y	0	35	W-C	0.005	300	10
038	v3 Meteo	Y	Y	Y	N	Y	0	35	W-C	0.005	400	10
039	v3 Meteo	Y	Y	Y	N	Y	0	35	W-C	0.005	500	10
040	v3 Meteo	Y	Y	Y	N	Y	0	35	W-C	0.005	600	10
041	v3 Meteo	Y	Y	Y	N	Y	0	35	W-C	0.005	700	10
042	v3 Meteo	Y	Y	Y	N	Y	0	35	W-C	0.005	800	10
043	v3 Meteo	Y	Y	Y	N	Y	0	35	W-C	0.005	900	10
044	v3 Meteo	Y	Y	Y	N	Y	0	35	W-C	0.005	1000	10
045	v3 Meteo	Y	Y	Y	Y	Y	0	35	W-C	0.005	400	10
046	v3 Meteo	Y	Y	Y	Y	Y	0	35	W-C	0.005	500	10
047	v3 Meteo	Y	Y	Y	Y	Y	0	35	W-C	0.005	600	10
048	v3 Meteo	Y	Y	Y	Y	Y	0	35	W-C	0.005	400	400
049	v3 Meteo	Y	Y	Y	Y	Y	0	35	W-C	0.005	300	300
050	v3 Meteo	Y	Y	Y	Y	Y	0	35	W-C	0.005	200	200

Table 5: Table of depth-averaged models evaluated for the work. Y = included; N = excluded; GB = Guaíba; CQ = Camaquã; SGC = São Gonçalo Channel; C = Chezy; Mn = Manning and W-C = White-Colebrook.

6. Behavior of the system

The behavior of the system was analyzed performing different tests with different forcings. All the forcing used was measured field data. The eigen frequency of the lagoon and the response of the hydrodynamics to the different forcings were analyzed. Measured wind speed and direction, measured river discharges, modeled water elevations from two stations, one close to Ponta da Feitoria area and the other in the mouth, and modeled cumulative discharge through the mouth were used.

One of the first tests done was to check the eigen frequency of the lagoon as mentioned and modeled by Moller et al (1996). Moller et al (1996) found a 20 hours of natural oscillation of the lagoon. So, one model was performed taking into account a constant NE wind with 7.5 m/s of speed (run_011). No river discharges and neither tide were considered. This 7.5 m/s of wind speed was used as average of the measured NE winds for the period of may to september of 1999 (Figure 13).

The simulation time was described for two months, starting on 01st of january and stopping on 01st of march, but the wind was prescribed to stop acting after the first month. In order to make easy the identification of the eigen frequency, a

transect through the lagoon was generated and the results of water elevation were plotted. In Figure 20 results for the last moment of wind action (a), 24 hours (b) and two week (c) after wind stop and the last time of simulation (d) are presented.

It is noticeable the pilling up of water in Ponta da Feitoria and a decrease of the water level in the north part of the lagoon (red line in Figure 20 (a)), these is due to the NE wind that blows parallel to the main axis of the lagoon. When looking to the green line, a decrease of the water level in the coast is shown due to the Ekman's transport that deflects the flow to the left, i.e., when NE winds are blowing a set down in the coast is expected. 24 hours after the wind stop, the same configuration still presented. No oscillation were found and so the eigen frequency either (Figure 20 (b)). Two weeks after the wind stop till the end of the simulation, the system is trying to come back to its initial level (Figure 20 (c) and (d)).

The model was not able to reproduce the eigen frequency of the system. A good reason for this behavior is that the grid elements inside the lagoon are too coarse to reproduce it. So, one should make a more refined grid elements and repeat the test. After the calibration process, the cumulative discharge through the mouth and a water elevation comparison between two stations were analyzed against measured wind and river discharges. The results are shown in Figure 21.

It is important to mention that the model started at 06th of may and stopped at 26th of september due to the 5 first and last days of water elevation lost to Thompson filter. From the Figure 21, it is possible to check the influence of the river discharges in the outflow mechanism. During the first month of simulation, the rivers discharges are low and the dominant wind is SW and its consequence is an average inflow. The first green balloon draw on the cumulative discharge graphic shows a huge inflow through the mouth and it is directly correlated to SW winds that promote a pressure gradient oceanwards with consequence to an inflow. This pressure gradient can be seen in the second graphic of Figure 21. This scenario starts to change after 10 days from the increasing of rivers discharges.

From the 5th until the 10th day of june, there is a big outflow going on. When looking for the same period to the wind data, from 5th to 7th of june SW winds are blowing but an outflow is shown. This behavior could be explained by the higher rivers discharges occurred 10 days before. After that period NE winds take place till the day 10. From the water elevation graphic it is noticeable a small pressure gradient for the period of 5 to 7 of june (30 cm), but during NE winds the gradient increases to

120 cm. This high value could be the consecutive NE winds and high river discharges actions. This immediately reaction of the system due to change in wind direction is in accordance to Fernandes (2001).

Some others periods of NE and SW winds are marked with blue and green balloons in Figure 21. The highest outflow found was between the day 16 and 22 of august. This higher event was generated from the long period of NE winds (6 days) blowing on the lagoon. During this long NE wind action, it could also be associated to the higher rivers discharges occurred few days ago. It is noticeable that the estuary area, mainly in the main canal, the water is completely fresh (Figure 22d).

These big outflows play an important rule in relation to the salinity intrusion. In Figure 22 it is shown four salinity patterns under NE winds and SW winds. Two of them (a) and (b) are related to the highest inflows (28-30/06 and 12-16/08) and the others two are related to the highest outflows (10-13/07 and 16-22/08). In the inflow figures (a) and (b), the lower salinity that goes to the north in the coast is caused by a previous outflow, which decreases the salinity in the coast, associated to SW winds, which drive this lower salinity mass of water northwards.

The residence time of the lagoon is the time required to replace the existing volume of freshwater at a rate equal to the river discharge (Dyer, 1997 in Fernandes et al, 2002). If the initial volume of the lagoon, not taking into account the inner shelf, was the same volume calculated by Fernandes et al (2002) ($V_o=58547.27 \times 10^6 \text{ m}^3$) and taking the average of the sum of the rivers discharges as $2000 \text{ m}^3/\text{s}$, the residence time would be 340 days. Similar result is achieved when dividing the initial volume of the lagoon by the last value of the cumulative discharge through the mouth (Figure 21) and then multiplies it by the number of simulated days.

7. Delft3D-Flow Module with Cohesive Sediment

In order to characterize the cohesive sediment transport to the coast, the cohesive sediment transport as a constituent of the hydrodynamics was used. First of all, after the whole process involving the hydrodynamics, the best modeled hydrodynamics was chosen (model run045). But due to the kind of horizontal diffusivity prescription, some anomalies occurred in the coastal area. So, new models with $400 \text{ m}^2/\text{s}$ of diffusivity for the whole domain (run048_Sed) were evaluated.

As there is no sediment data for this period, some parameters were chosen in accordance to previous works executed in the area and a small data of suspended matter concentration from the Brazilian Water National Agency (ANA) website.

To prescribe the inputs of suspended matter for the rivers, data from the ANA website and Hartmann et al (1990) were used. From Hartmann et al (1990c), that during 15 hours of observations (before and during a cold front) at the mouth of São Gonçalo Channel, the concentration of the suspended matter increased from 75 to 320 mg/l in 5 hours, so, the concentration of 80 mg/l was chosen to use in the model as an average for this contribution since 320 mg/l was observed as a extreme value for a non-dominant event. From the ANA website data (Figure 15) the concentration for the Camaquã river was chosen between three data observed for the period of simulation (may, july and september of 1999); the concentration of 50 mg/l was used. But for the Guaíba river there was no enough data, so, in accordance to Hartmann et al (1990b) that said that the Guaíba river is the most important in sediment contribution to the lagoon, its value was set to 100 mg/l.

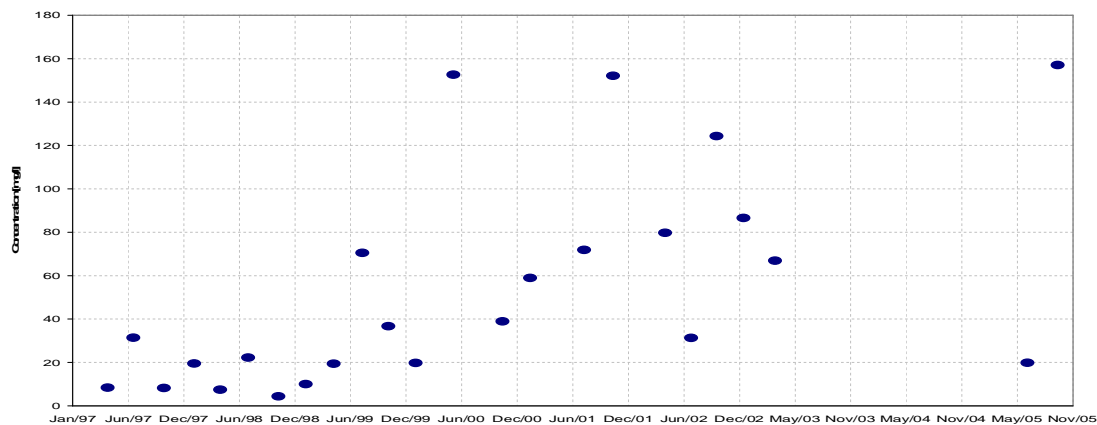


Figure 15: Suspended matter from ANA website data for the Camaquã river. The concentration for the Camaquã river was chosen to 60 mg/l as a mean value of the may, july and october/99 data.

The settings used were prescribed to make the sediments to deposit in the coastal zone, so the critical shear stress for sedimentation was set to 1000 N/m^2 . Both the settling velocity and the critical shear stress for erosion were varied (0.0003 and 0.0006 m/s and 0.1 and 0.5 N/m^2). See Table 6 for the complete settings. The results of these for models are shown in Figure 64. It seems that when increasing the erosion shear stress from 0.1 to 0.5 N/m^2 , there is no bank formation in front Cassino beach for both settling velocity. But these patterns could be changeable due to changes in diffusivity coefficient. The models used were all set to $400 \text{ m}^2/\text{s}$ for the whole domain. Hence, four new models (run048_Sed_045 to run048_Sed_048) were

evaluated using a constant diffusivity for the whole domain equal to $10 \text{ m}^2/\text{s}$. The others settings used were the same as the last four models. The results are presented in Figure 65. The results showed a more widespread southward mud bank from the jetties than in the last models. Still, when using critical shear stress for erosion equal to 0.5 N/m^2 , there is no bank in front of Cassino beach, but in comparison to Figure 64 (b) and (c) there is more southward mass around the jetties. The results of models run048_Sed_045 and run048_Sed_047 are in accordance to Calliari et al (1993 & 2000), that said observed mud bank between 6 and 20 meters depth.

8. Conclusions and recommendations

- From the beginning of the work, from the first models only with wind action, it is noticeable the wind driving behavior of the system, as the tides are small (0.50 m in average). The mechanism of set up and set down in the lagoon and in the coast is mainly responsible for the exchange of waters between the lagoon and the coast. It is in accordance to Fernandes et al (2002 & 2004) and Moller et al (1996 & 2001).
- NE winds tend to pill up water in the south part of the lagoon while action on the coast promote a decrease of the water level due to the Ekman's transport, favoring a pressure gradient towards the estuary and a outflow is achieved. The same mechanism is valid to SW winds but in opposite direction. It is in accordance to Fernandes et al (2002 & 2004) and Moller et al (1996 & 2001).
- When performing the model with a constant NE wind during a month and then stops it, it was supposed that an eigen frequency of approximately 20 hours would be shown, but the model was not able to do it. There is an assumption that could explain that, it might be the coarser grid elements created inside the lagoon that it can not see it. So, for a first step, one should make a refined grid inside the lagoon and test it again.
- When including the river discharges to the only wind model, a big difference in the cumulative discharge through the mouth is noticeable and also the variation in water level inside the lagoon as in the estuary. While the winds are the mainly responsible for the set up/down mechanism, the discharges from the rivers are responsible to increase the pressure gradient between the lagoon and the coast favoring a dominating outflow. And they are also responsible to limit the penetration of saline water into the estuary.

- The use of FES99 constituents was very satisfactory since showed a small deviation from the harmonic analyses of the measured data from Praticagem. The harmonic analyses showed three quarter-diurnal constituents that summing those 6 cm of amplitude would be resulted. FES99 does not have those constituents and they were not considered in this work. It would be better if one could find some data to fill this blank in order to increase the accuracy of the open boundary time series.
- The use of Thompson filter (Thompson, 1983) to remove high frequencies (less than 1 day of period) in order to obtain a meteorological signal that could reproduce the remote wind action was a good tool. It is important to remind that when performing this filter, 240 data are lost.
- During the calibration process, the use of the *t_predic* tool from *T_Tide* (Pawlowicz et al, 2002) showed a great result in terms of water elevation in comparison to measurements done in station Praticagem. Correlation coefficients for water elevation of 0.60 were being calculated before its use and 0.91 after its use.
- Several tests were performed varying the bottom frictional law and roughness coefficient. While calibrating the currents the best bottom frictional law and roughness coefficient were achieved when using White-Colebrook and 0.005 m.
- For the salinity calibration, several models were executed varying the horizontal diffusivity in order to compare the average of the measured salinities in station Praticagem, since this is a depth-averaged model. First it was applied a space varying diffusivity and the best result was achieved using 400 m²/s. But this kind of prescription interfered in the sediment models. Furthermore, it was prescribed a constant diffusivity for the entire domain and the best one was achieved with 400 m²/s again, despite the higher salinity values when stratification occurs but fitted when homogeneous salinity was found.
- For the simulated period, the result showed a dominance of outflow due to the predominant NE winds and the residence time of the lagoon was calculated to 340 days.
- From the sediment models, when using a critical shear stress for erosion equal to 0.5 N/m², there is no mud deposition in front Cassino beach for both settling velocities tested.
- When decreased the horizontal diffusivity from 400 to 10 m²/s, a more widespread bank is observed in the model results.

9. References

- Calliari, L. J.; Gomes, M. E. V.; Griep, G. H.; Möller, O. O. (1980). Características sedimentológicas e fatores ambientais da região estuarial da Lagoa dos Patos. Anais do XXXI Congresso Brasileiro de Geologia, Balneário Camboriú, Santa Catarina, vol. 2: 862-875;
- Calliari, L. J.; Fachin, S. (1993). Laguna dos Patos. Influência nos depósitos lamíticos costeiros. Pesquisas vol 20 (1): 57-69, Instituto de Geociências, UFRGS, Porto Alegre, Rio Grande do Sul, Brasil;
- Calliari, L.; Sperranski, N. S.; Torronteguy, M.; Oliveira, M. B. (2000). The mud banks of Cassino beach, southern Brazil: characteristics, processes and effects. Journal of Coastal Research vol. ICS 2000 Proceedings: 318-325, Nova Zelândia;
- Caltabiano, A. C. V. (1994). Análise quali-quantitativa do material em suspensão no estuário da laguna dos Patos, RS. Monografia de Graduação, Departamento de Geociência, Laboratório de Oceanografia Geológica, FURG, Rio Grande, Rio Grande do Sul, Brasil, 50p.;
- Castelão, R. M.; Möller, O. O.; Fetter F, A. F.; Campos, E. J. D. (____). Dinâmica da Lagoa dos Patos (RS-Brasil) forçada por ventos. Submetido a edição especial do XII SNO, 10p.;
- Fernandes, E. H. L. (2001). Modelling the hydrodynamics of the Patos Lagoon, Brazil. Ph.D. Thesis, University of Plymouth, United Kingdom, 219p.;
- Fernandes, E. H. L.; Dyer, K. R.; Möller, O. O.; Niemcheski, L. F. H. (2002). The Patos Lagoon hydrodynamics during na El Niño event (1998). Continental Shelf Research vol. 22: 1699-1713;
- Fernandes, E. H. L.; Dyer, K. D.; Möller, O. O. (2004a). Spatial gradients in the flow of southern Patos Lagoon. Journal of Costal Research vol. 20: 102-112;
- Fernandes, E. H. L.; Marino-Tápia, I.; Dyer, K. D.; Möller, O. O. (2004b). The attenuation of tidal and subtidal oscillations in the Patos Lagoon estuary. Ocean Dynamics vol. 54: 348-359;
- Fernandes, E. H. L.; Monteiro, I. O.; Möller, O. O. (2004c). On the dynamics of Saco da Mangueira embayment – Patos Lagoon (Brazil). Submetido ao Journal of Coastal Research em dezembro de 2004, 14p.;
- Hartmann, C.; Silva, O. F. (1988). Dinâmica sazonal da pluma de sedimentos na desembocadura da laguna dos Patos, analisada através de imagens Landsat. IVO Simpósio Brasileiro de Sensoriamento Remoto, Natal, Rio Grande do Norte, 8p.;
- Hartmann, C.; Silva, O. F.; Mendes, C. A. B.; Haertel, V.; Nunes, J. C. (1990a). Estudo por sensoriamento remoto das “frentes” costeiras na região da desembocadura da laguna dos Patos, RS. VI Simpósio Brasileiro de Sensoriamento Remoto 24-29/06/1990, Anais vol. 3, Manaus, Amazônia;
- Hartmann, C.; Calliari, L.; Möller, O. O. (1990b). Material em suspensão no estuário da laguna dos Patos (RS) Fase I – Observações preliminares – Abril/1979 a Março/1980. Sociedade & Natureza, Uberlândia, vol. 2 (4): 73-95;

- Hartmann, C.; Harkot, P. F. C. (1990c). Influência do Canal São Gonçalo no aporte de sedimentos para o estuário da laguna dos Patos – RS. *Revista Brasileira de Geociências*, vol. 20 (1-4): 329-332;
- Hartmann, C.; Calliari, L. (1995). Composição e qualidade do material em suspensão durante alta turbidez na extremidade sul da laguna dos Patos, RS, Brasil. *Pesquisas* vol. 22 (1-2): 74-83, Instituto de Geociências, UFRGS, Porto Alegre, Rio Grande do Sul, Brasil;
- Lefèvre, F.; Lyard, F.H.; Le Provost, C. (2002). FES99: A global tide finite element solution assimilating tide gauge and altimetric information. *Journal of Atmospheric and Oceanic Technology* (September 2002), vol. 19, 1345-1356;
- Möller, O. O.; Lorenzzenti, J. A.; Stech, J. L.; Mata, M. M. (1996). The Patos lagoon summertime circulation and dynamics. *Continental Shelf Research* vol. 16 (3): 335-351;
- Möller, O. O.; Castaing, P. (1999). Hydrographical characteristics of the estuarine area of Patos Lagoon (30o S, Brazil). *Estuaries of South América (their Geomorphology and Dynamics) - Environmental Science*. Berlin: Springer, 83-100;
- Möller, O. O.; Castaing, P.; Salomon, J-C.; Lazure, P. (2001). The influence of local and non-local forcing effects on the subtidal circulation of Patos Lagoon. *Estuarine Research Federation* vol. 24, no 2: 297-311;
- Piola, A. R.; Matano, R. P.; Palma, E. D.; Möller, O. O. (2005). The influence of the Plata River discharge on the western South Atlantic shelf. *Geophysical Research Letters*, vol. 32, 4p.;
- Thompson, R. O. R. Y. (1983). Low-pass filters to suppress inertial and tidal frequencies. *American Meteorological Society*, vol. 13, no. 06 (june): 1077-1083;
- Zaviolov, P. O.; Möller, O. O.; Campos, E. (2002). First direct measurements of currents on the continental shelf of southern Brazil. *Continental Shelf Research*, 22, 1975-1986;
- Zaviolov, P. O.; Kostianoy, A. G., Möller, O. O. (2003). SAFARI cruise: mapping river discharge effects on Southern Brazilian shelf. *Geophysical Research Letters*, vol. 30, no. 21, 2126, 4p.;

10. Appendix

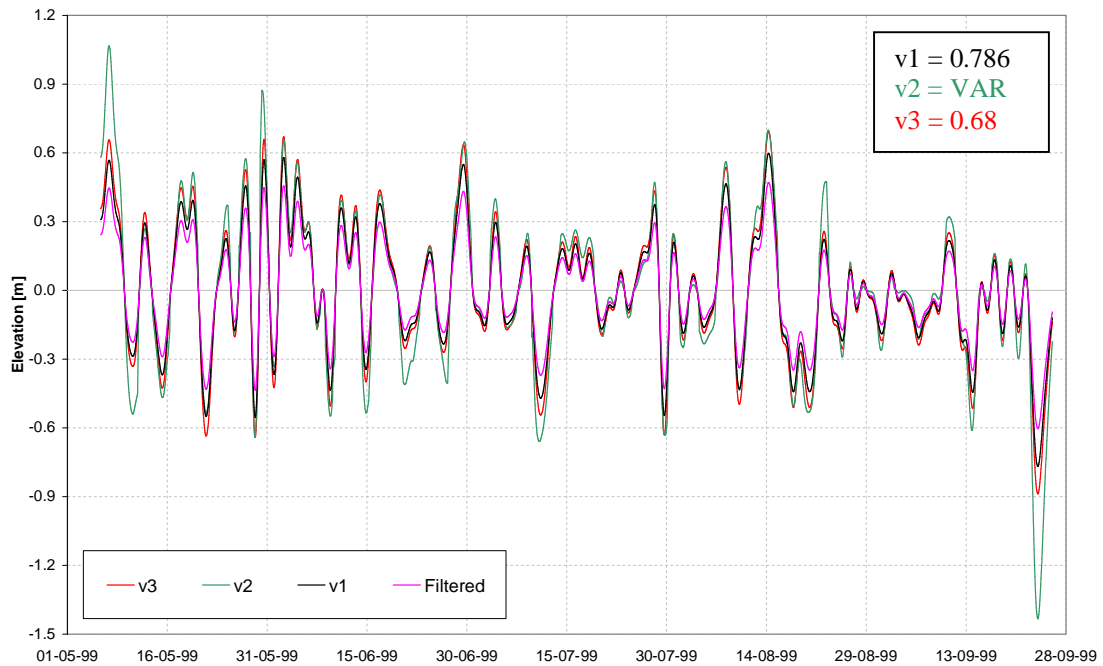


Figure 16: Amplified meteorological tide. Three different factors were used.

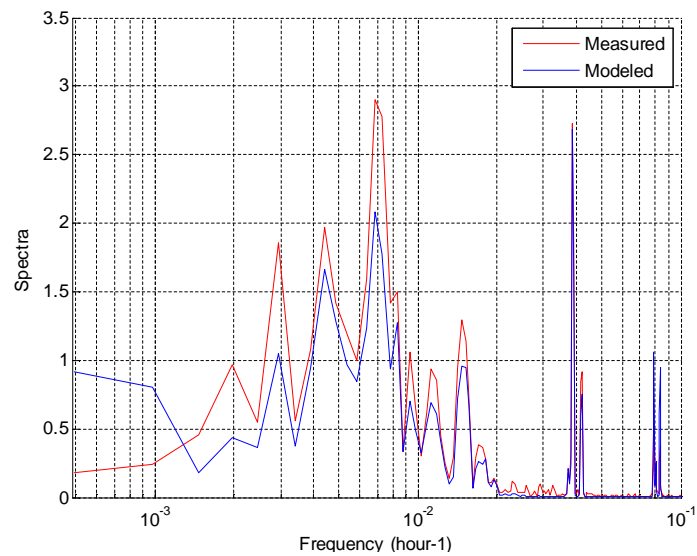


Figure 17: Water elevation spectral density at station Praticagem, using v1 amplification factor – run016. Ordinates in log scale.

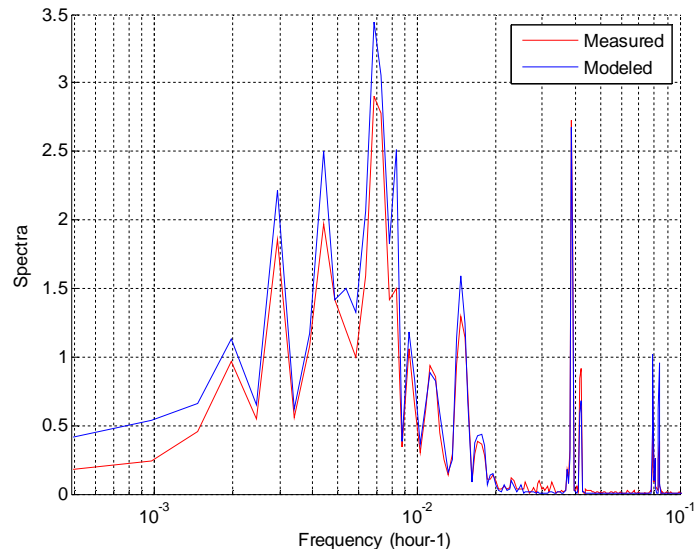


Figure 18: Water elevation spectral density at station Praticagem, using v2 amplification factor – run017. Ordinates in log scale.

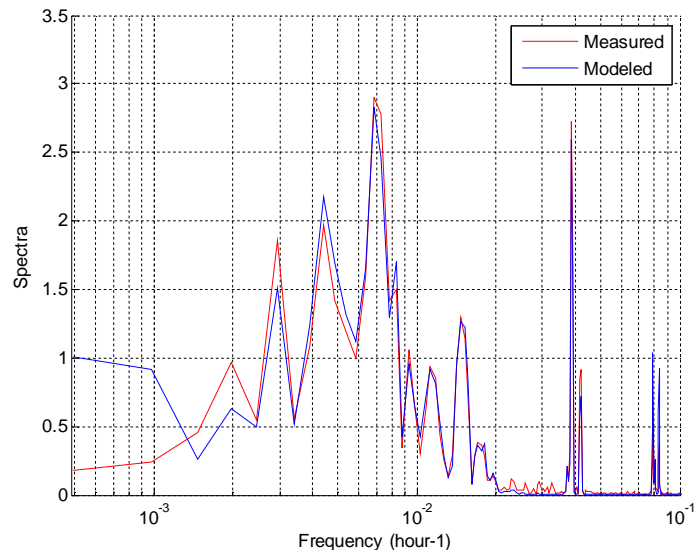


Figure 19: Water elevation spectral density at station Praticagem, using v3 amplification factor – run018. Ordinates in log scale.

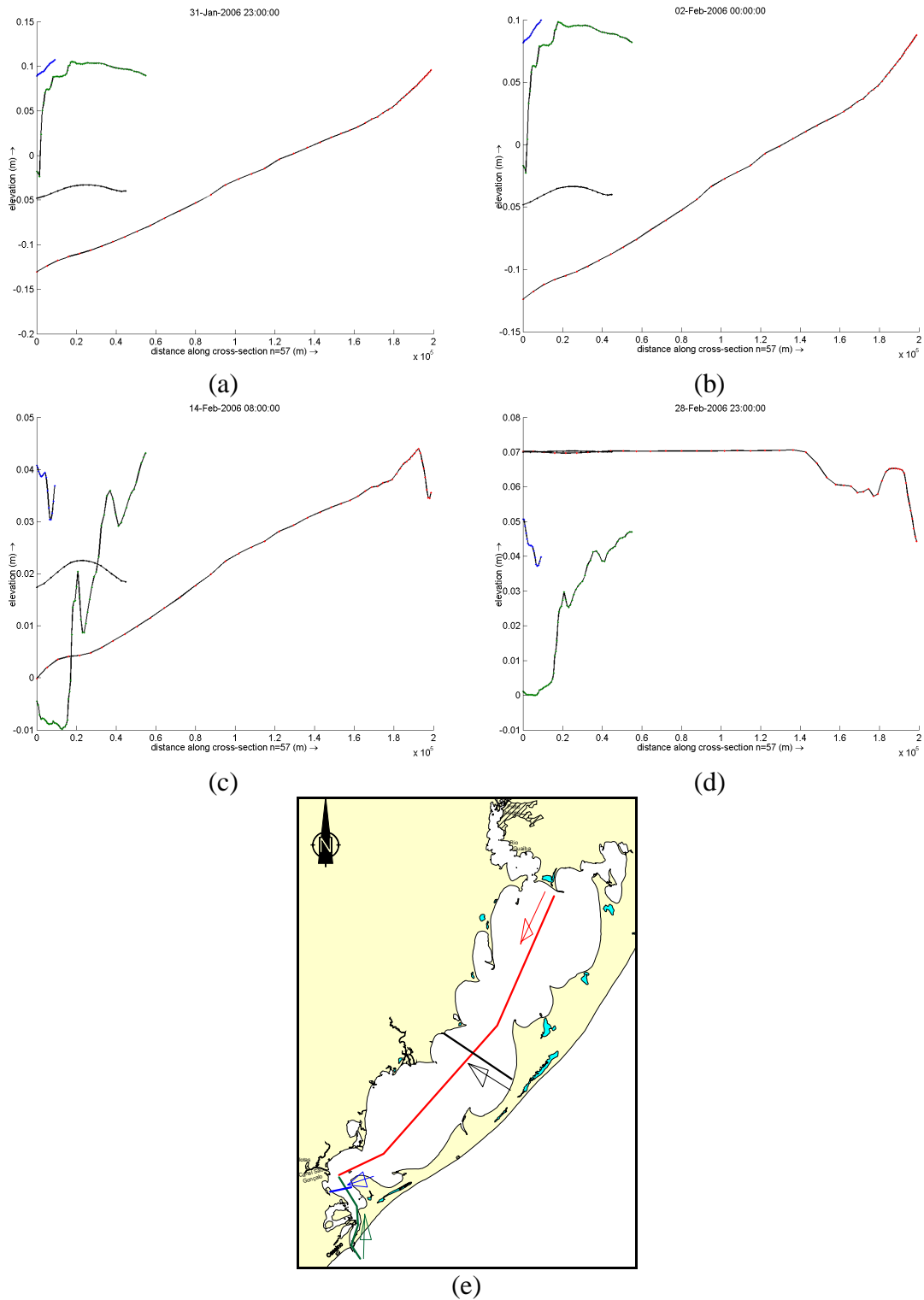
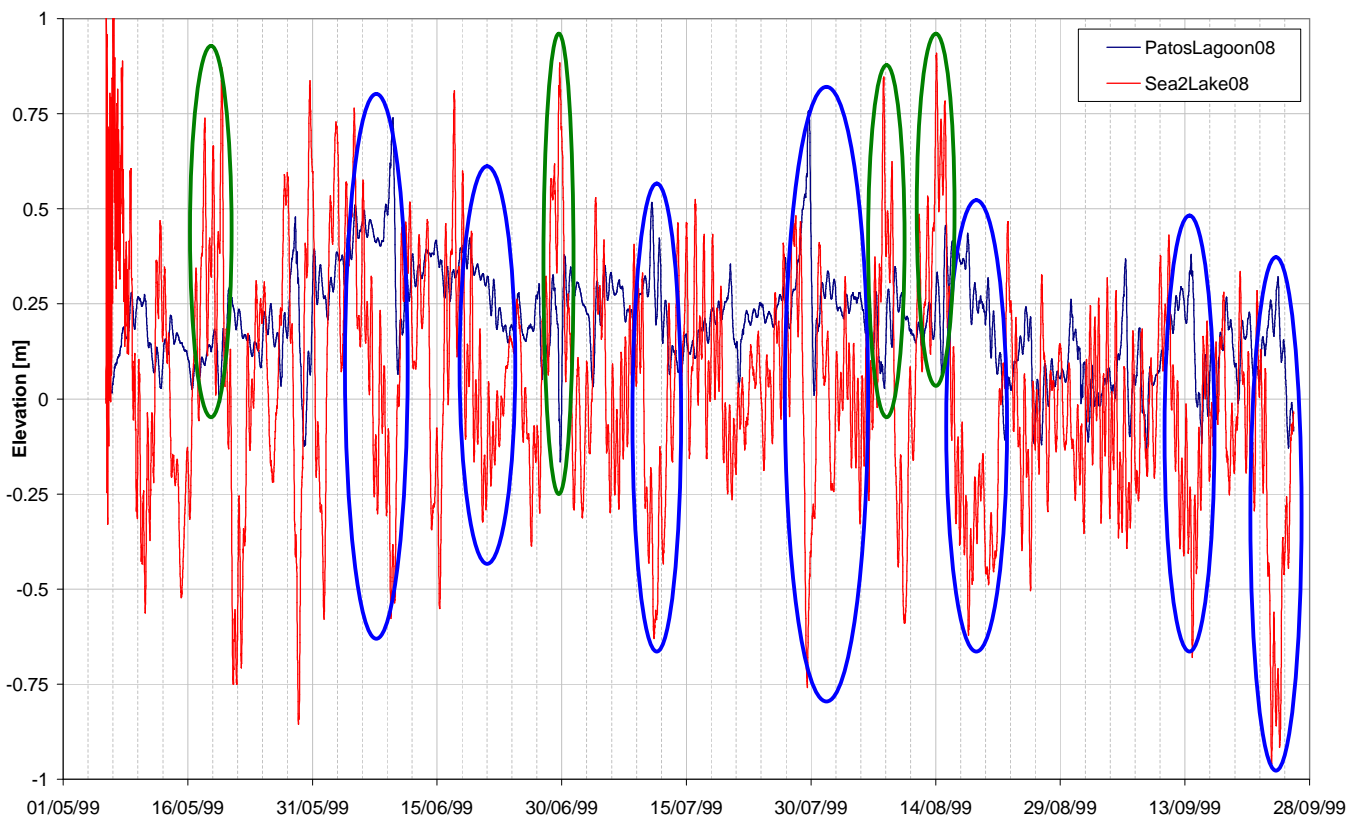
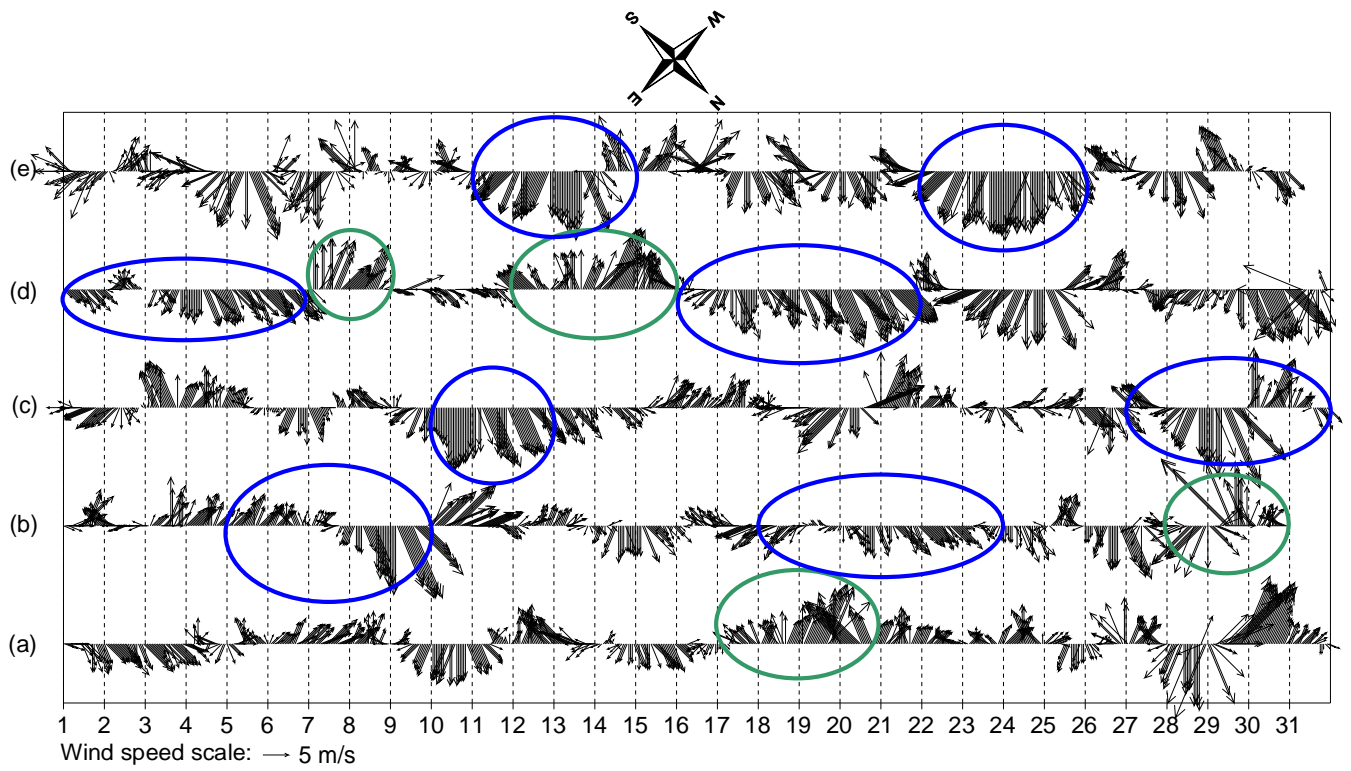


Figure 20: Water elevation plotted for transects. The red line is the lagoon transect. The black line is the middle lagoon transect. The blue line is the cross-estuary transect. The green is the along-estuary transect. The arrows indicate the beginning of each plotted transect in the graphics ($x=0$).



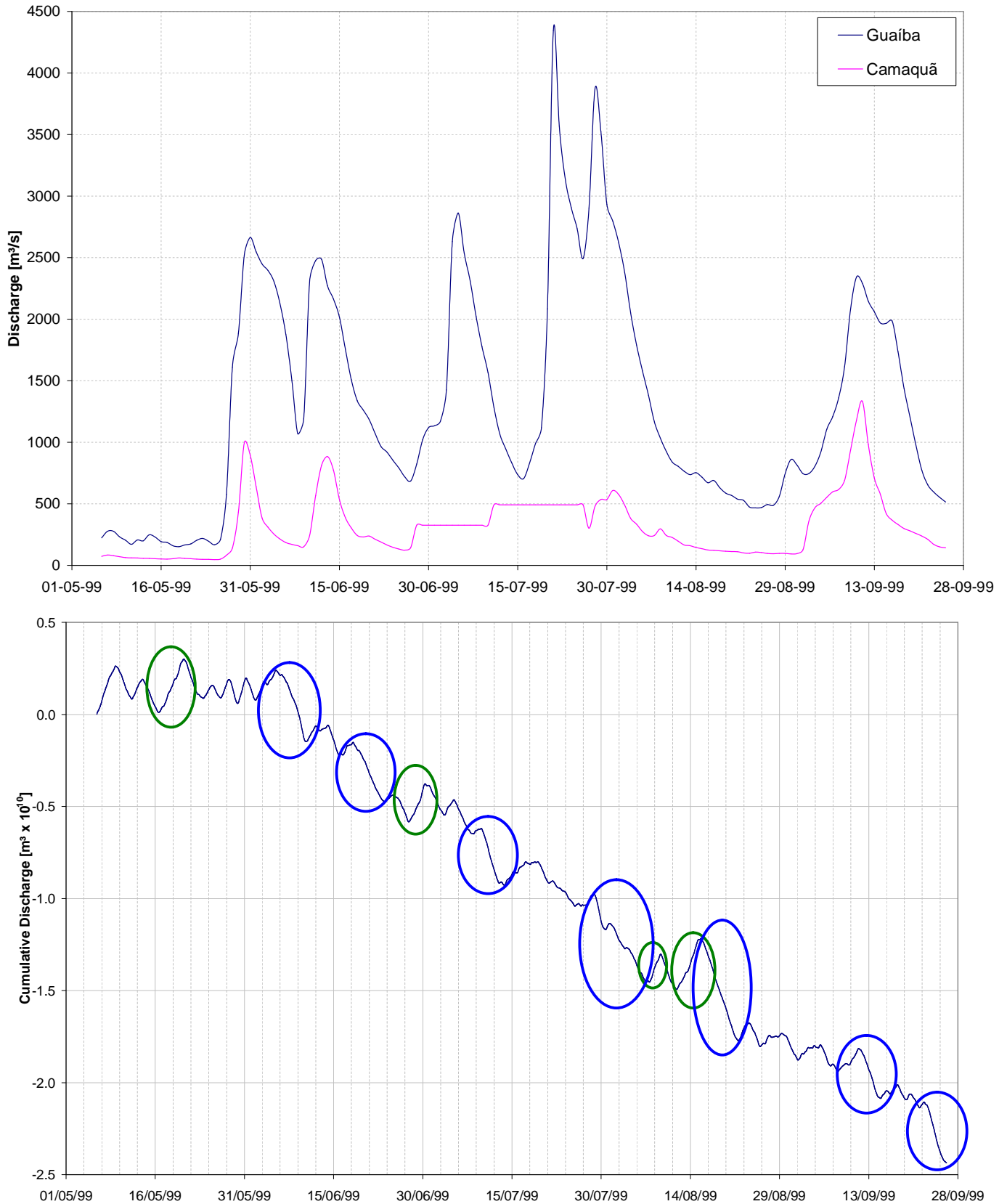


Figure 21: Comparison of wind, water elevation, river discharges and cumulative discharge through the mouth for the modeled period. The blue balloons are correlated to NE winds and the green ones are to SW winds. In the upper graphic, the letters mean: (a) may, (b) june, (c) july, (d) august and (e) september of 1999.

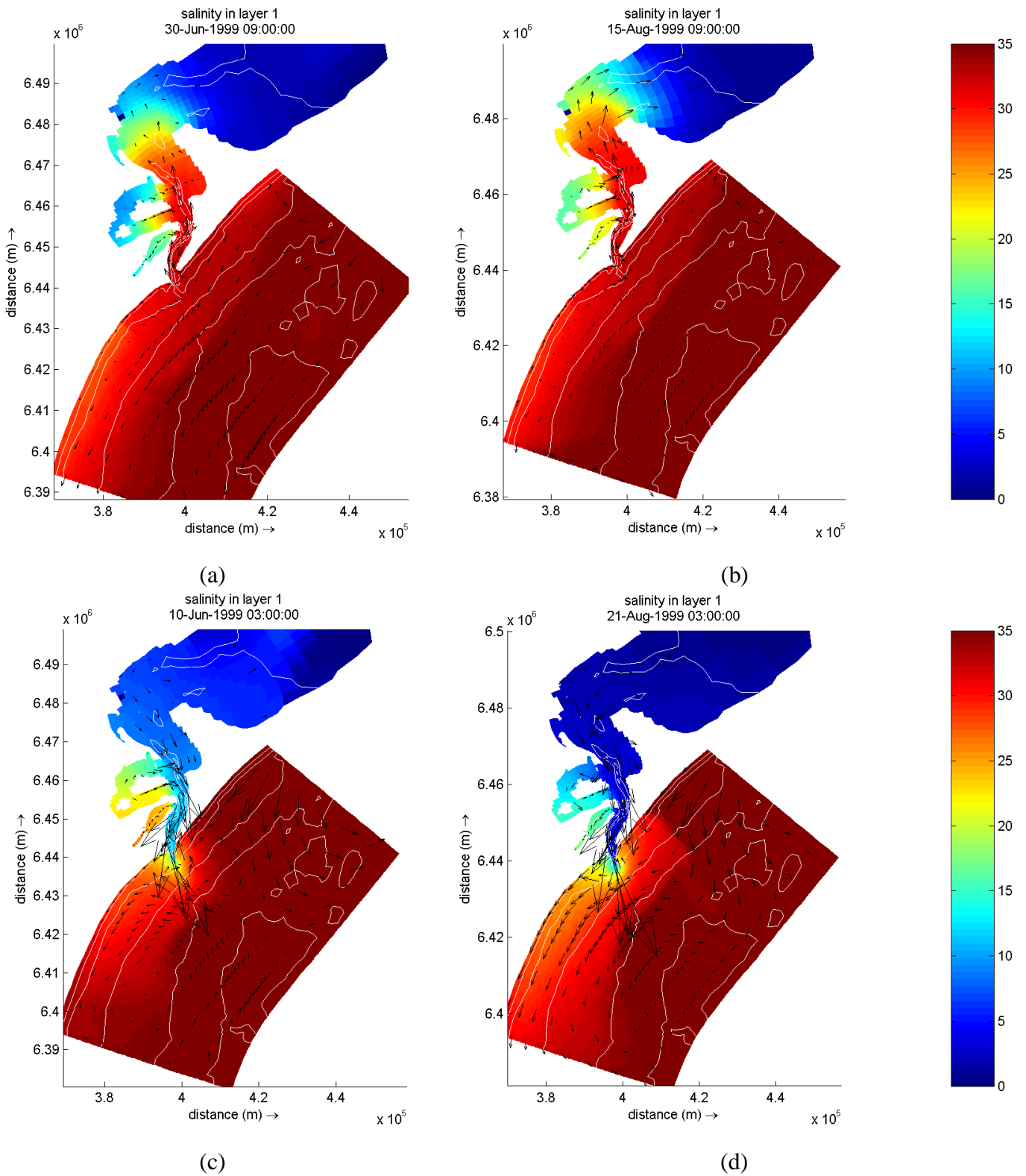


Figure 22: Salinity patterns under NE winds (a), (c) and (d) and SW winds (b). The upper part of each graphics is the location of Ponta da Feitoria. The color bar is in ppt. Results from model run_045.

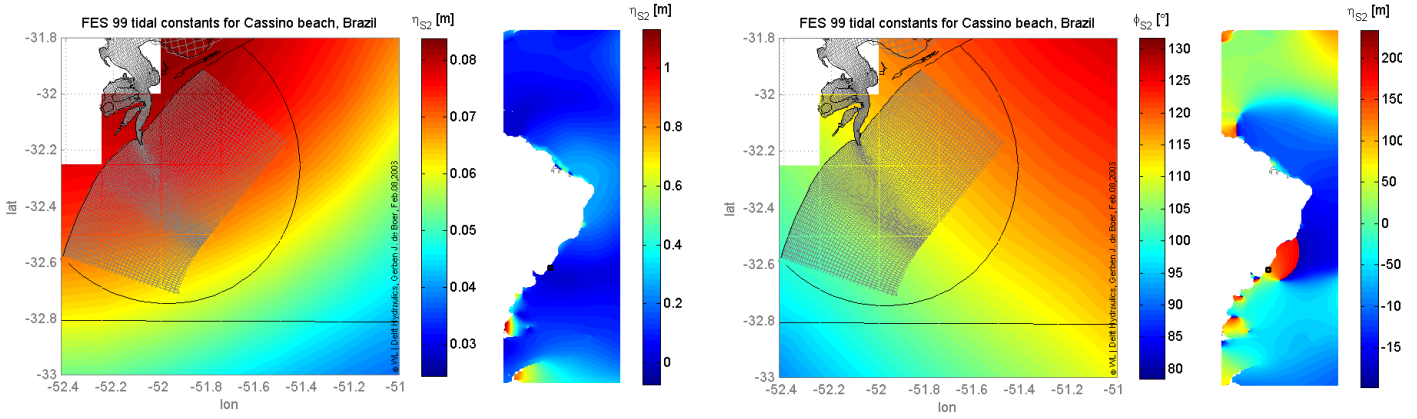


Figure 23: Constituent S2: amplitude and phase used to interpolate to the open boundary.

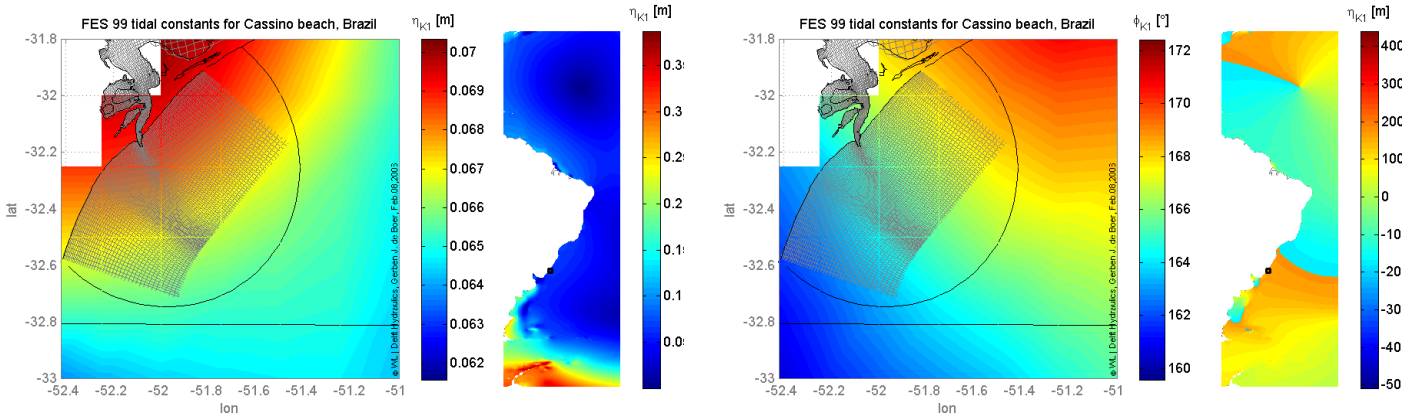


Figure 24: Constituent K1: amplitude and phase used to interpolate to the open boundary.

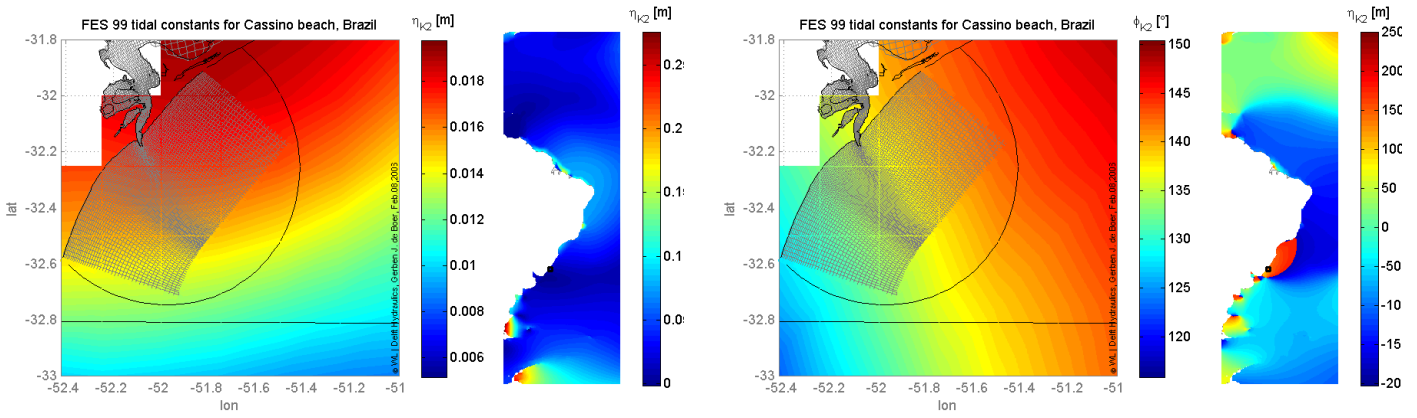


Figure 25: Constituent K2: amplitude and phase used to interpolate to the open boundary.

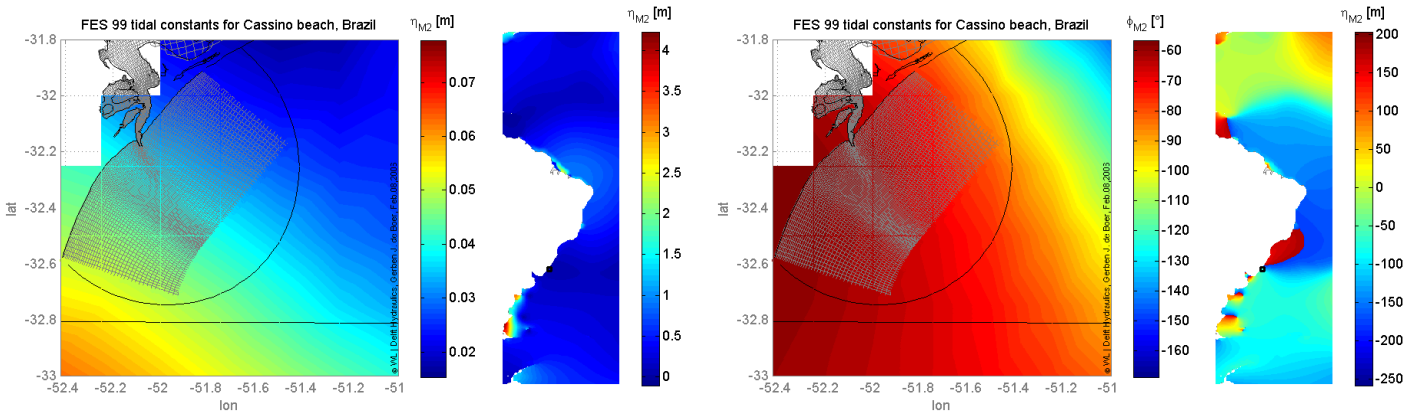


Figure 26: Constituent M2: amplitude and phase used to interpolate to the open boundary.

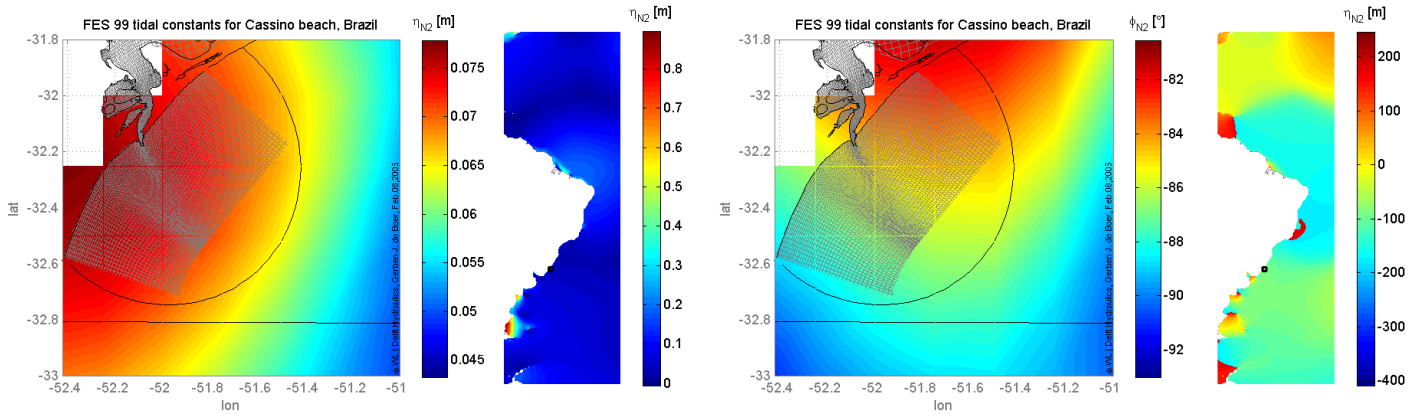


Figure 27: Constituent N2: amplitude and phase used to interpolate to the open boundary.

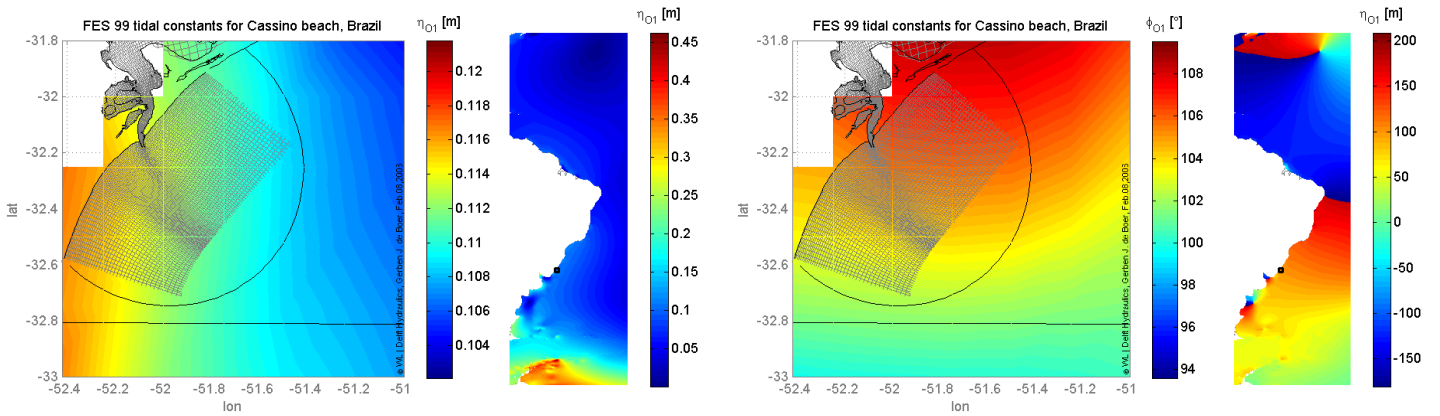


Figure 28: Constituent O1: amplitude and phase used to interpolate to the open boundary.

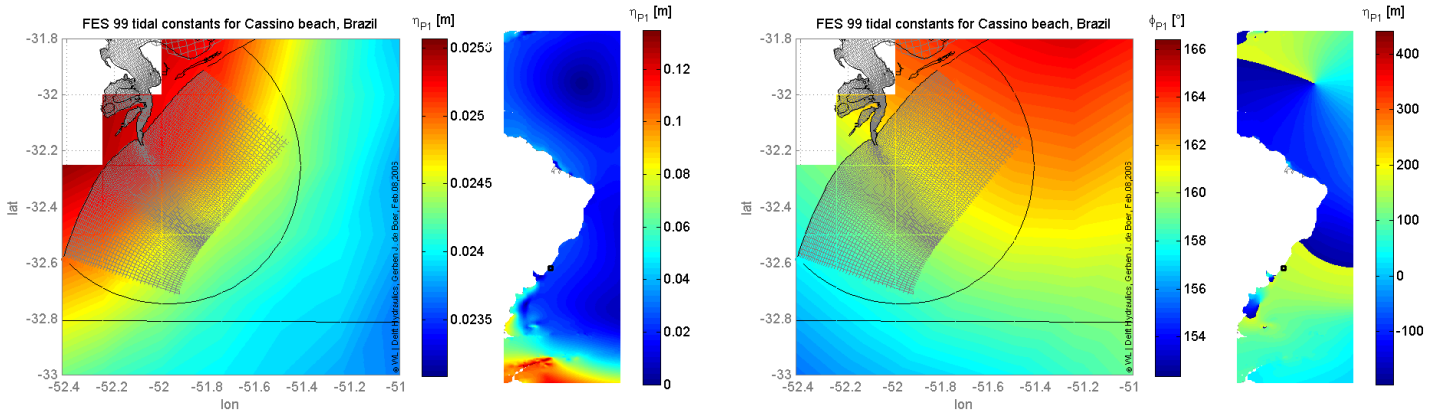


Figure 29: Constituent P1: amplitude and phase used to interpolate to the open boundary.

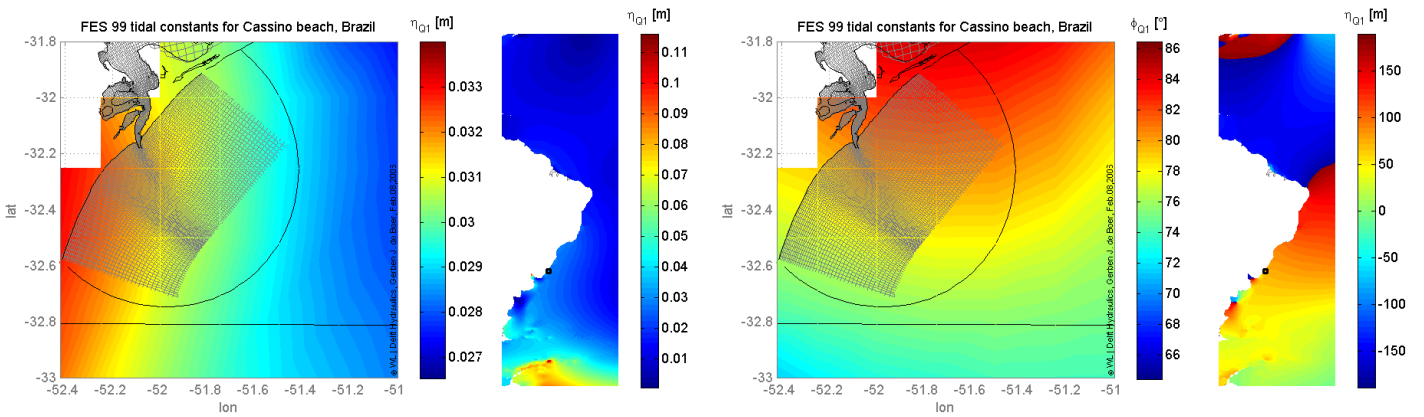


Figure 30: Constituent Q1: amplitude and phase used to interpolate to the open boundary.

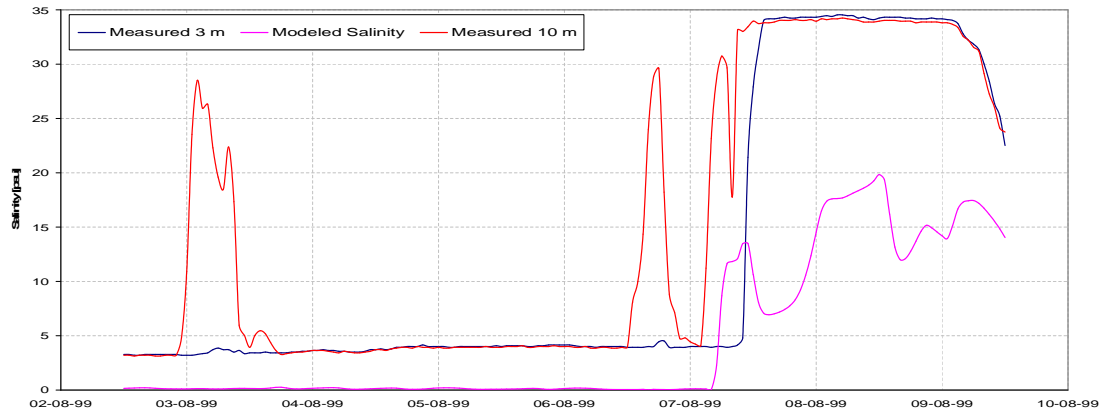
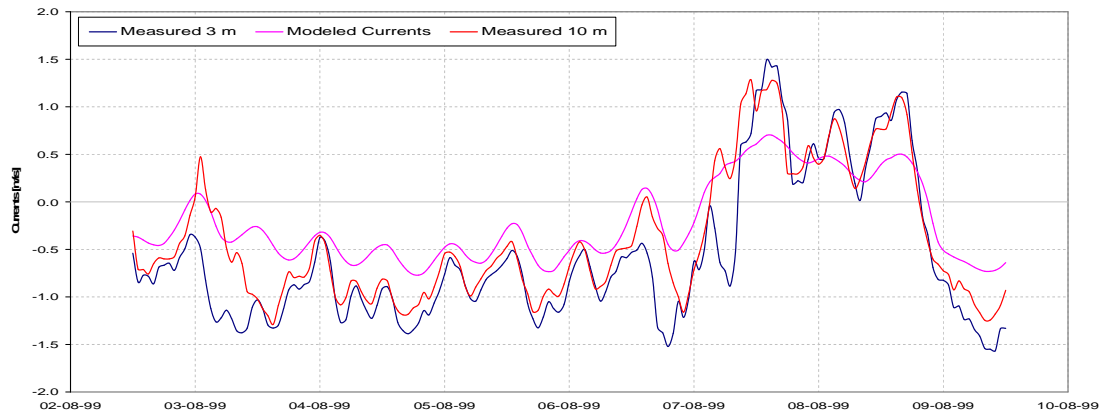


Figure 31: Currents and salinity modeled comparison against measured data. Chezy bottom frictional law ($C=50$). Y units are in m/s (upper graphic) and ppt (lower graphic).

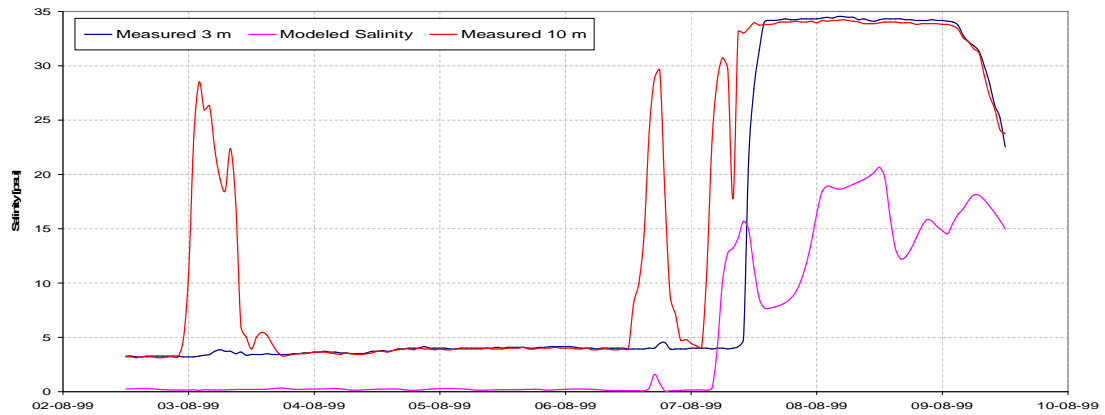
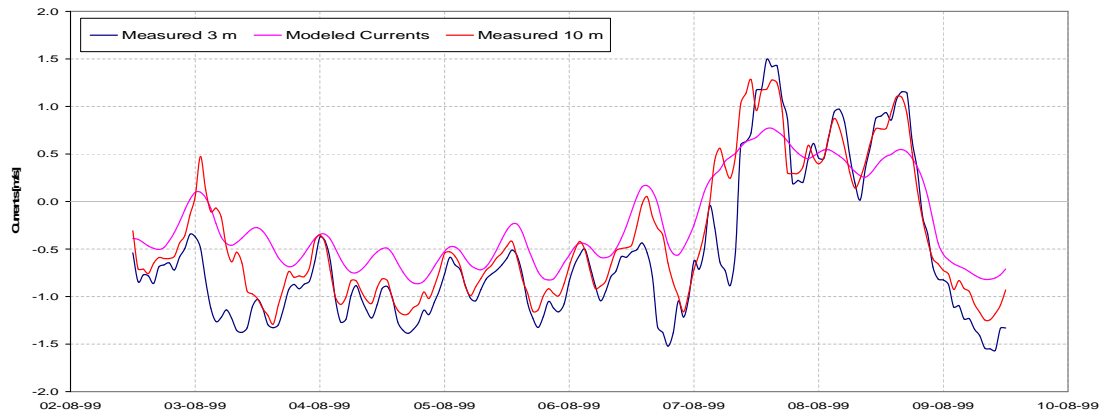


Figure 32: Currents and salinity modeled comparison against measured data. Manning bottom frictional law ($M=0.025$). Y units are in m/s (upper graphic) and ppt (lower graphic).

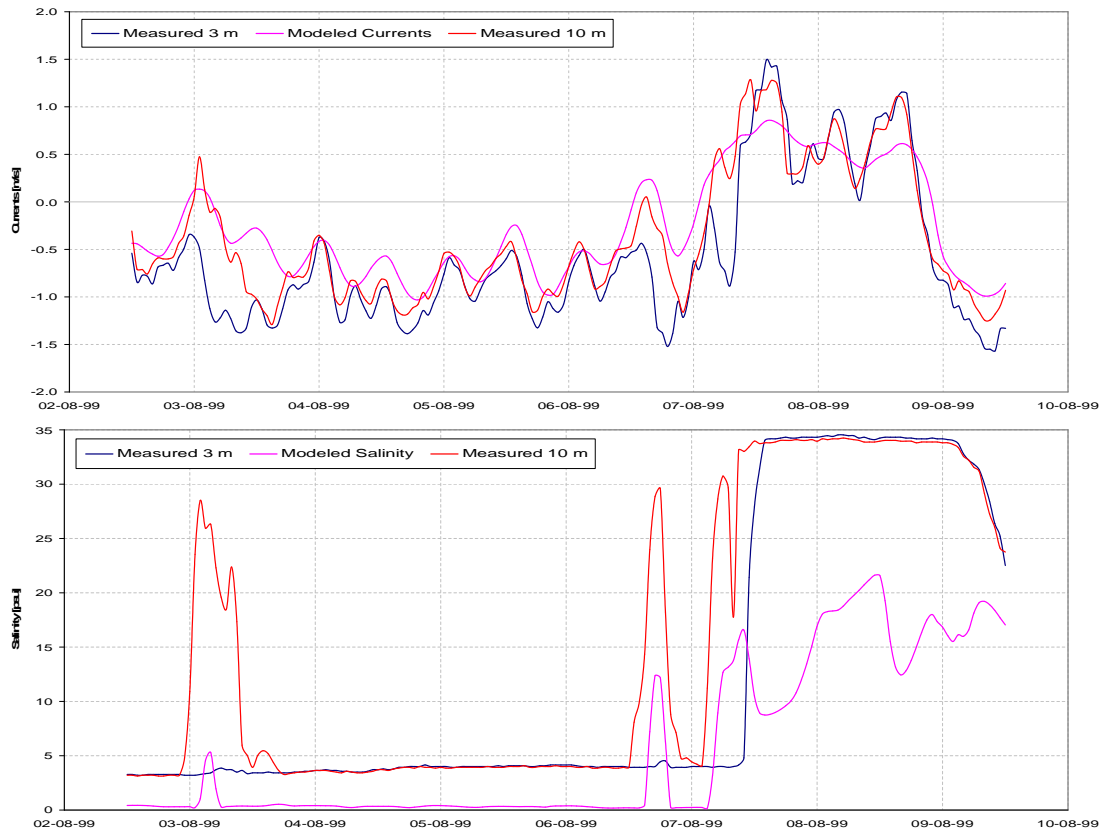


Figure 33: Currents and salinity modeled comparison against measured data. White-Colebrook bottom frictional law ($k=0.01$). Y units are in m/s (upper graphic) and ppt (lower graphic).

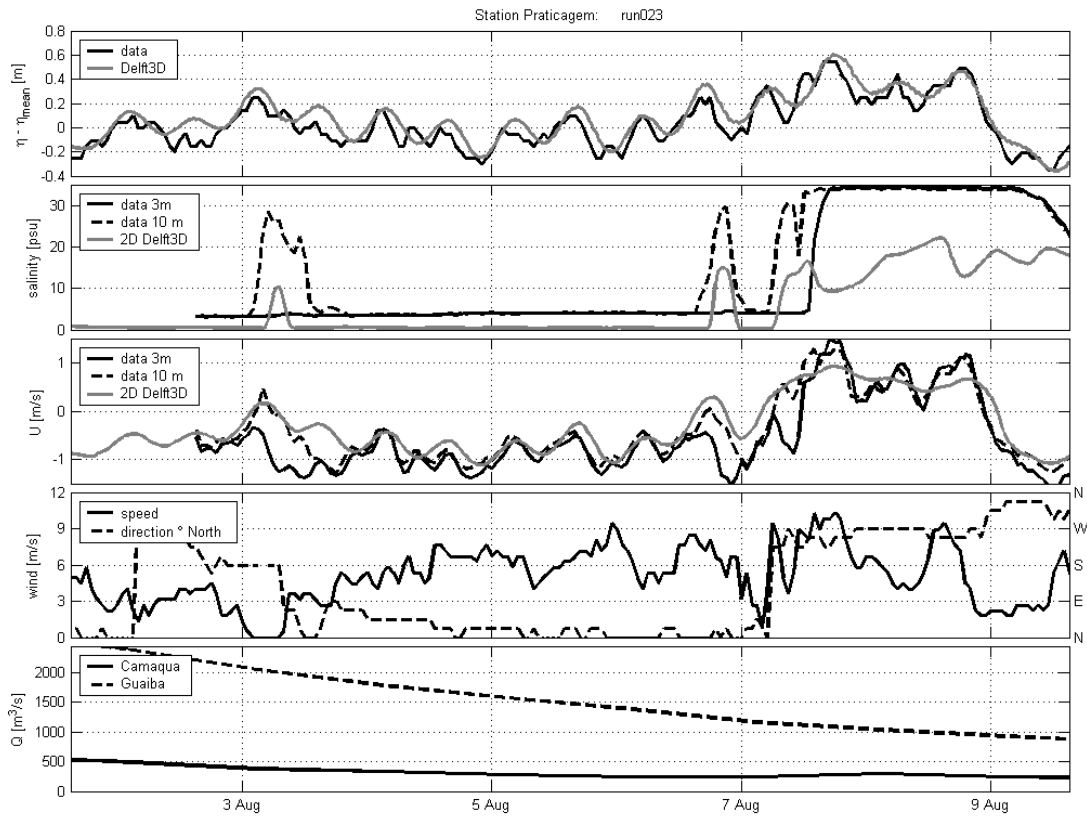


Figure 34: Modeled current and salinity comparison against measured data. $k=0.005$ and SGC discharge.

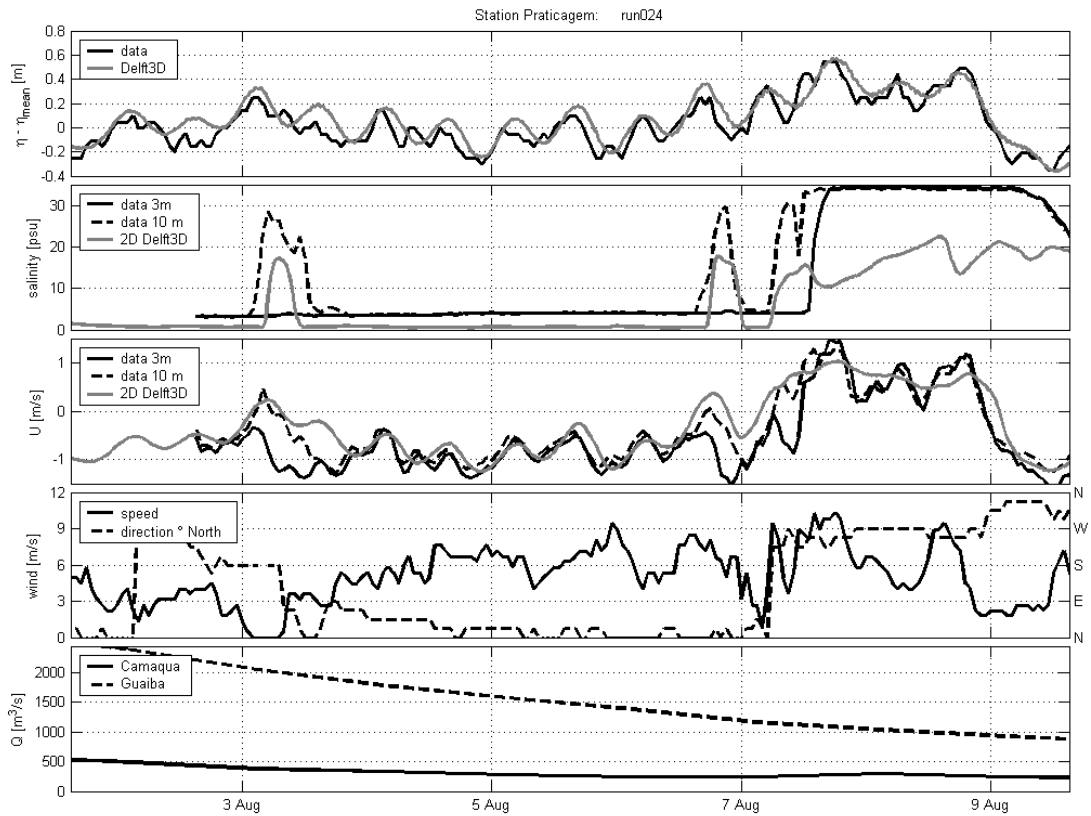


Figure 35: Modeled current and salinity comparison against measured data. $k=0.001$ and SGC discharge.

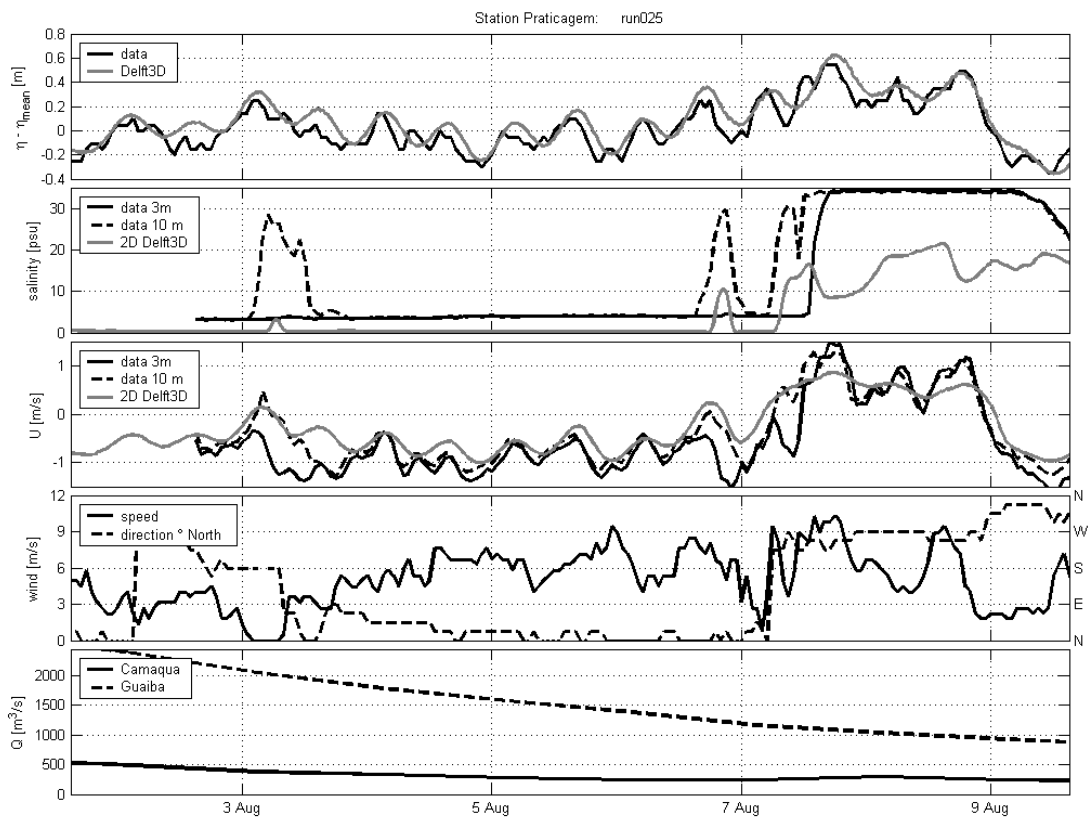


Figure 36: Modeled current and salinity comparison against measured data. $k=0.015$ and SGC discharge.

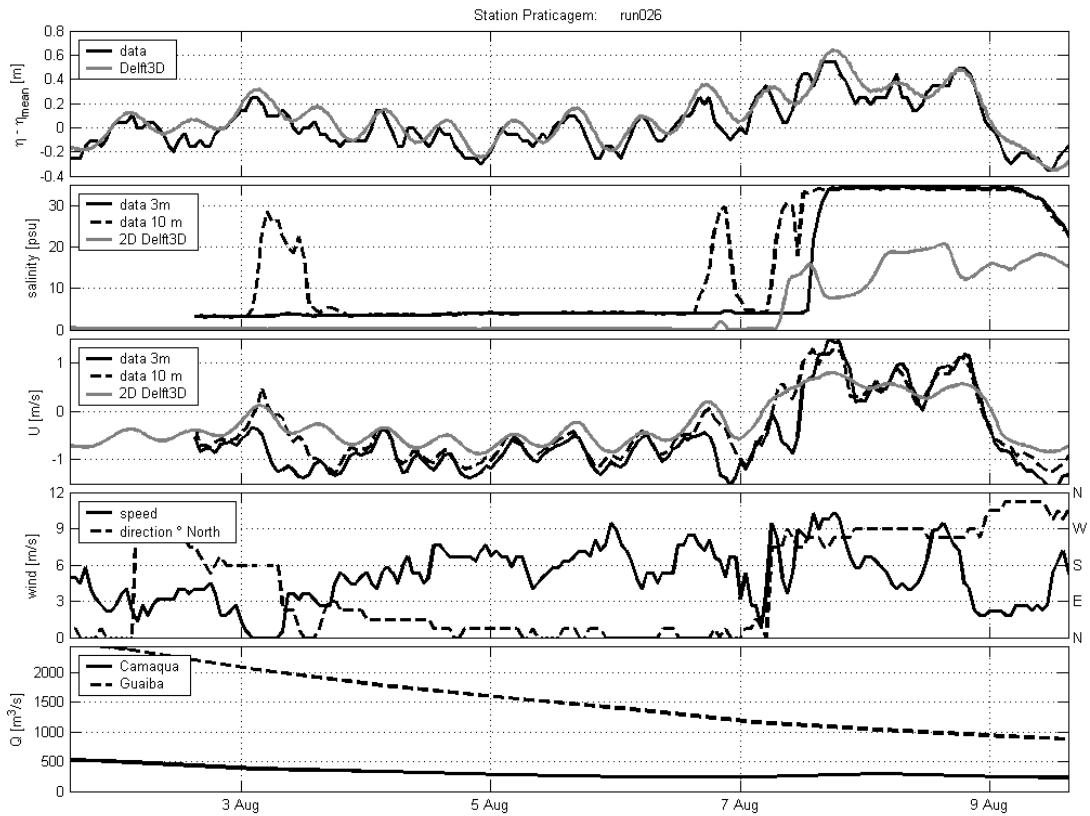


Figure 37: Modeled current and salinity comparison against measured data. $k=0.05$ and SGC discharge.

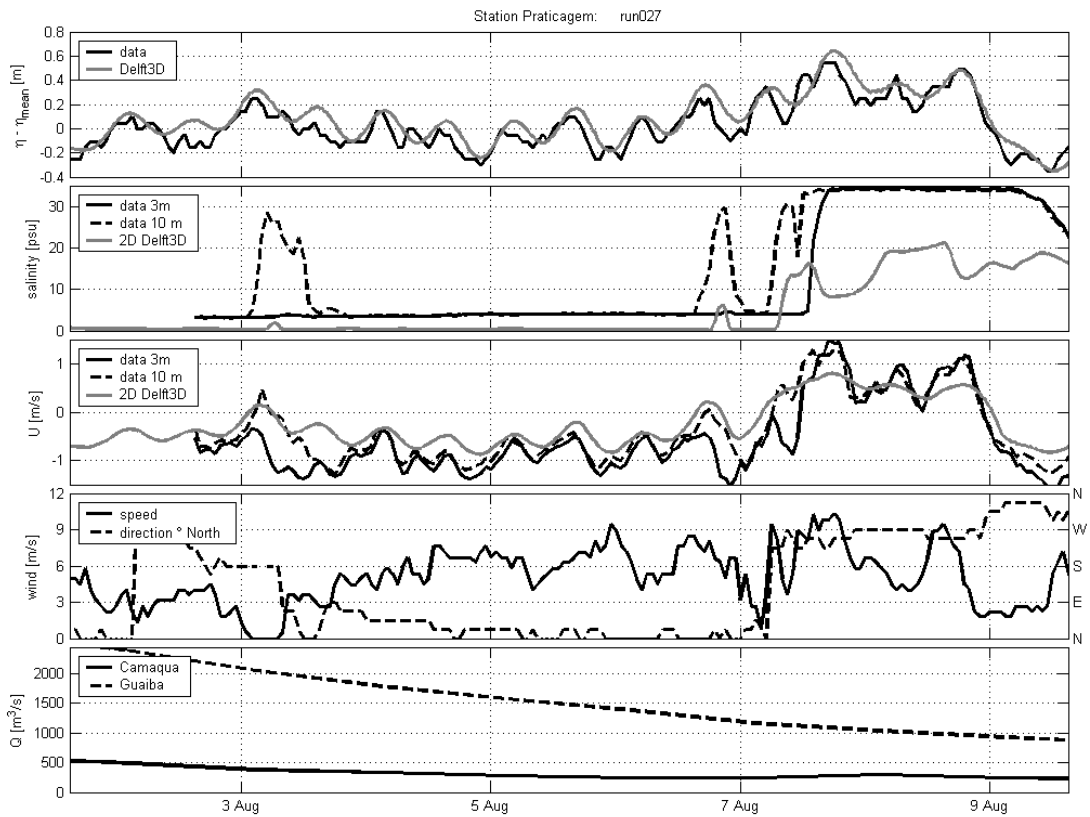


Figure 38: Modeled current and salinity comparison against measured data. $k=0.05$ and no SGC discharge.

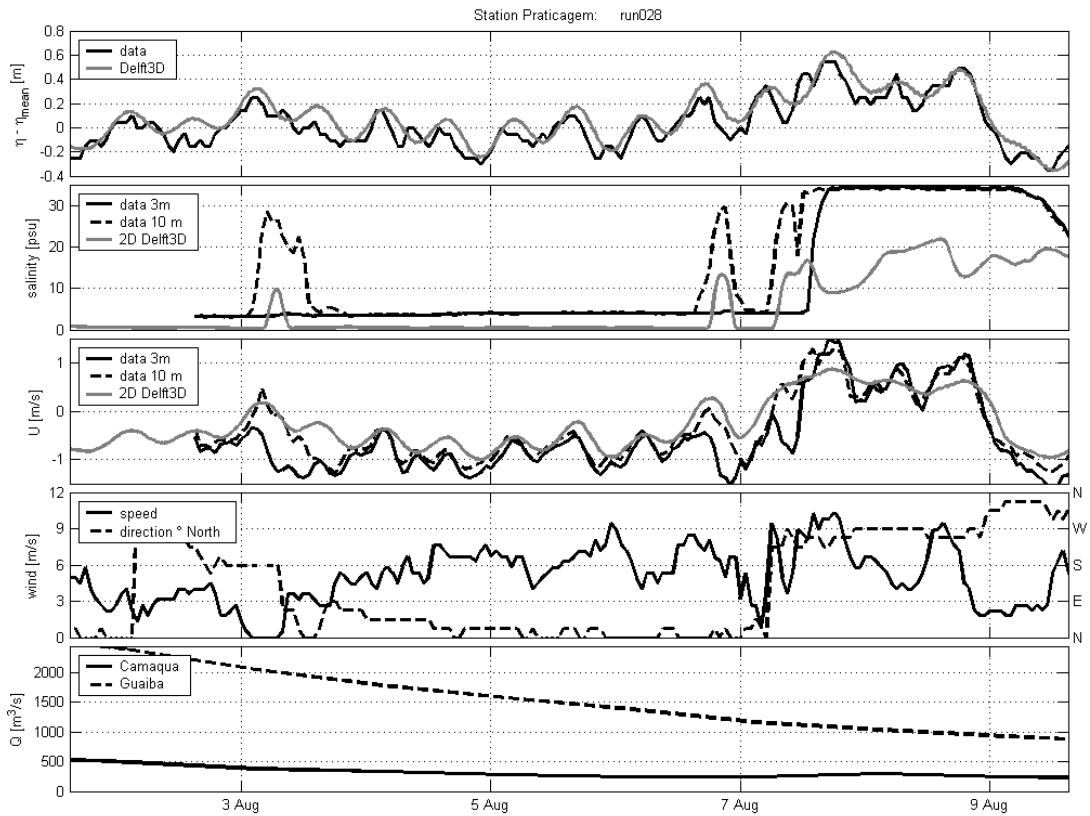


Figure 39: Modeled current and salinity comparison against measured data. $k=0.015$ and no SGC discharge.

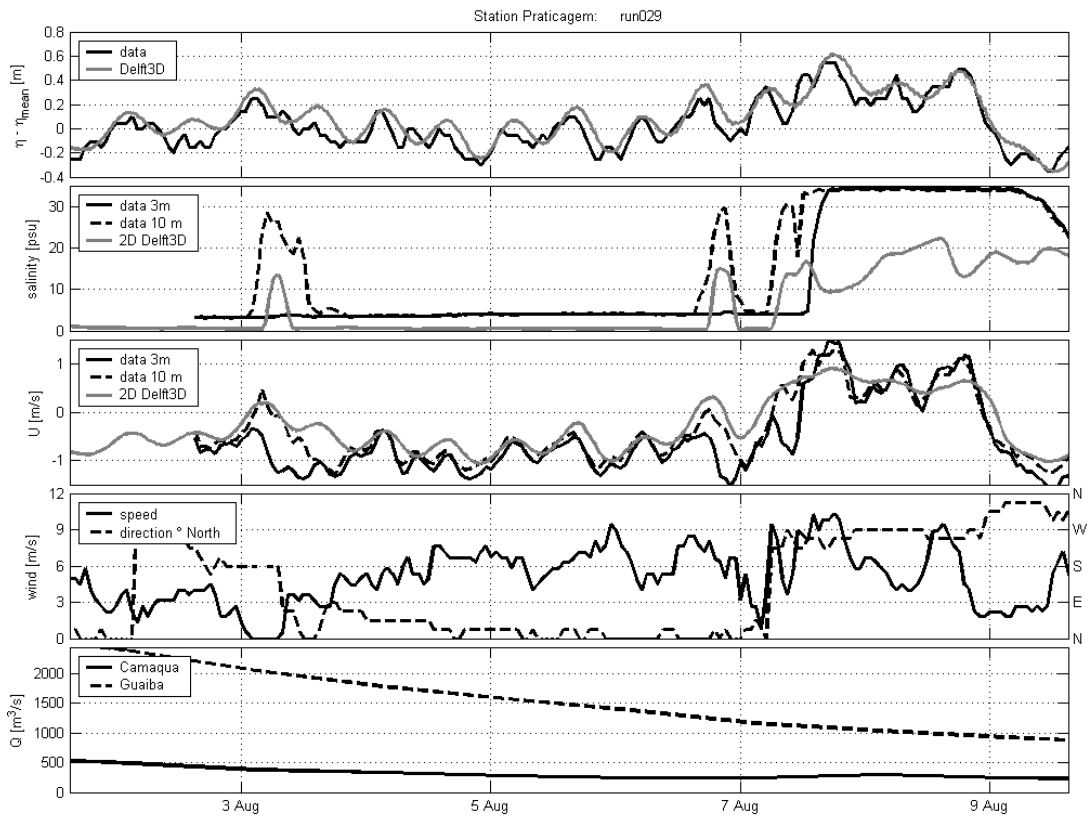


Figure 40: Modeled current and salinity comparison against measured data. $k=0.008$ and no SGC discharge.

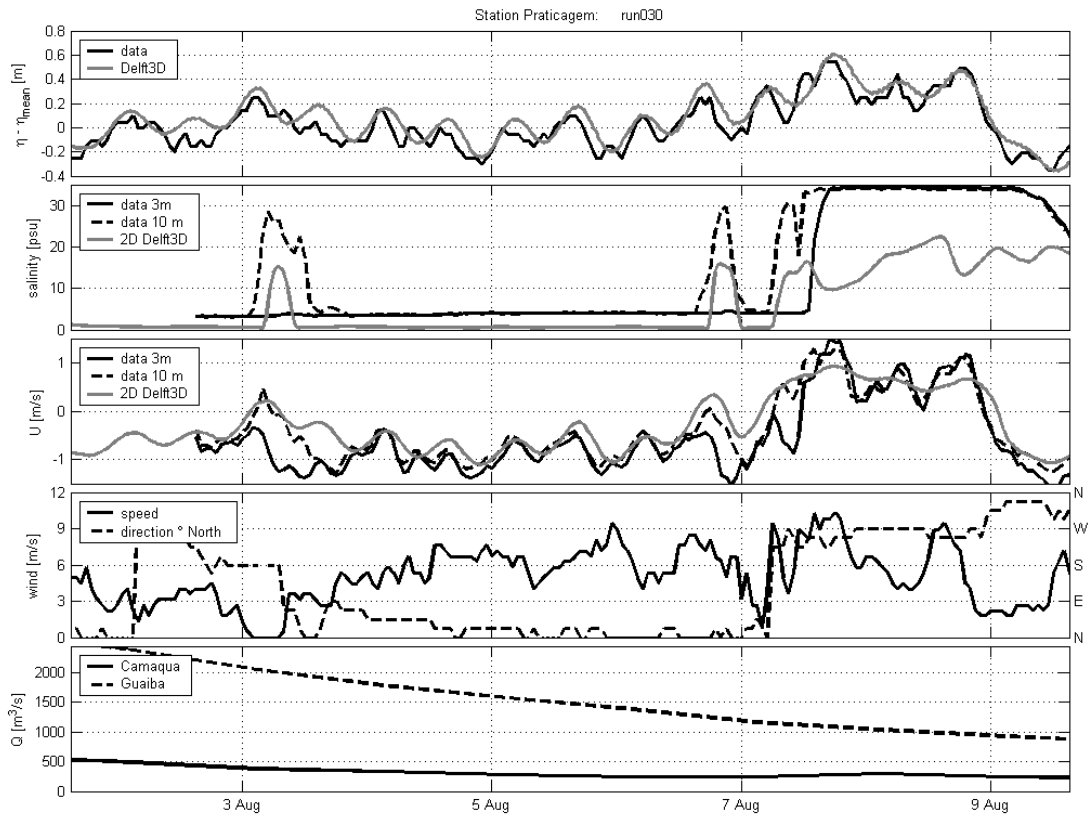


Figure 41: Modeled current and salinity comparison against measured data. $k=0.005$ and no SGC discharge.

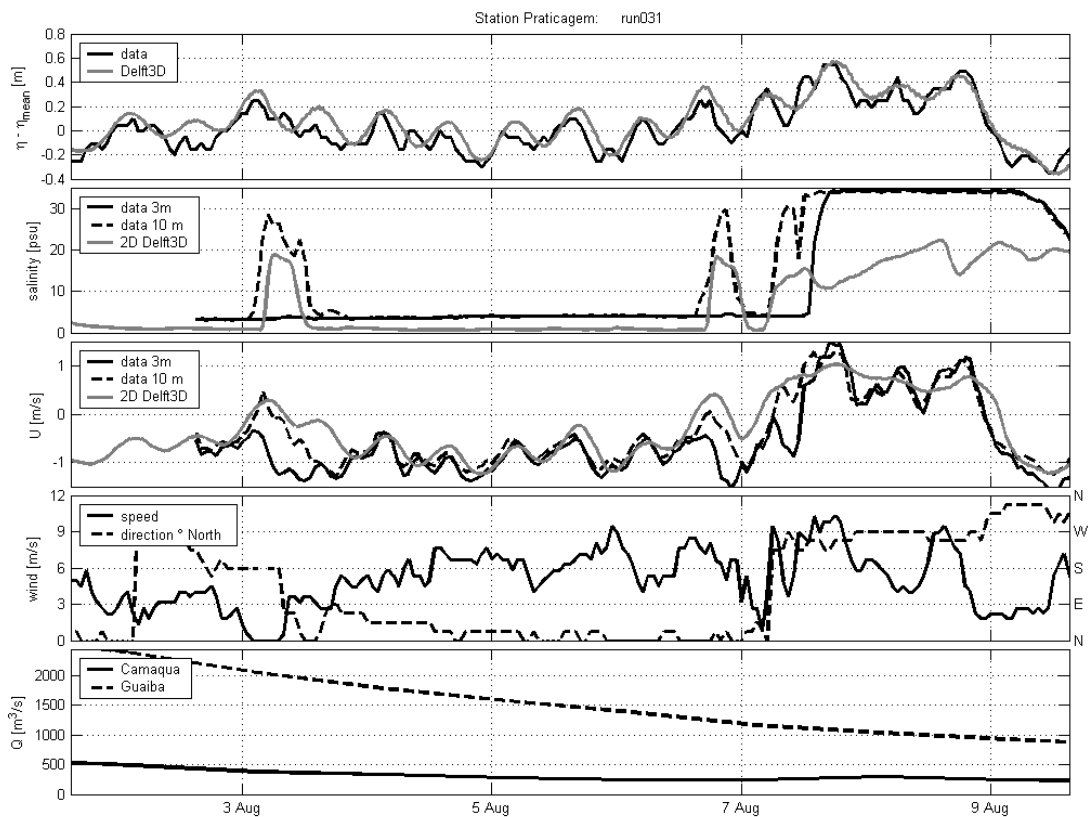


Figure 42: Modeled current and salinity comparison against measured data. $k=0.001$ and no SGC discharge.

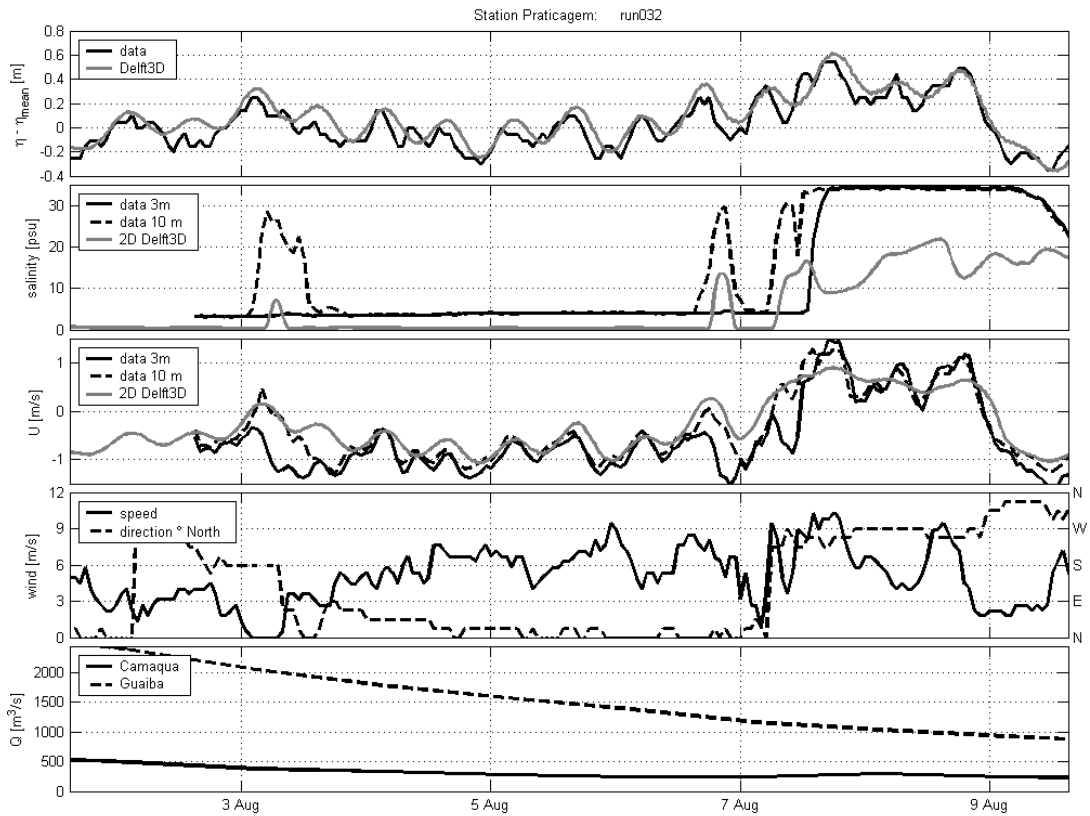


Figure 43: Modeled current and salinity comparison against measured data. $k=0.008$ and SGC discharge.

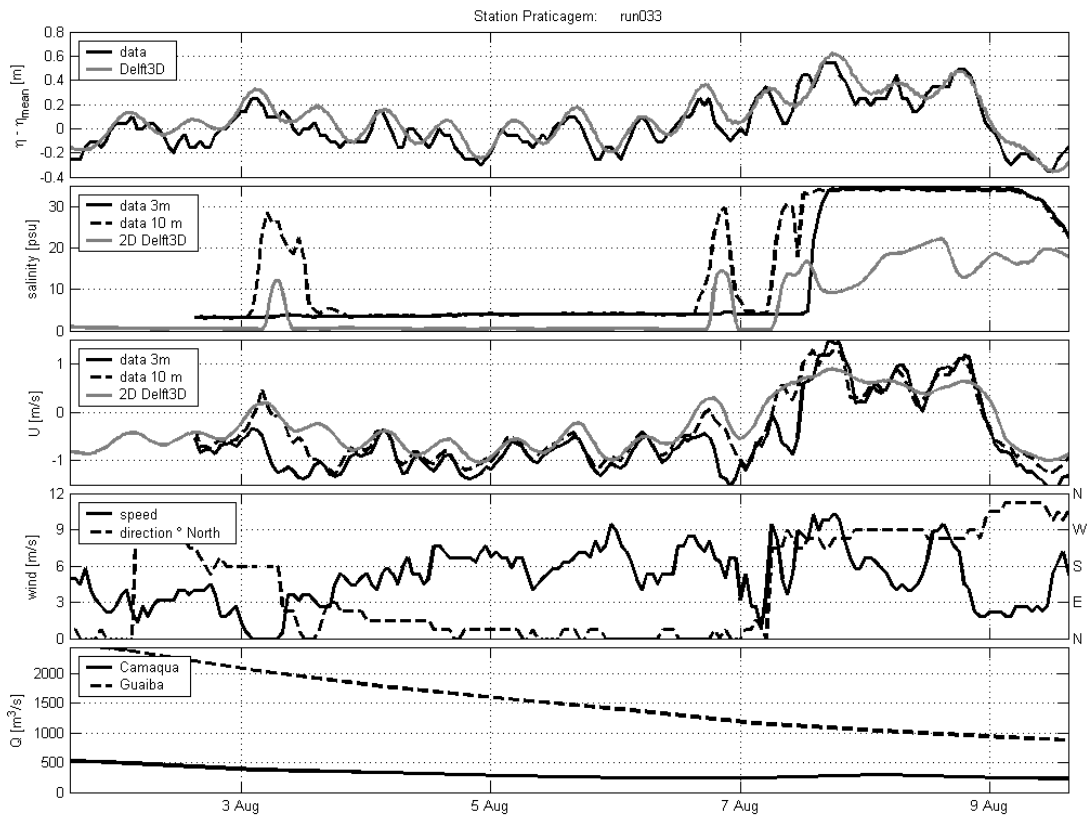


Figure 44: Modeled current and salinity comparison against measured data. $k=0.01$ and no SGC discharge.

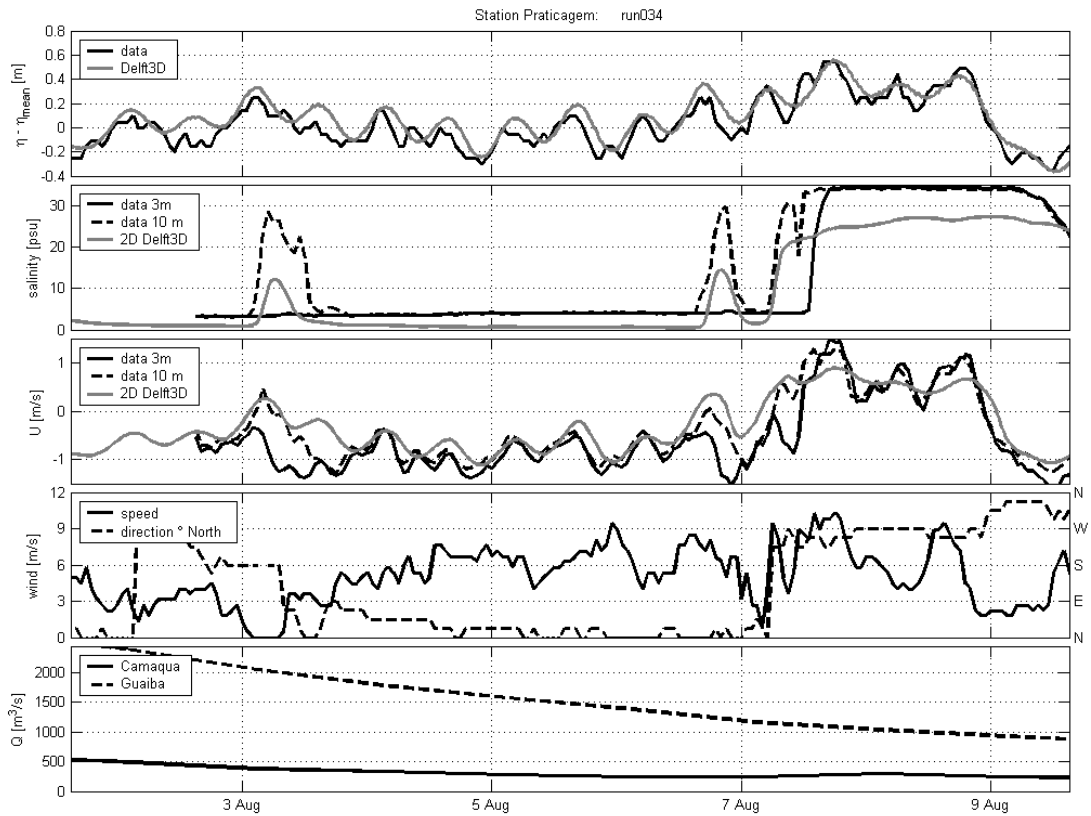


Figure 45: Modeled current and salinity comparison against measured data. Horizontal diffusivity in the estuary area set to 100 m²/s.

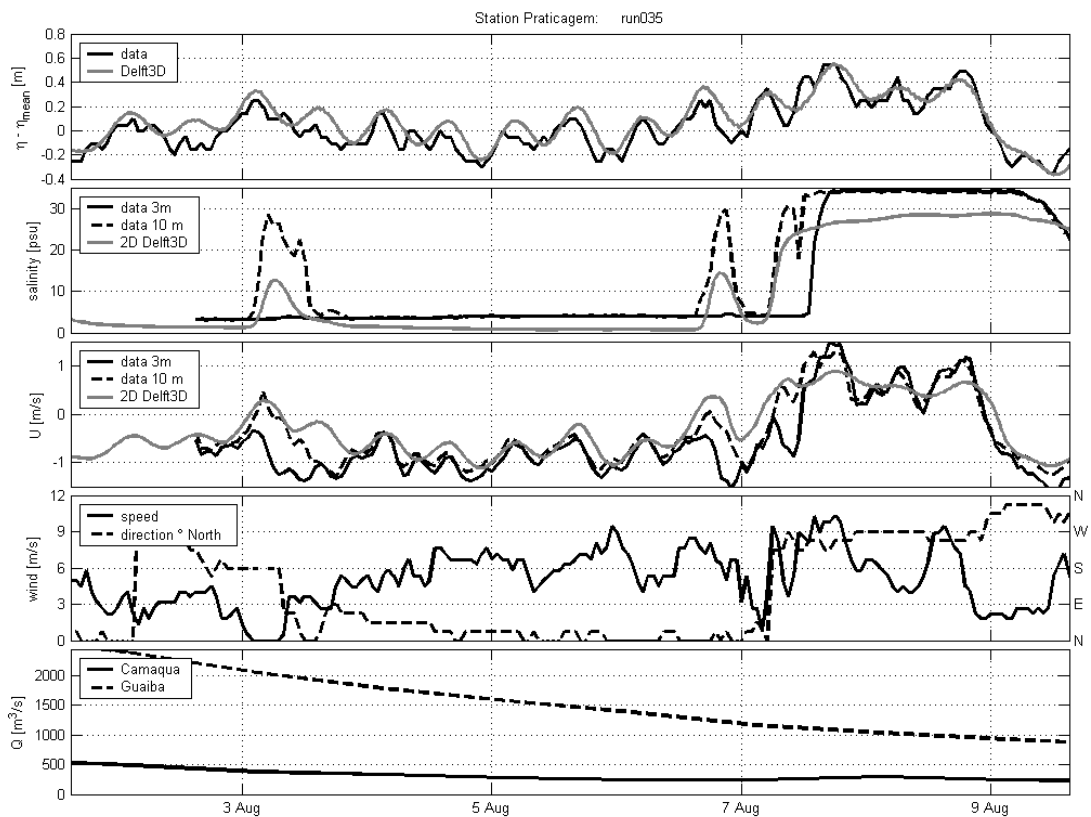


Figure 46: Modeled current and salinity comparison against measured data. Horizontal diffusivity in the estuary area set to 150 m²/s.

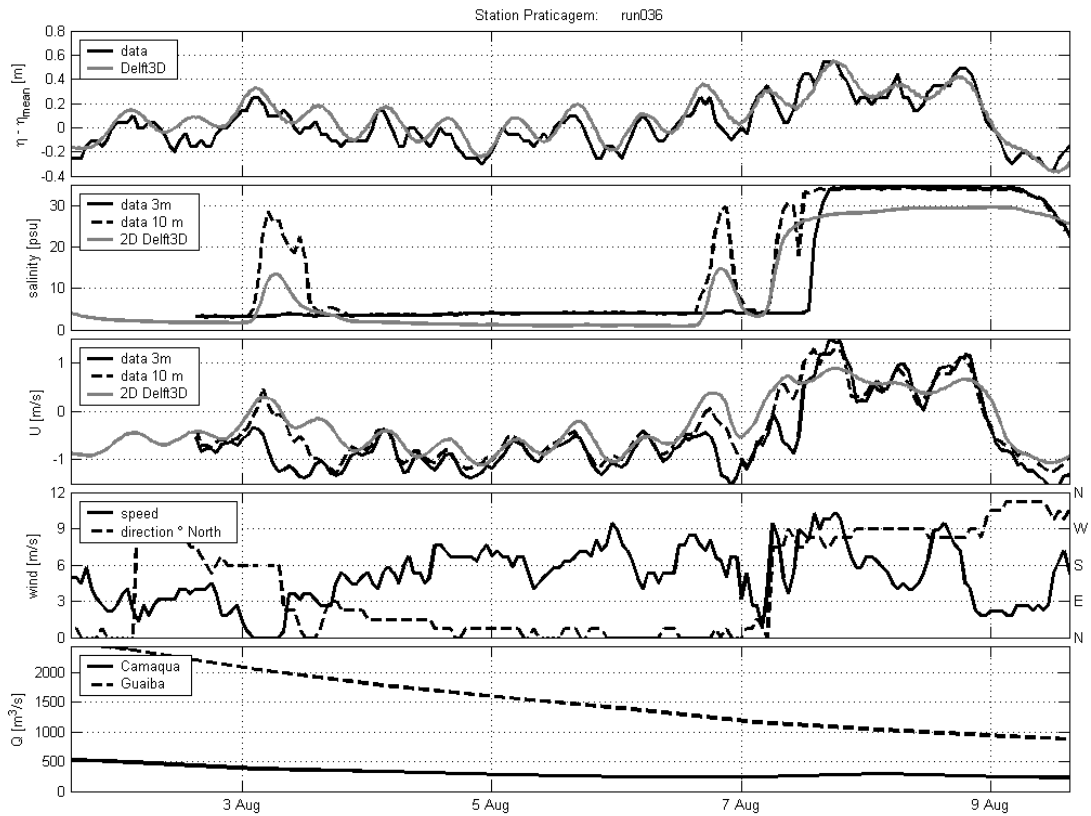


Figure 47: Modeled current and salinity comparison against measured data. Horizontal diffusivity in the estuary area set to 200 m²/s.

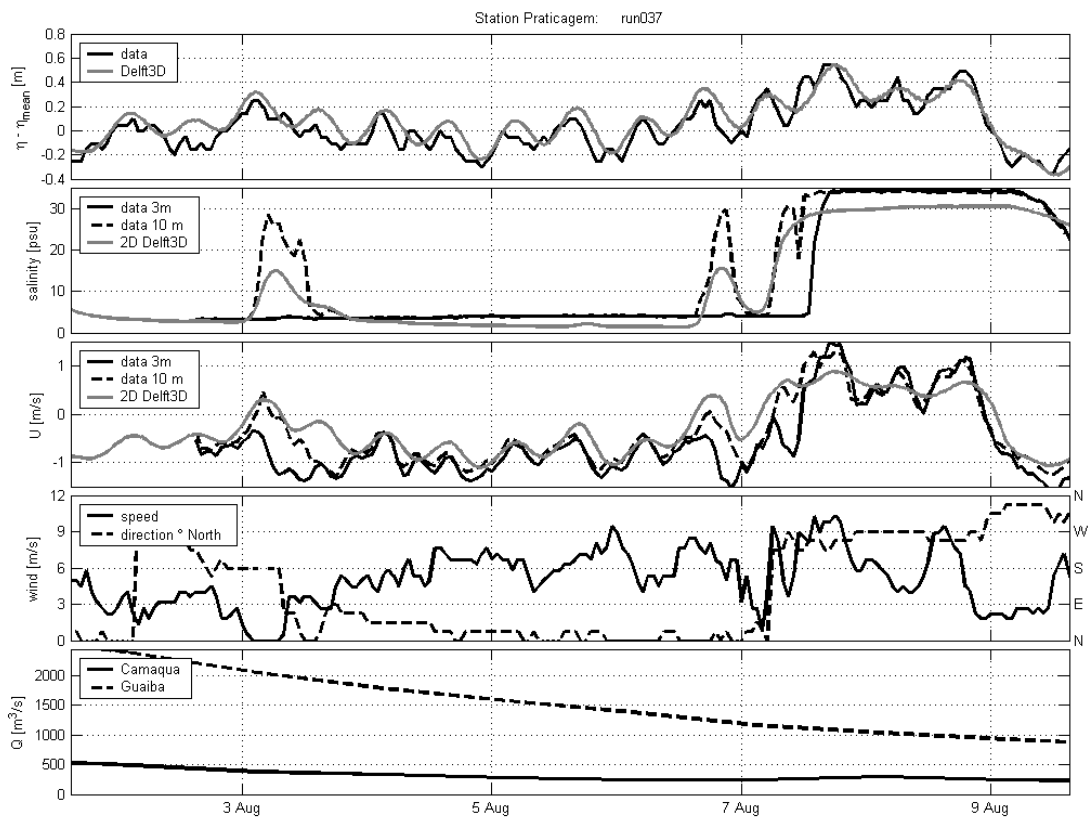


Figure 48: Modeled current and salinity comparison against measured data. Horizontal diffusivity in the estuary area set to 300 m²/s.

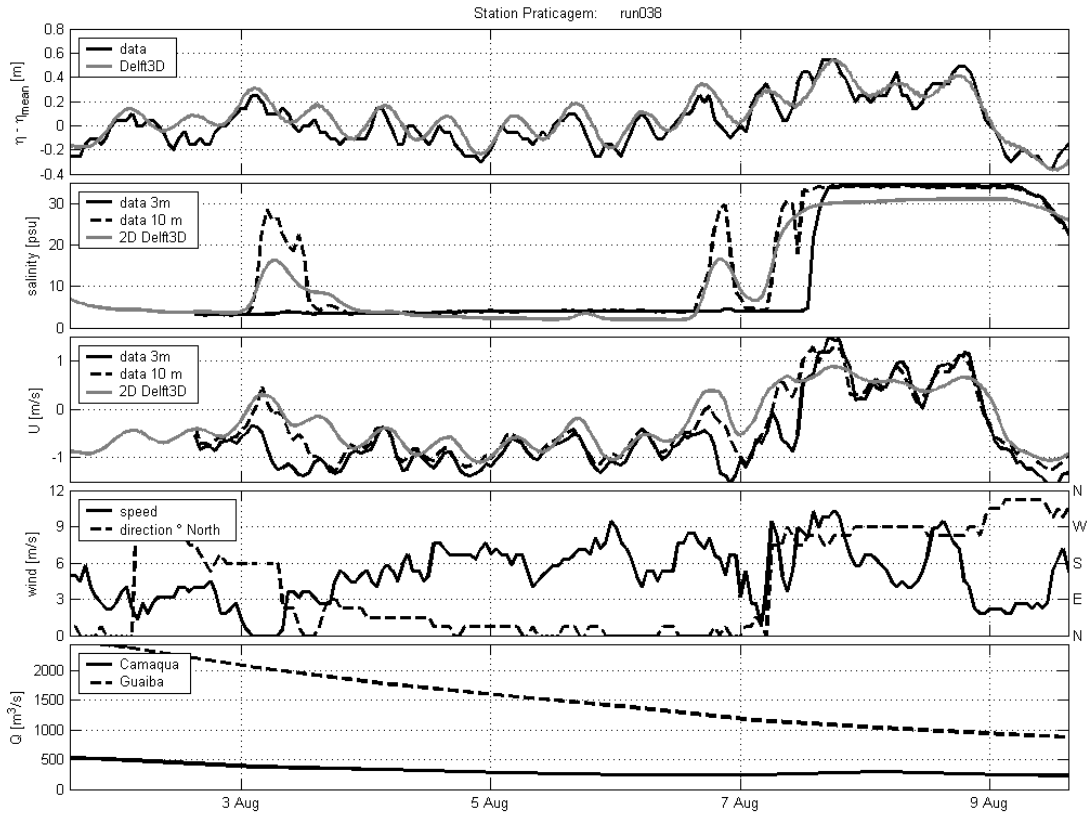


Figure 49: Modeled current and salinity comparison against measured data. Horizontal diffusivity in the estuary area set to 400 m²/s.

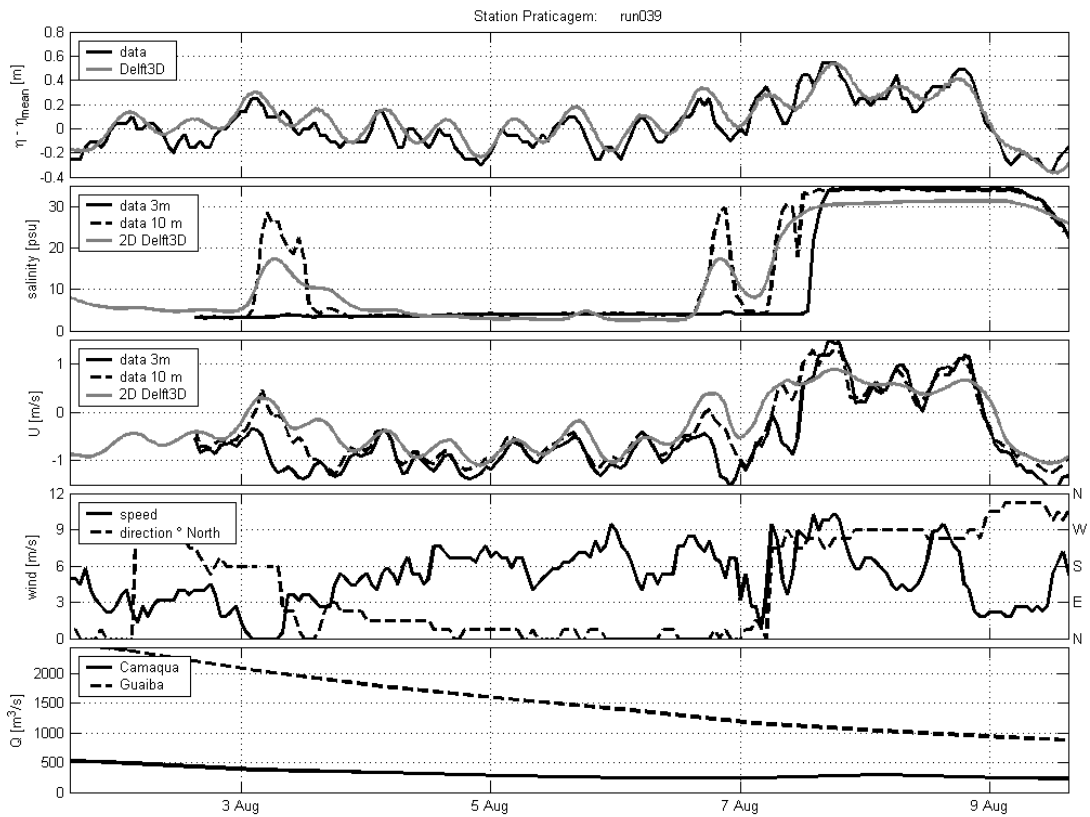


Figure 50: Modeled current and salinity comparison against measured data. Horizontal diffusivity in the estuary area set to 500 m²/s.

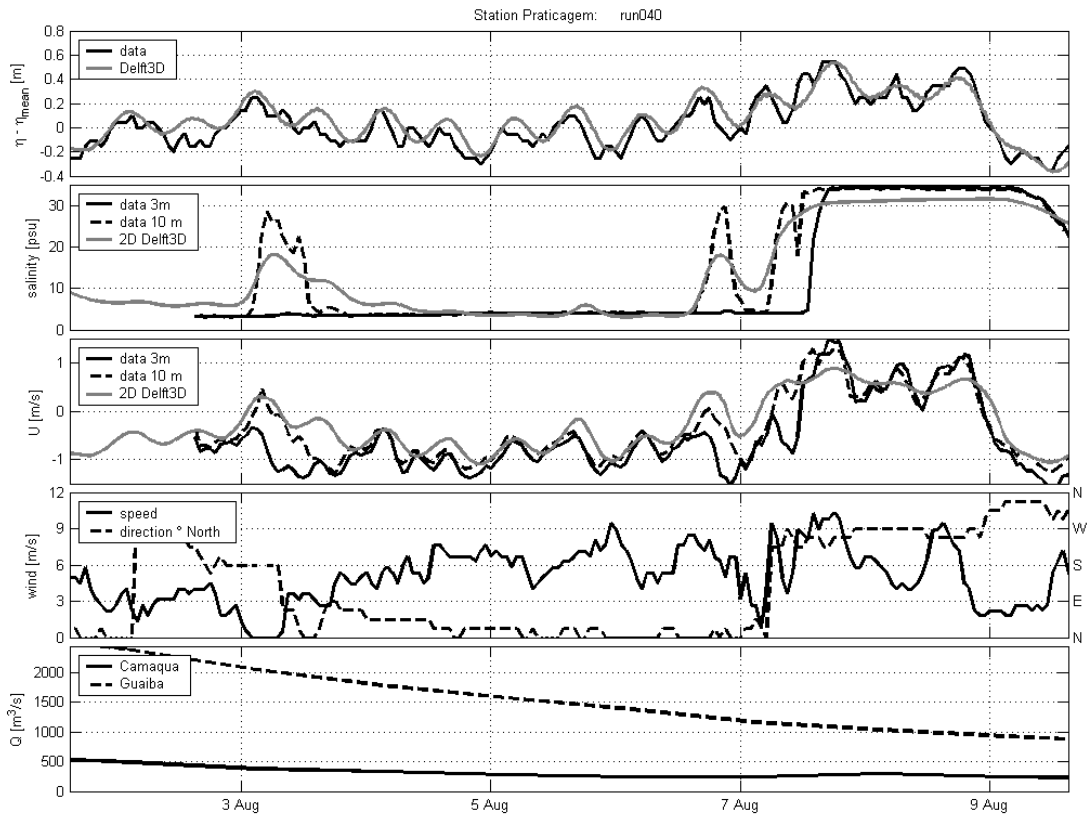


Figure 51: Modeled current and salinity comparison against measured data. Horizontal diffusivity in the estuary area set to 600 m²/s.

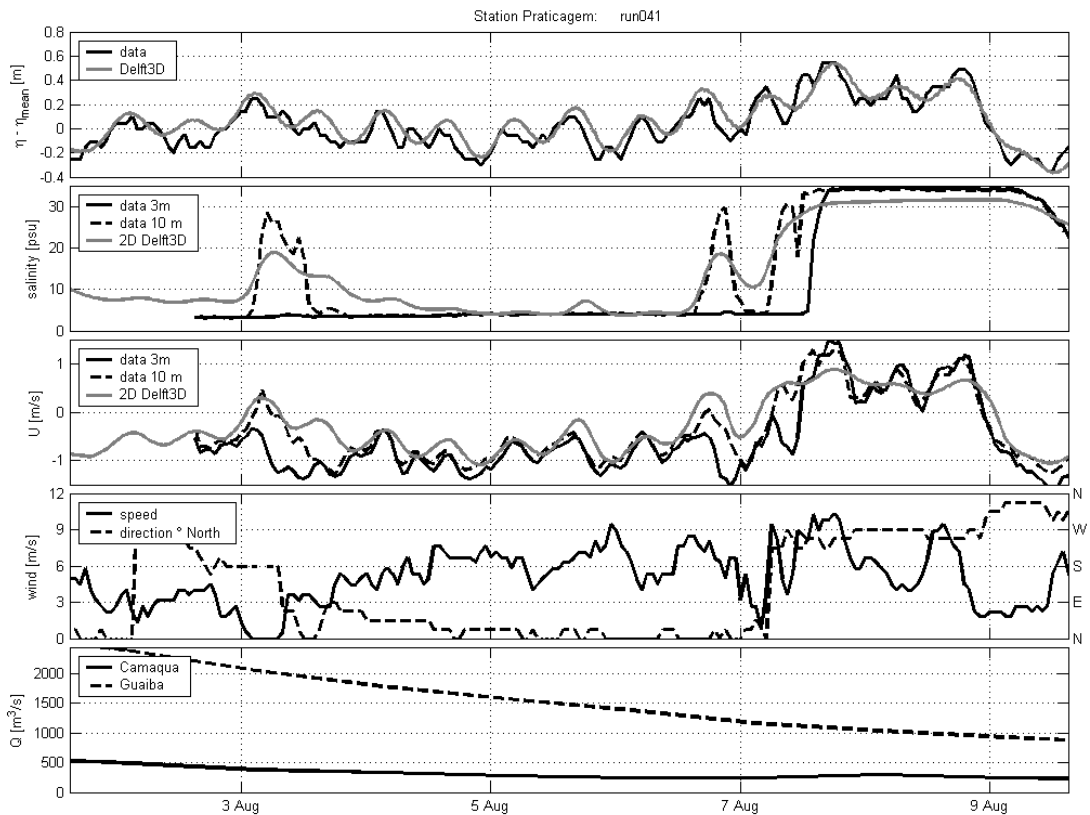


Figure 52: Modeled current and salinity comparison against measured data. Horizontal diffusivity in the estuary area set to 700 m²/s.

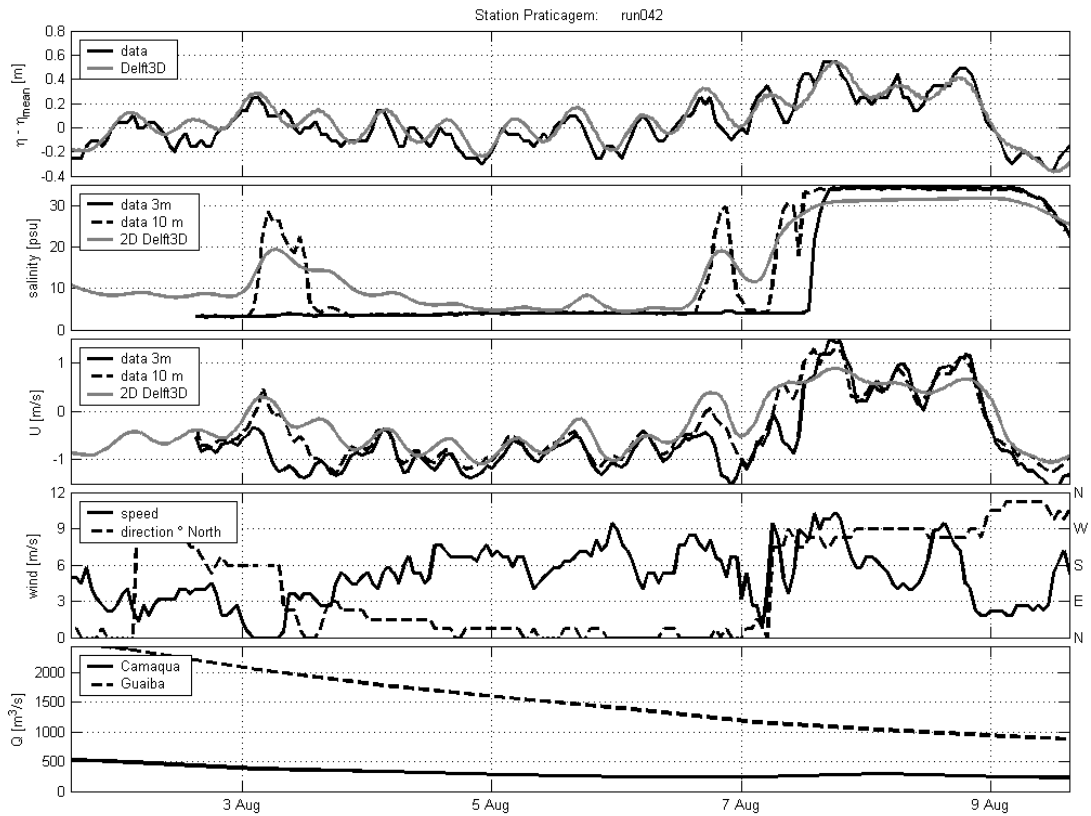


Figure 53: Modeled current and salinity comparison against measured data. Horizontal diffusivity in the estuary area set to 800 m²/s.

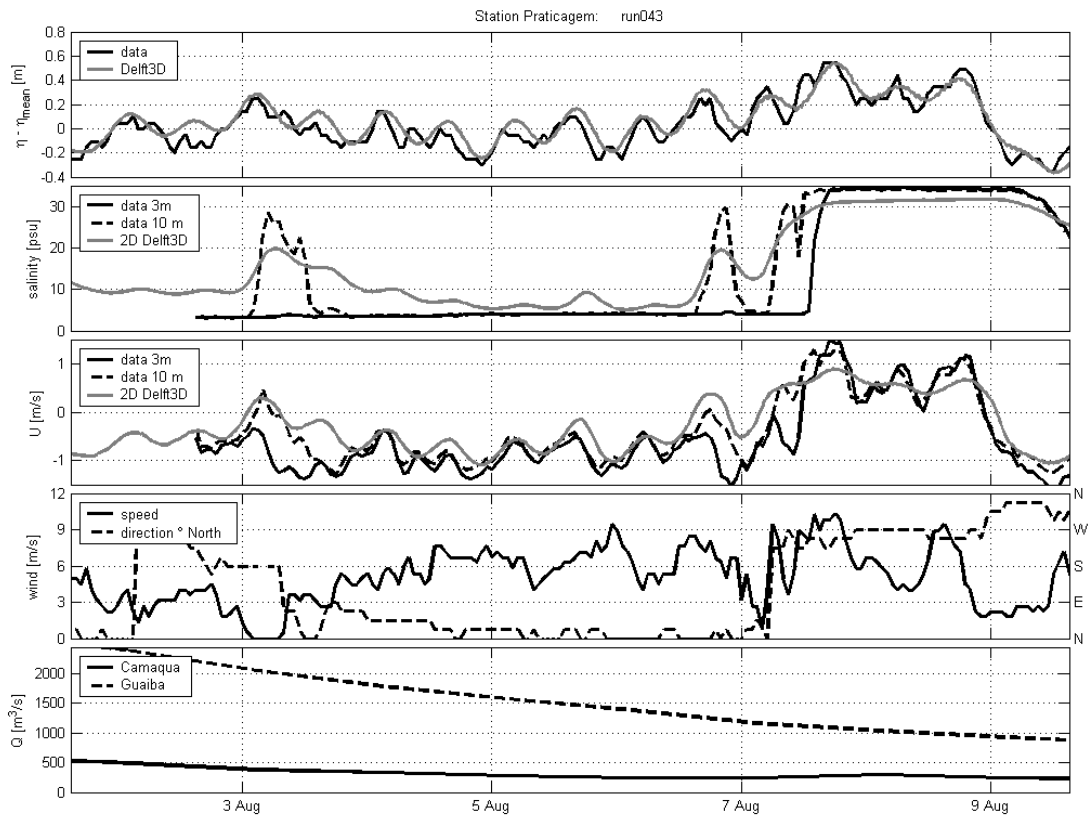


Figure 54: Modeled current and salinity comparison against measured data. Horizontal diffusivity in the estuary area set to 900 m²/s.

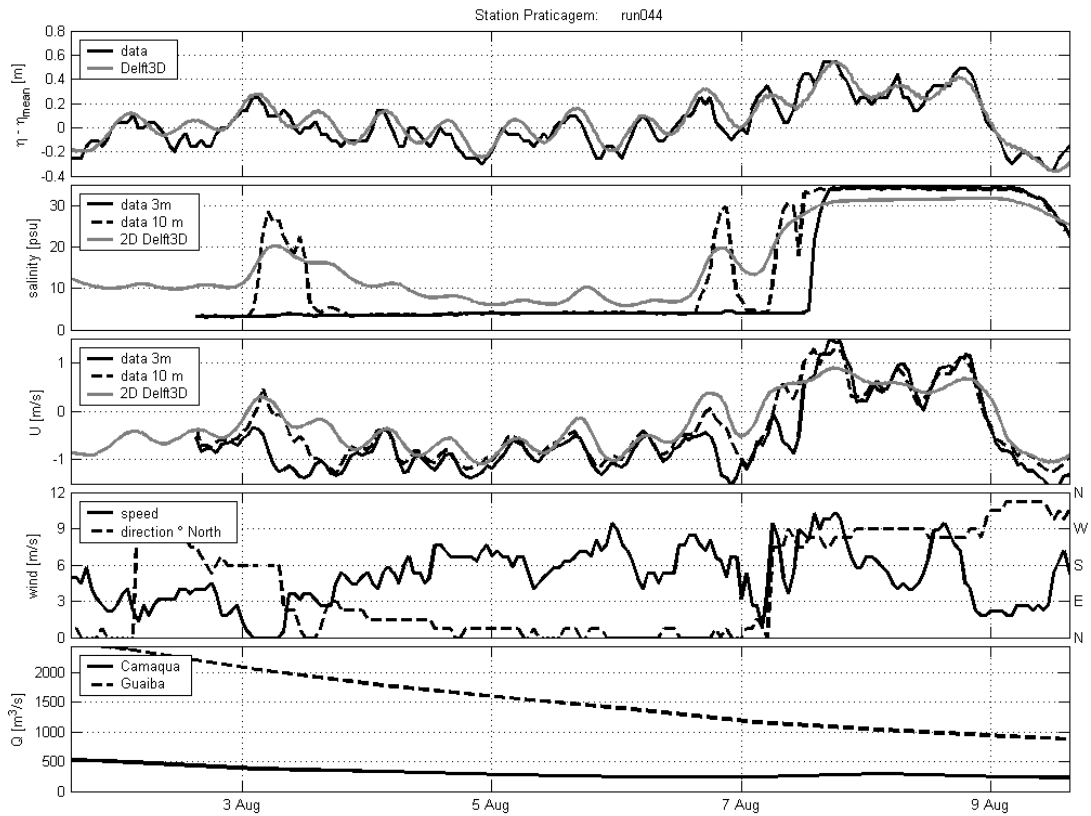


Figure 55: Modeled current and salinity comparison against measured data. Horizontal diffusivity in the estuary area set to 1000 m²/s.

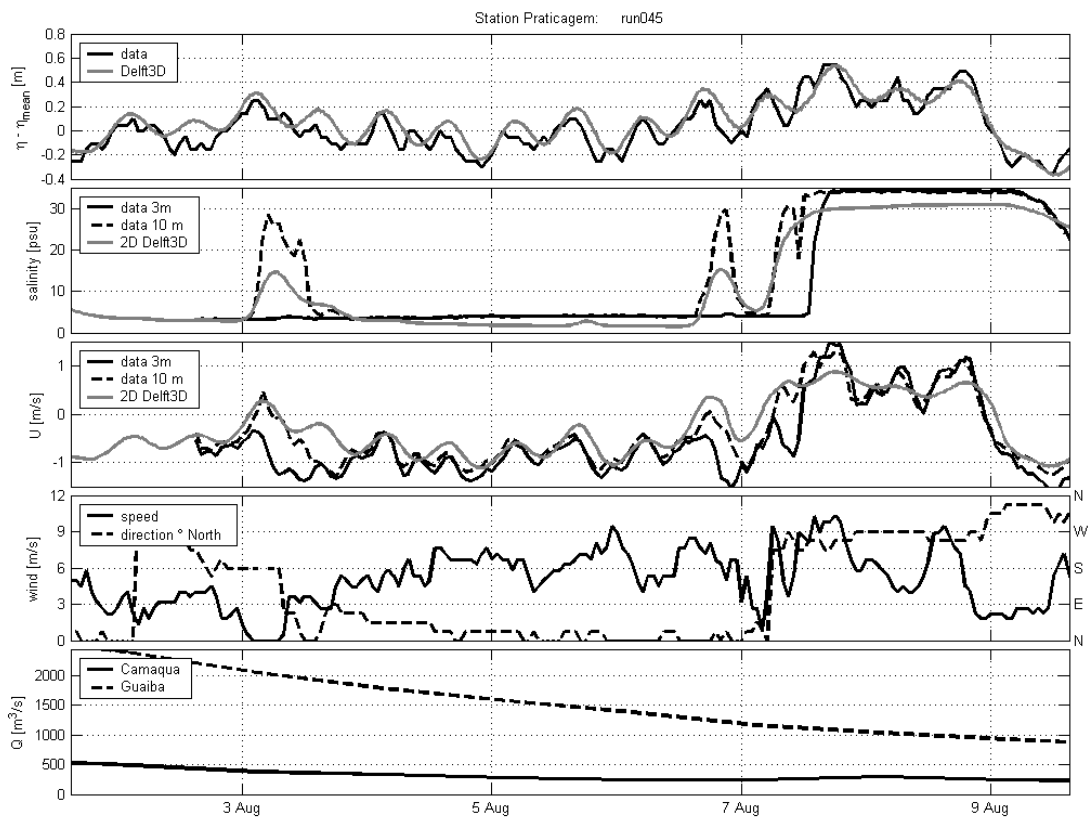


Figure 56: Modeled current and salinity comparison against measured data. Horizontal diffusivity in the estuary area set to 400 m²/s and SGC discharges included.

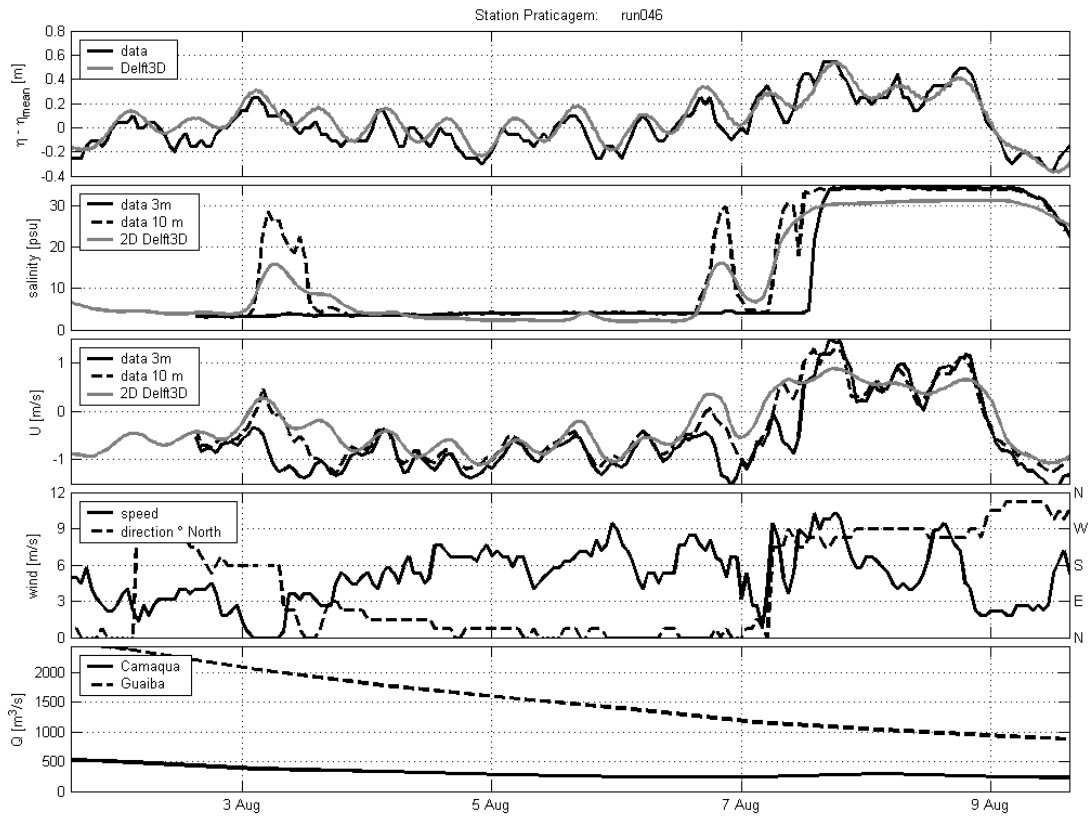


Figure 57: Modeled current and salinity comparison against measured data. Horizontal diffusivity in the estuary area set to 500 m²/s and SGC discharges included.

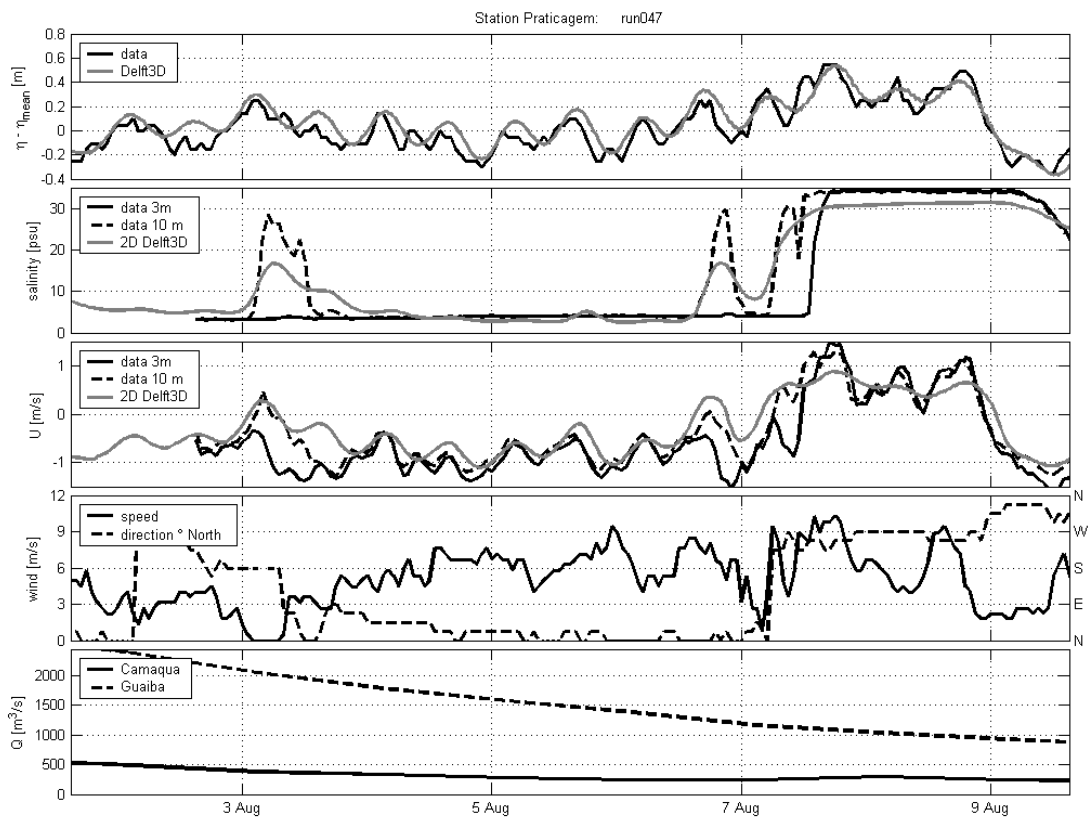


Figure 58: Modeled current and salinity comparison against measured data. Horizontal diffusivity in the estuary area set to 600 m²/s and SGC discharges included.

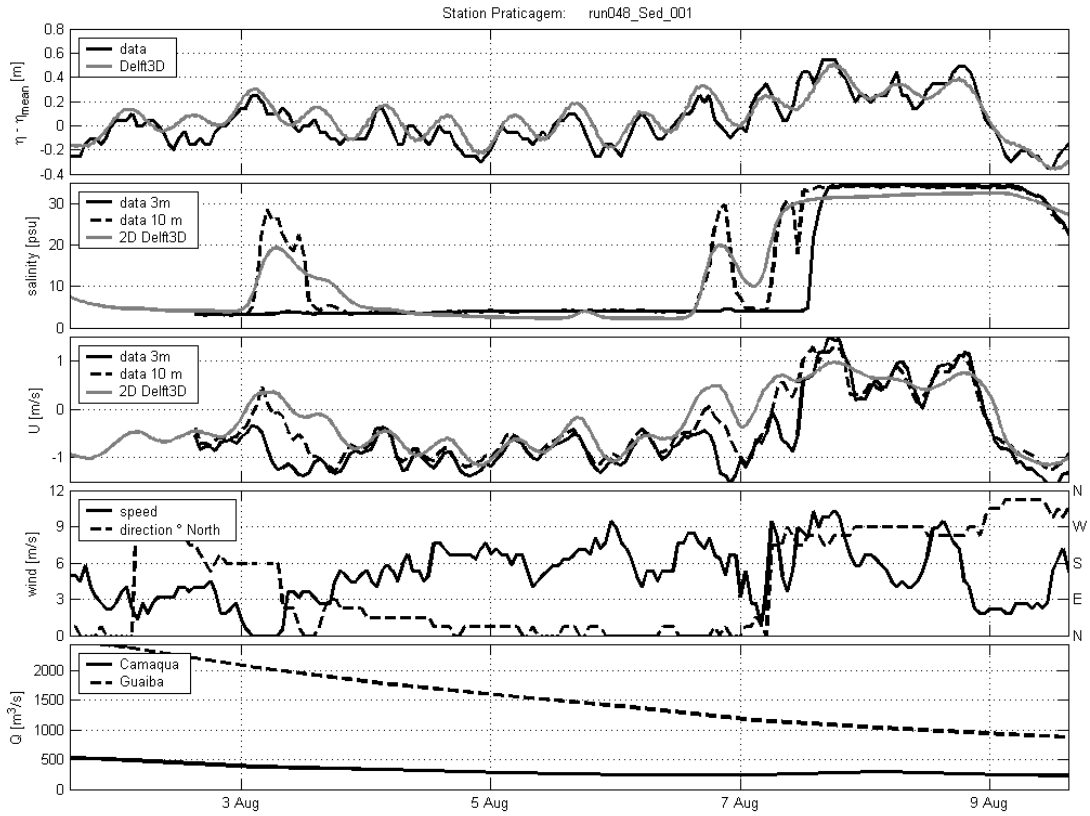


Figure 59: Modeled current and salinity comparison against measured data. Horizontal diffusivity for the whole domain set to 400 m²/s and SGC discharges included.

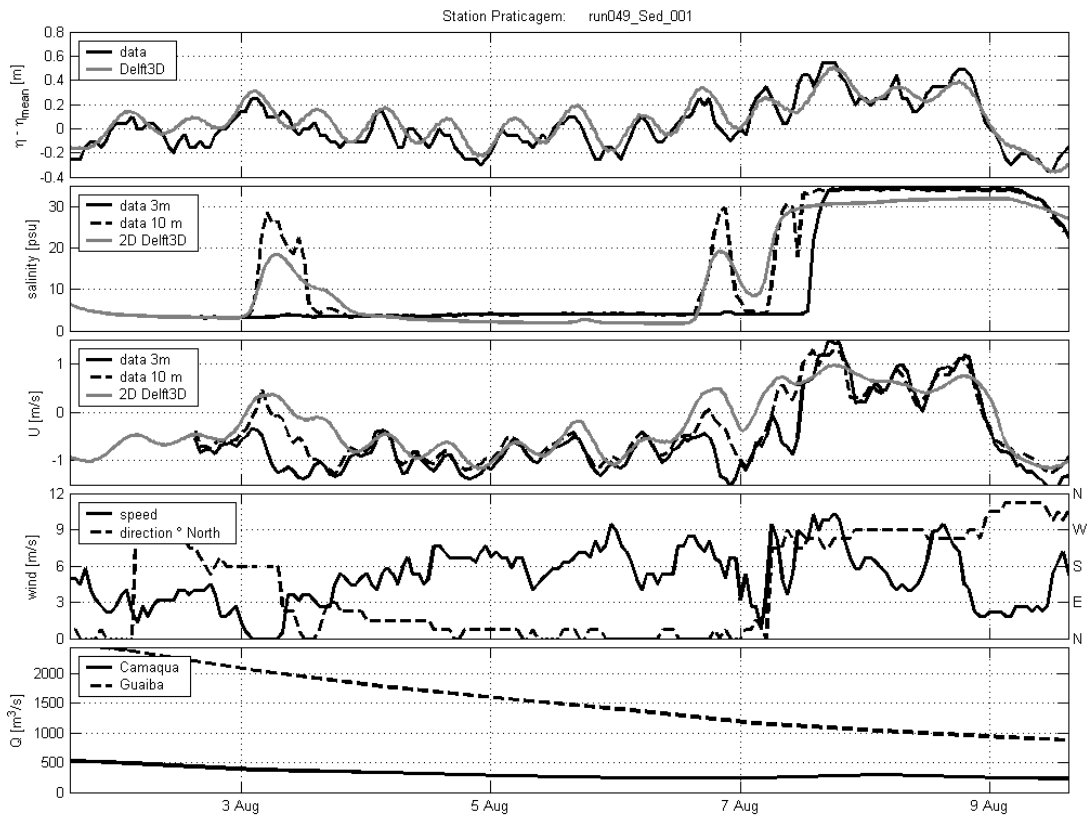


Figure 60: Modeled current and salinity comparison against measured data. Horizontal diffusivity for the whole domain set to 300 m²/s and SGC discharges included.

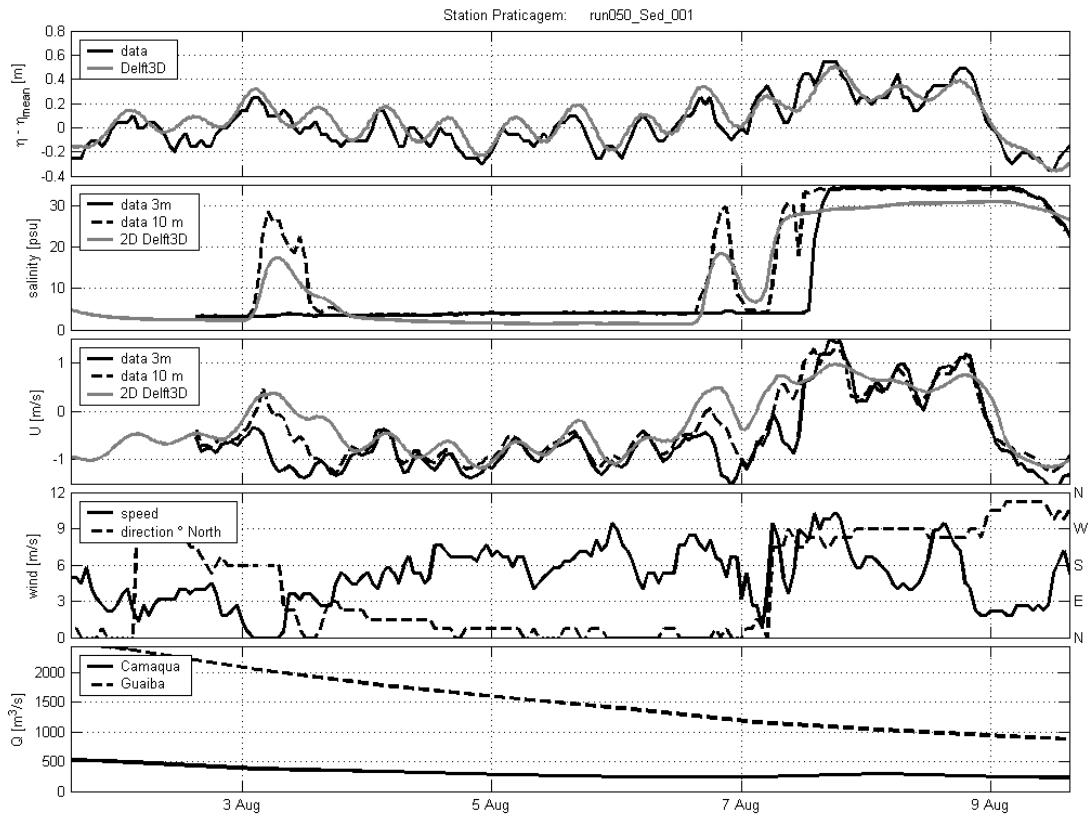


Figure 61: Modeled current and salinity comparison against measured data. Horizontal diffusivity for the whole domain set to 200 m²/s and SGC discharges included.

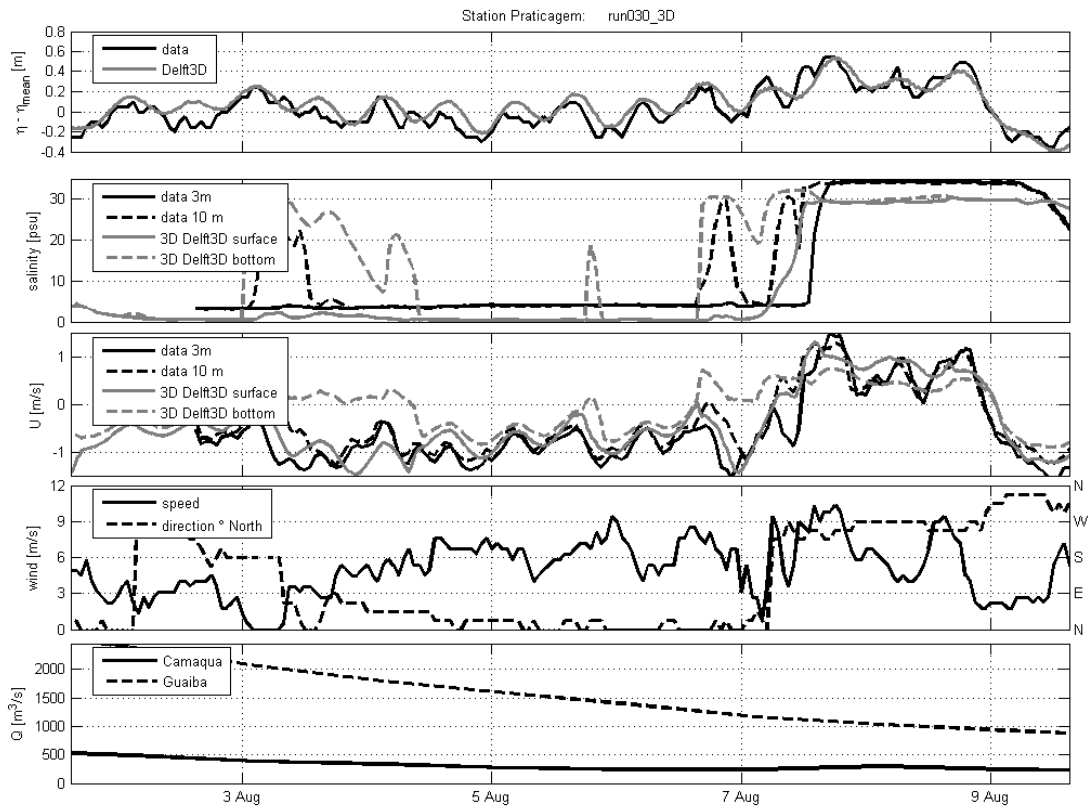


Figure 62: Modeled current and salinity comparison against measured data for Delft3D-Flow three dimensional module, 10 layers were used.

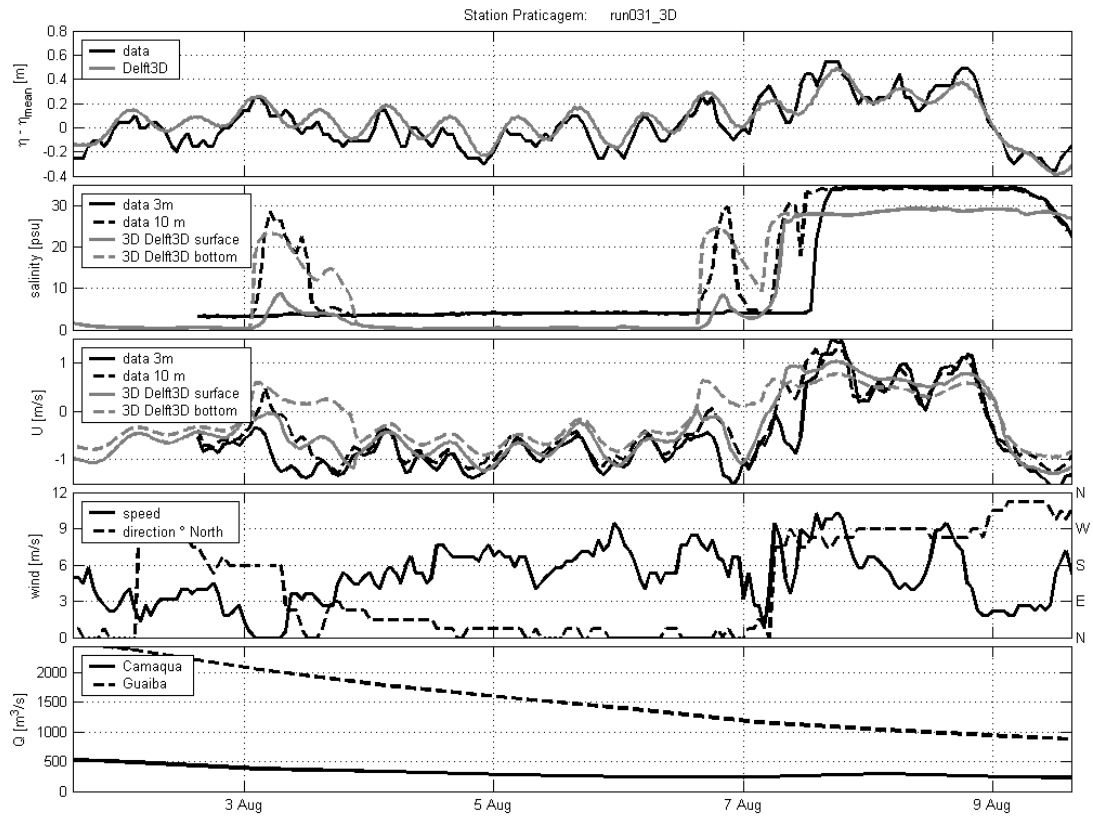
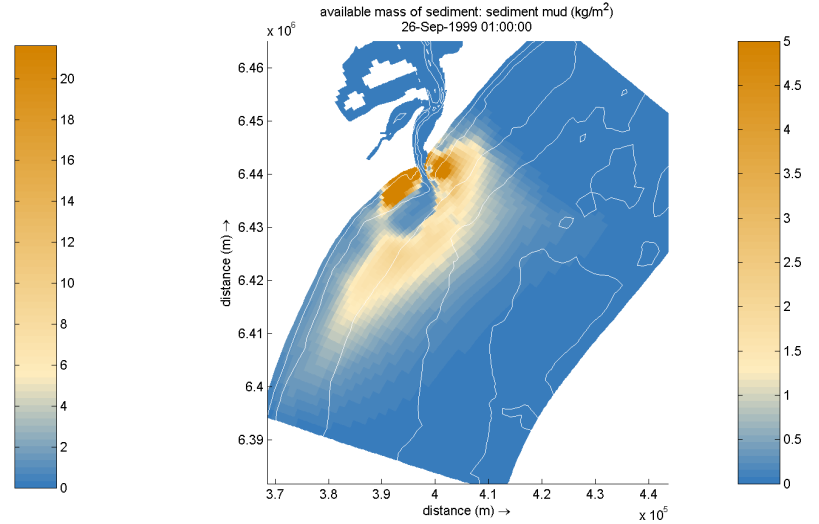
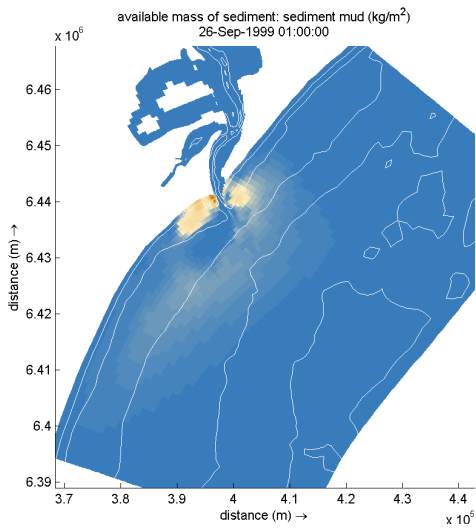
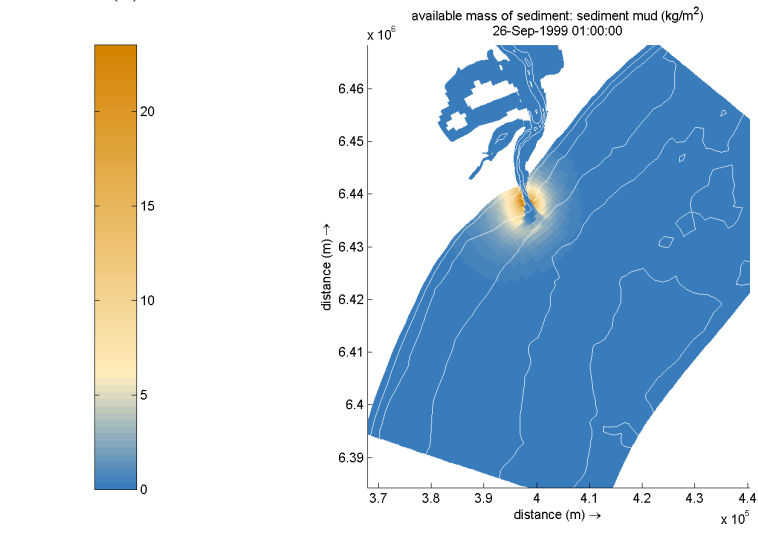
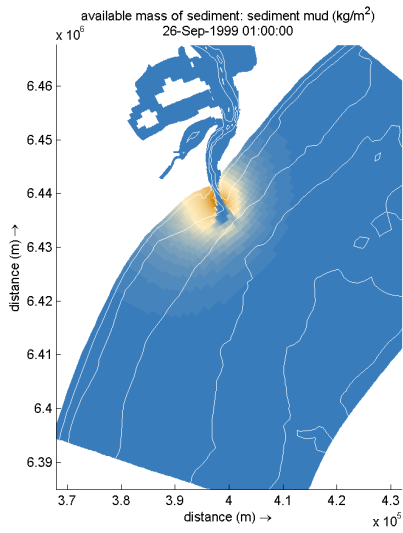


Figure 63: Modeled current and salinity comparison against measured data for Delft3D-Flow three dimensional module, 10 layers were used.

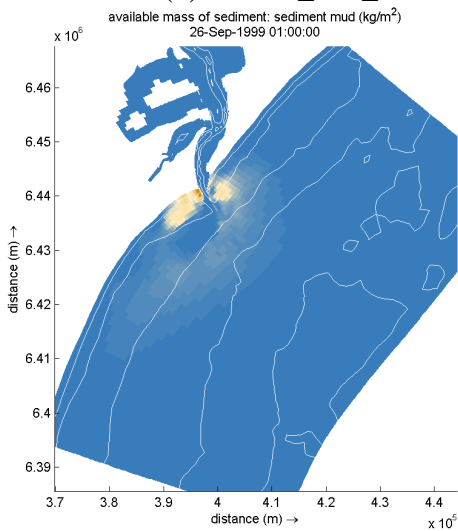


(a) run048_Sed_041



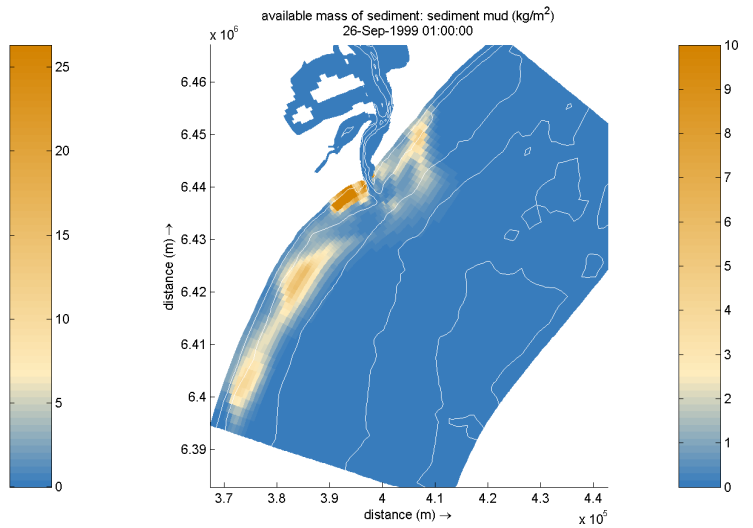
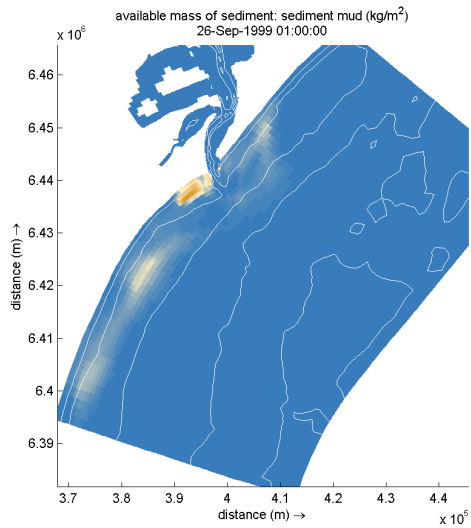
(b) run048_Sed_042

(c) run048_Sed_044

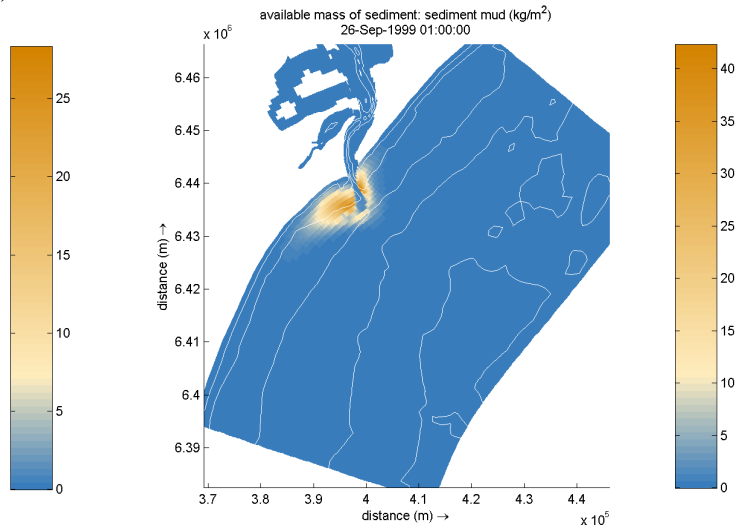
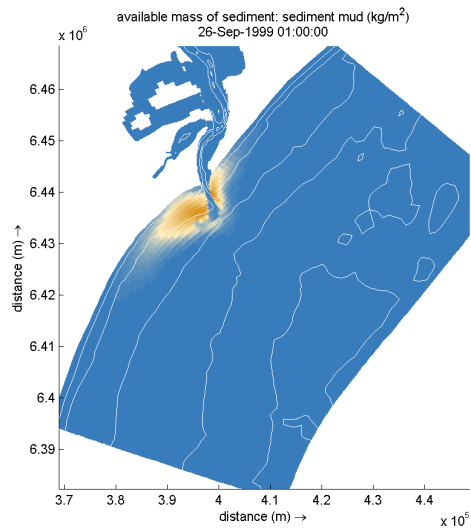


(d) run048_Sed_043

Figure 64: Available mass of sediments results for the models run048_Sed_041 (a), run048_Sed_042 (b), run048_Sed_043 (d) and run048_Sed_044 (c). Bathymetry isolines are spaced in 5 meters. Figures (a) and (d) are the same results but in different scales in order to better visualize the mud bank.

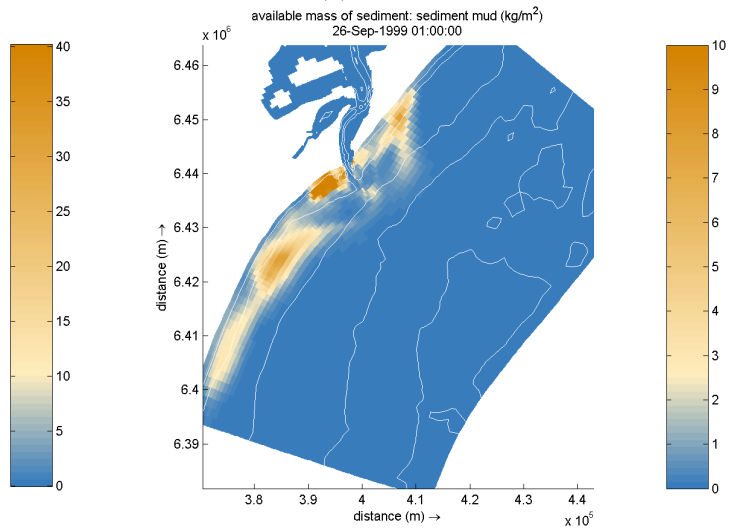
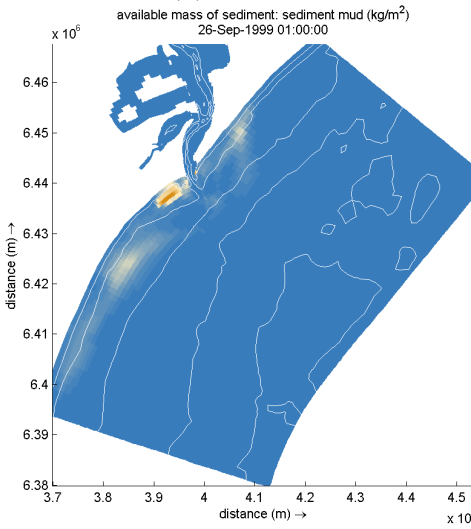


(a) run048_Sed_045



(b) run048_Sed_046

(c) run048_Sed_048



(d) run048_Sed_047

Figure 65: Available mass of sediments results for the models run048_Sed_045 (a), run048_Sed_046 (b), run048_Sed_047 (d) and run048_Sed_048 (c). Bathymetry isolines are spaced in 5 meters. Figures (a) and (d) are the same results but in different scales in order to better visualize the mud bank.

Depth-Averaged Transport Sediment Models													
Model Number	Hindered Settling Density (kg/m ³)	Specific Density (kg/m ³)	Dry Bed Density (kg/m ³)	Settling Velocity (m/s)	Critical Shear Stress Sedimentation (N/m ²)			Critical Shear Stress Eros (N/m ²)	Erosion Rate (kg/m ² s)	Initial Susp Matter Lagoon (mg/l)	Rivers Susp Matter Input (mg/l)		
					Lagoon	Estuary	Sea				GB	CQ	SGC
048_Sed_041*	1043	2650	200	0.0003	0	0	1000	0.1	0.001	60	100	50	80
048_Sed_042*	1043	2650	200	0.0003	0	0	1000	0.5	0.001	60	100	50	80
048_Sed_043*	1043	2650	200	0.0006	0	0	1000	0.1	0.001	60	100	50	80
048_Sed_044*	1043	2650	200	0.0006	0	0	1000	0.5	0.001	60	100	50	80
048_Sed_045**	1043	2650	200	0.0003	0	0	1000	0.1	0.001	60	100	50	80
048_Sed_046**	1043	2650	200	0.0003	0	0	1000	0.5	0.001	60	100	50	80
048_Sed_047**	1043	2650	200	0.0006	0	0	1000	0.1	0.001	60	100	50	80
048_Sed_048**	1043	2650	200	0.0006	0	0	1000	0.5	0.001	60	100	50	80

Table 6: List of sediment models performed. The models with * means that the horizontal diffusivity was set to 400 m²/s for the whole domain and ** were set to 10 m²/s for the whole domain. GB = Guaíba river; CQ = Camaquã river and SGC = São Gonçalo Channel.